NTNU

Norwegian University of
Science and Technology

Evaluation of Microbial Enhanced Oil Recovery using the MRST Simulator

Dayo Akindipe

Petroleum Engineering
Submission date: June 2016
Supervisor: Ole Torsæter, IPT
Co-supervisor: Robert Drysdale, SINTEF Petroleum

Norwegian University of Science and Technology
Department of Petroleum Engineering and Applied Geophysics

Abstract

Microbial enhanced oil recovery (MEOR), as a field of study, exploits the benefits of microbes for the purpose of improving microscopic as well as macroscopic displacement of oil by water. This work has been carried out to investigate certain mechanisms that affect the displacement process and limit the effectiveness of MEOR as an enhanced oil recovery technique. It was implemented via one-dimensional modelling and simulation of the MEOR displacement process with the MATLAB Reservoir Simulation Toolbox (MRST). By applying the dynamic modelling approach, mechanisms such as interfacial tension reduction by the action of biosurfactants, and component (bacteria and food) adsorption resulting in the formation of a biofilm have been studied. Simulation results generally revealed improved oil recovery compared to the base case of pure waterflooding. The effect of biosurfactants in mobilising residual oil in the reservoir has been found to result in the creation of a water saturation profile with two displacement fronts characterised by a travelling oil bank. Oil mobilisation commences much earlier when the combined effect of biofilm formation and IFT reduction by biosurfactants is active. The presence of indigenous microbes has been observed to limit the MEOR displacement process; however, this effect becomes less significant when high concentrations of exogenous bacteria are injected. Overall, MRST as a simulation tool has provided the necessary flexibility and robustness required for microbial EOR modelling making it suitable and recommendable for further modelling studies.

Dedicated to God Almighty,

my help in ages past and my

hope for greater years to come

Acknowledgement

Someone once said, “Silent gratitude isn't much use to anyone”. For this reason, I would like to take this opportunity to explicitly declare my gratitude to all that have contributed in one measure or another to the completion of this project. First of all, I would like to formally thank my supervisor, Professor Ole Toræsater for giving me the opportunity to work on this project and for showing interest every step of the way. Immense gratitude also goes to my co-supervisor, Robert Drysdale of SINTEF Petroleum, who has been the major facilitator of this work and has been available whenever his assistance was sought. Appreciation also goes to Xavier Raynaud of SINTEF Applied Mathematics for his timely help when problems with running MRST codes seemed intractable. Katherine Aurand has been very helpful with the design of some illustrations in this report; for which I am truly grateful. I would like to specially thank my wonderful family, particularly my parents, for their weekend calls and prayers that always gave me the courage to strive on. Mirhossein Taheriotaghsara has been a good friend here at NTNU, thanks for encouraging me to take that bold step last autumn. Not forgetting other friends I have met here in Trondheim – Reizky, Alua, Anna, Mehari, Laura, Anisa and Priya. You made my stay very pleasant. Finally, I would like to officially thank my sponsors – National Oilwell Varco (NOV) and Total Nigeria – for facilitating and funding my master’s programme at NTNU.

Contents

List of Figures

List of Tables

Nomenclature

Latin Alphabets

Symbol	Unit	Description
M	-	Oil-water mobility ratio
k_{rw}	-	Relative permeability of water
k_{ro}	-	Relative permeability of oil
p_c	Pa or bar	Capillary pressure
p	Pa or bar	Pressure
p_{bh}	bara	Constant boundary pressure
K	mD	Absolute permeability
k_o	mD	Effective permeability to oil
k_w	mD	Effective permeability to water
N_o	-	Corey exponent for oil
N_w	-	Corey exponent for water
S_{on}	-	Normalized oil saturation
S_{wn}	-	Normalized water saturation
S_{or}	-	Residual oil saturation
S_{wi}	-	Initial/irreducible water saturation
S	-	Saturation
q	m^3/s or m^3/day	Volumetric flow rate (flux)
u	m/s	Darcy velocity
g	m/s^2	Acceleration due to gravity
z	m	Elevation vector
c	-	Mass composition
t	day or s	Time
B	m^3/Sm^3	Formation volume factor
R_s	Sm^3/Sm^3	Solution gas-oil ratio
C	kg/m^3	Mass concentration
C_j	kg/m^3	Mass concentration of component *j*
C_{ji}	kg/m^3	Mass concentration of component j in phase *i*
K_{bn}	kg/m^3	Half saturation constant for bacteria
K_{mn}	kg/m^3	Half saturation constant for metabolite
$C_{n,crit}$	kg/m^3	Critical mass concentration of nutrients
R_j	kg/m^3.day	Reaction term for component *j* in conservation equation
Y_j	-	Yield coefficient of component *j*
D_i	-	Distribution coefficient for surfactant partitioning
l_1,l_2, l_3	-	Constants that define surfactant efficacy
f	-	Coats' interpolation function
$\tilde{A}_S$-	m^2/m^3 total vol.	Specific surface area
A_S	m^2/m^3 of PV	Effective surface area
R_1,R_2	m	Principal radii of curvature

Greek Symbols

Symbol	Unit	Description
μ_w	cp	Dynamic viscosity of water
μ_o	cp	Dynamic viscosity of oil
θ	°	Contact angle
τ	-	Adhesion tension
σ_{wo}	mN/m	Oil/water interfacial tension
σ_{so}	mN/m	Oil/rock interfacial tension
σ_{sw}	mN/m	water/rock interfacial tension
ρ	kg/m3	Density
ϕ	-	Porosity
$\mu_{b,max}$	day^{-1}	maximum growth rate (bacteria)
$\mu_{m,max}$	day^{-1}	maximum growth rate (metabolite)
μ_b	day^{-1}	Specific growth rate of bacteria
μ_m	day^{-1}	specific growth rate of metabolite
κ	day^{-1}	Rate constant
χ	-	Mass of adsorbed component per unit surface area
ω_1, ω_2	kg/m^2 and m^3/kg	Langmuir adsorption isotherm constants
ψ	-	Biofilm partition
γ	-	Kozeny-Carman exponent
ϕ_{rel}	-	Relative porosity
δ	day^{-1}	Diffusion rate

Subscripts

Symbol	Description
i	Represents a particular phase - oil, water or gas
j	Represents a particular component within phase *i* (e.g. bacteria, metabolite)
o	oil
w	water
g	gas
b	bacteria or biofilm phase
n	nutrient
m	metabolite
s	Measurement based on surface conditions
c	Microbial competition

Superscripts

n	time step
*	modified parameter
′	endpoint values (relative permeability curve)

Abbreviations

EOR	Enhanced oil recovery
BT	Breakthrough
EPS	Extracellular polymeric substances
IFT	Interfacial tension
MRST	MATLAB Reservoir Simulation Toolbox
MEOR	Microbial enhanced oil recovery
NCS	Norwegian continental shelf
NRB	Nitrate-reducing bacteria
PV	Pore volume
REV	Representative elementary volume
UTCHEM	University of Texas Chemical Compositional Simulator
CSTR	Continuous stirred-tank reactor
OIIP	Oil Initially in Place
WAG	Water-alternating gas injection
SWAG	Simultaneous water and gas injection
FAWAG	Foam-assisted water-alternating gas injection
SAGD	Steam-assisted gravity drainage
GAGD	Gas-assisted gravity drainage
SINTEF	Stiftelsen for industriell og teknisk forskning
CMG	Computer Modelling Group

1 Introduction

Over the years, since the advent of the modern day discovery of crude oil in 1859, the demand for oil and gas for energy and ancillary purposes has been on an exponential rise. Oil production has also followed the same trend from a meagre 25 bbl/day recorded in Titusville, Pennsylvania in 1859 to first quarter 2016 global supply of about 96.49 million bbl/day (IEA, 2016). As we gradually move towards peak oil production globally, it follows that there will be a disproportionate growth in oil demand compared to oil production.

In many reservoirs today, primary and secondary methods for recovering oil can only deliver about 30% of the oil initially in place leaving about 70% behind (Lake, et al., 1992). This is largely due to certain limitations that range from technical issues like water/gas coning to economic limitations like well profitability. This creates a need for more effective, efficient and environmentally-friendly methods of producing oil within the limits of uncertainty and cost. Enhanced oil recovery (EOR) has been proposed as a veritable solution to breaking these limits. Essentially, EOR is a term used to describe the third step of oil recovery (tertiary recovery) which covers processes beyond the simple application of gas and water to improve the recovery of a well (Lake, et al., 1992). It is fast becoming an integral part of the present-day petroleum industry as the need for higher oil production rates and recovery factor increases. Generally, EOR processes can be classified as thermal, gas (miscible and immiscible), chemical and other processes as illustrated in Table 1.1 below.

Table 1.1: Classification of EOR process (Adapted from Lake & Walsh, 2008 and Lake, et al.1992)

EOR Process	**Types of Mechanisms**
Thermal	Steam flooding, cyclic steam stimulation, in-situ combustion, hot water flooding, steam-assisted gravity drainage (SAGD)
Gas	Hydrocarbon (miscible and immiscible), carbon dioxide (CO_2) (miscible and immiscible), nitrogen, flue gas (miscible and immiscible), gas-assisted gravity drainage (GAGD)
Chemical	Micellar-polymer, polymer, caustic/alkaline, alkaline/surfactant, caustic, nanoflood
Others	Microbial, electrical, mechanical, electromagnetic heating, carbonated waterflood, low salinity waterflood

Many of these processes seek to mobilise the oil by lowering the oil-water interfacial tension or by changing the contact angle both of which have an effect in decreasing the capillary entry pressure. Others are aimed at producing more oil by increasing the capillary number which is the ratio of the viscous force due to a drive pressure and capillary force at the driven interface (Abdallah, et al., 2007). Higher capillary numbers can be achieved by increasing water viscosity and/or reducing oil viscosity.

1.1 History of EOR in Norway

Oil and gas activity in Norway is limited to offshore exploration and development projects majorly in the North Sea and partly in the Barents Sea. About 63% of all the reported EOR field applications in the North Sea have been initiated on the Norwegian continental shelf, 32% on the United Kingdom (UK) continental shelf and the remainder on the Danish continental shelf (Awan, et al., 2008). The average recovery in the Norwegian continental shelf (NCS) currently stands at about 47% of the oil in place; way over the global average (OED and NPD, 2015). Recently, the state-owned oil firm, Statoil, recorded an increase in recovery from its fields from 49% to about 50% (Statoil, 2012). This indeed has been due to advances in both secondary recovery and EOR technologies. Major EOR techniques employed over the years are hydrocarbon miscible gas injection, water-alternating gas (WAG) injection, simultaneous water-and gas (SWAG) injection, microbial EOR (MEOR), foam-assisted water-alternating gas (FAWAG) injection (Awan, et al., 2008). Other EOR techniques currently being proposed and/or screened are low-salinity water injection, polymer injection and surfactant flooding.

1.2 Microbial EOR as a Tertiary Oil Recovery Technique

Microbes have been used in many parts of the world for specialized applications in different fields of science and technology. This could vary from simple bacterial conversion of milk into curd to complex processes that are encountered in the field of biotechnology. In the oil industry, they have found wide application in petroleum exploration, drilling technology, bioremediation of crude oil spills, well stimulation and enhanced oil recovery.

The first suggestion about the use of microbes for improved oil production from porous media was made by Beckman (1926). Later on, ZoBell (1947) carried out extensive experimental studies which involved inoculating oil-bearing cores with two types of sulphate-reducing bacteria. He suggested that oil release from the cores were as a result of

decomposition of inorganic carbonates, evolution of gases, the affinity of bacteria for solids and the action of surface tension depressants (Jang & Yen, 1990). The first successful field trial carried out by Kuznetsov, et al. (1962) in the Sernovodsk oilfield indicated an increase in oil production from 37 tons to 40 tons. However, this success was short-lived as production fell back to around 36.5 tons after just four months (Jang & Yen, 1990). Other field tests were implemented in Eastern Europe and the United States in the 1960s through to the early 1970s but were halted because of low oil prices at the time. In the recent past, successful field tests have been executed globally with the Asia-Pacific region currently spearheading these trials (Hou, et al., 2011; Tingshan, et al., 2005; Ghazali Abd. Karim, et al., 2001; Brown, et al., 2000; Deng, et al., 1999). Statoil is one of the only two companies in the world currently applying MEOR in an offshore field – the Norne field in the Norwegian Sea (Statoil, 2014; Awan, et al., 2008).

Basically, every microbial enhanced oil recovery (MEOR) process seeks to achieve two major things – mobilisation of residual oil after secondary recovery processes and improvement of the volumetric sweep efficiency of the recovery process (Bryant & Lockhart, 2002). This is usually achieved through the introduction or stimulation of in-situ or external microbes into the reservoir followed by metabolic activities that result in microbial growth and generation of metabolic products (chemicals). MEOR addresses the same physical parameters (e.g. viscosity, interfacial tension) just like other chemical EOR processes. Therefore, they are subject to the same technical challenges that are encountered in the application of chemicals to improve oil recovery (Bryant & Lockhart, 2002). A major advantage however is the lower cost incurred in applying MEOR as compared to mainstream chemical and other EOR processes. Another major advantage is that they are environmentally friendly, using natural substances instead of potentially harmful ones. They do not essentially depend on the price of crude oil because microbial growth occurs at exponential rates; hence, large amounts of useful metabolic products are rapidly produced from inexpensive renewable resources (Youssef, et al., 2009).

1.3 Project Objectives

The purpose of this work is to investigate and evaluate the mechanisms observed in microbial EOR through a comprehensive literature study and to perform numerical modelling and simulation of surfactant production as a major MEOR mechanism within the limits of nutrient availability, adsorption and microbial competition. Implementation of the MEOR

model for an oil/water system will be carried out by adopting various model input parameters developed by Nielsen (2010) and modifying the MRST simulation scheme developed by Amundsen (2015). It is postulated that MRST will be sufficient and flexible enough to perform the various simulations and scenario analyses that this project will entail.

1.4 Project Methodology

This project is implicitly divided into four phases. The first phase involves a review of relevant literature that border around the waterflooding technique and various parameters – interfacial tension, wettability, capillary pressure and relative permeability, which affect the oil recovery process. The literature review will also discuss some concepts behind microbial enhanced oil recovery such as types of microbes and metabolic products, fluid displacement mechanisms observed during MEOR laboratory and field tests, as well as modelling and simulation studies.

The second phase covers the subject of reservoir modelling which is viewed from the perspective of the combination of a static geological model and a dynamic flow model. MEOR modelling will be discussed but limited to areas covering modelling of microbial growth, biosurfactant production, biofilm formation and microbial competition.

The third phase covers the implementation of these models in MRST, and will commence will a concise description of the specific features of this novel reservoir simulation software. Going further, the model implementation strategy and methodology will be discussed.

The final phase involves one-dimensional modelling and simulation of waterflooding and microbial EOR using MRST. Initially, simulations of idealized MEOR models will cover bacteria growth, biosurfactant, production and biofilm formation as a result of bacteria or nutrient adsorption. A sensitivity analysis on the model input parameters will be performed in order to understand the flexibility of the model. Further simulations will be carried out to determine the effect of microbial competition on oil recovery during MEOR.

2 Literature Review

It is insufficient to talk about any enhanced oil recovery process without initially describing their precursors. In this section, waterflooding as antecedent to microbial enhanced oil recovery is initially discussed. Parameters necessary for sufficient recovery via water injection into reservoirs are also highlighted. These go a long way in determining the extent of microscopic displacement of oil by water and the volumetric sweep efficiency of the entire process. Moving further, microbial enhanced oil recovery (MEOR) is described by highlighting the different microbes that alter the physical and chemical properties of reservoir rock and fluids. Mechanisms encountered as a result of microbial activities during MEOR processes and their effects on recovery of residual oil are also discussed.

2.1 Waterflooding

This is the most common method of increasing oil production after natural flow through primary recovery methods become uneconomical. Waterflooding, also known as water injection, entails the injection of water (usually brine) typically via an injection well on one side of a reservoir in order to serve as an additional source of energy required to raise the pressure in the field and to sweep mobile oil towards the producing wells. Water injection wells are normally completed either at the oil layer itself (Figure 2.1) or at the water layer with or without an active aquifer.

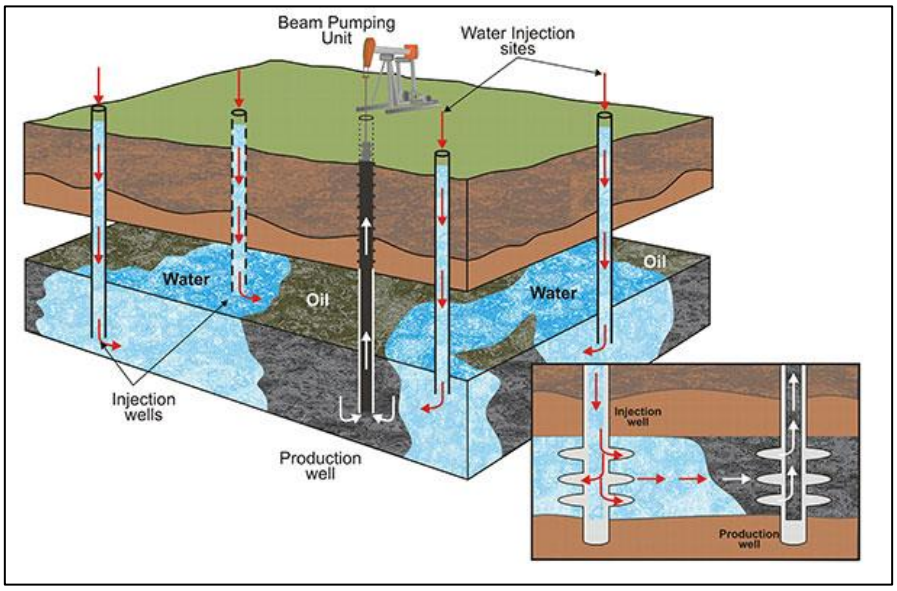

Figure 2.1: Water Injection in a 5-spot well pattern (Range Resources, n.d.)

In general, according to Thomas et al. (1987) there are some important factors that must be accounted for in order to fully describe a reservoir as being suitable for waterflooding. These factors can be categorized as:

- Geometrical factors: reservoir depth, reservoir geometry
- Petrophysical factors: lithology, porosity, permeability, reservoir heterogeneity, fluid saturations
- Intrinsic fluid properties: Viscosity, density, interfacial tension

However for an efficient overall displacement process via waterflooding, two properties stand out – viscosity (μ) and relative permeability (k_r) of both oil and water. These determine the mobility of each phase during the displacement process. Water/oil mobility ratio describes the water mobility with respect to the presence of an oil phase. It is expressed as:

$$M = \frac{k_{rw}.\mu_o}{\mu_w.k_{ro}} \tag{2.1}$$

M is the mobility ratio, μ_o & μ_w are oil and water viscosities, and k_{rw} & k_{ro} are water and oil relative permeabilities. Generally, mobility ratios less than 1 are favourable for efficient oil displacement by water with the displacement efficiency increasing as this value gets smaller.

In laboratory waterflooding analysis with small cores, efficient fluid displacement is usually analysed on a pore scale. Major factors that affect the microscopic (pore scale) displacement efficiency are wettability and pore geometry. Pore geometry factors typically describe the size and connectivity of the pore spaces and their effects on oil-water capillary pressure and relative permeability.

2.1.1 Interfacial Tension and Wettability

The interfacial tension (IFT) between fluids is the force that acts at the interface (boundary) of the contacting phases. IFT mostly applies to liquid/liquid or liquid/solid systems which are highly impacted by adhesive forces in contrast to liquid/gas systems that are majorly influenced by cohesive forces within the liquid. Hence, surface tension is the more appropriate term for the latter systems. Oil-water IFT plays a major role in the microscopic displacement of oil during waterflooding; hence, lower IFT values are usually preferred.

The wetting characteristics of a formation describe its ability to preferentially allow a fluid to be in contact with its solid surface in the presence of another fluid. This preference is

essentially due to the interplay of surface and interfacial forces and it is termed as the wettability of the formation (Abdallah, et al., 2007). The most important yardstick for measuring the wettability of a rock surface is the contact angle. The contact angle of any liquid/liquid/solid system is a function of the interfacial tension (IFT) between each liquid surface and the adhesion tension between the liquid and solid surface. Young (1805) defined the contact angle of an oil/water/rock system as:

$$Cos\theta = \frac{\tau}{\sigma_{wo}} = \frac{\sigma_{so} - \sigma_{sw}}{\sigma_{wo}} \tag{2.2}$$

where, θ is the contact angle measured from the water phase, τ is the adhesion tension, σ_{wo} is the oil/water IFT, σ_{so} is the oil/rock IFT, and σ_{sw} is the water/rock IFT.

Depending on the value and range of the contact angle, we can generally classify an oil/water homogeneous system as strongly water-wet, intermediate-wet or strongly oil-wet. For a non-homogeneous system, the term mixed-wet, fractional-wet or dalmatian-wet is usually encountered as variants of the intermediate-wet state (Abdallah, et al., 2007). Figure 2.2 below illustrates the variation of wettability with increasing contact angle as we move from a strongly water-wet scenario to a strongly oil-wet case.

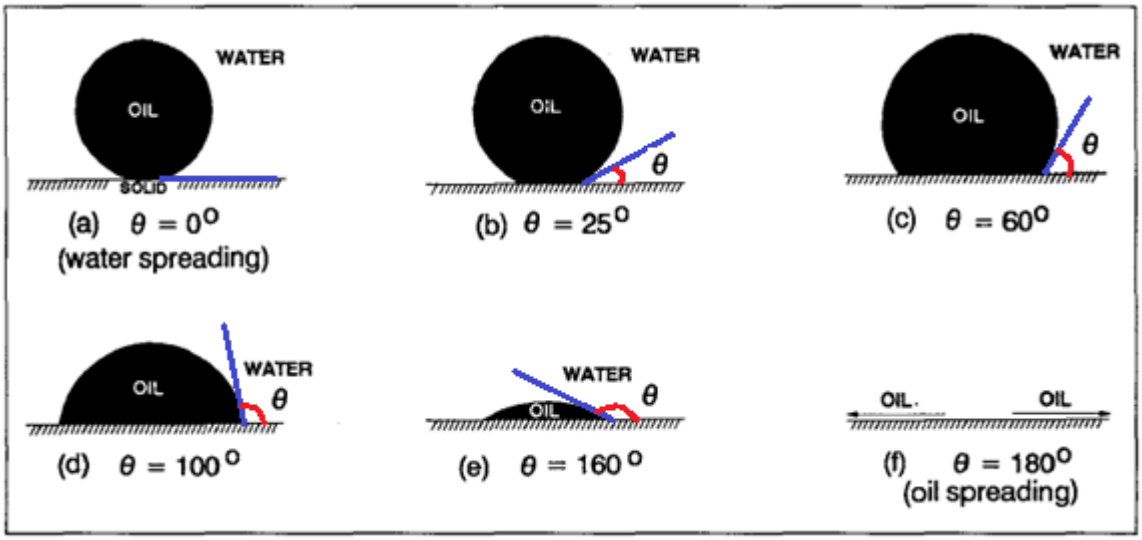

Figure 2.2: An ideal spreading case showing variation in contact angle and change in wettability (Morrow, 1990)

2.1.2 Capillary Pressure

When the surfaces of two immiscible fluids come in contact with each other in a capillary-like tube, a certain curvature at the point of surface contact is observed. This is due to the

interfacial tension that tends to exist at this interface. The shape of the curvature however depends on the individual pressures exerted by each fluid in the presence of the other fluids which tends to counteract the effect of the interfacial tension. This relative pressure is known as the capillary pressure. It is generally expressed by the Young-Laplace equation as:

$$p_c = \sigma\left(\frac{1}{R_1}+\frac{1}{R_2}\right) \tag{2.3}$$

where, p_c is capillary pressure, σ is surface tension and R_1 & R_2 are the principal radii of curvature.

In the displacement of one fluid by another in a porous medium, the wetting characteristics are very important because the difference between the pressure exerted by the non-wetting phase (P_{NW}) and the wetting (P_W) phase define the capillary pressure (Ahmed, 2010). This relationship is expressed as:

$$p_c = p_{NW} - p_W \tag{2.4}$$

Therefore for an oil/water system where water is the wetting fluid, the oil-water capillary pressure P_{cow} can be expressed as:

$$p_{cow} = p_o - p_w \tag{2.5}$$

where, p_o and p_w are the oil and water pressures respectively.

Two primary capillary processes exist during fluid displacement in a porous medium – drainage and imbibition. The drainage process involves the displacement of a wetting fluid by a non-wetting fluid; for instance, the displacement of in-situ reservoir brine by oil during accumulation. The brine saturation after drainage becomes connate in nature. The second process involves the displacement of the non-wetting fluid by the wetting fluid such that the connate saturation of the wetting fluid increases to a capillary-determined saturation. This process could be either spontaneous or forced. Figure 2.3 illustrates the capillary processes for typical Berea sandstone. Generally, during the drainage process, there is hysteresis in capillary pressure as the saturation is varied, making drainage and imbibition curves different (Anderson W. G., 1987). Therefore, the more the hysteresis effect, the greater the difference between these two curves.

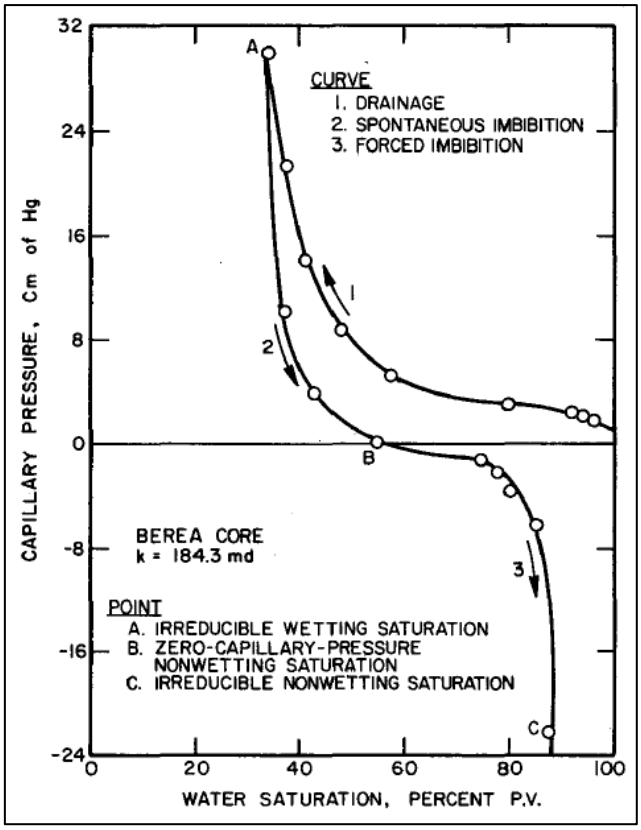

Figure 2.3: Drainage and imbibition processes for a Berea sandstone core sample (Anderson W. G., 1987)

2.1.3 The Relative Permeability Concept

An essential property of a reservoir that describes its ability to allow for fluid flow through its pore spaces (voids) is called permeability. In the presence of no other fluid, the permeability of a reservoir to a fluid is termed as its absolute permeability (K). Typically, oil reservoirs exist as gravity-separated layers of fluids (water, oil and gas) in phases and the ability of one fluid to flow in the presence of another is described as the effective permeability. Ahmed (2010) elucidates that the effective permeability of any reservoir fluid is a function of the reservoir fluid saturation and the wetting characteristics of the formation. Therefore, in a two-phase oil-water system, the effective permeability to oil, k_o is dependent on the amount of oil and the tendency of the oil or water to occupy the smaller pores. The ratio of the effective permeability to the absolute permeability for a given reservoir fluid saturation is termed as the relative permeability of that fluid (k_{ri}; where i = gas, oil or water). Figure 2.4 illustrates the analogous nature of effective permeability curves with relative permeability curves.

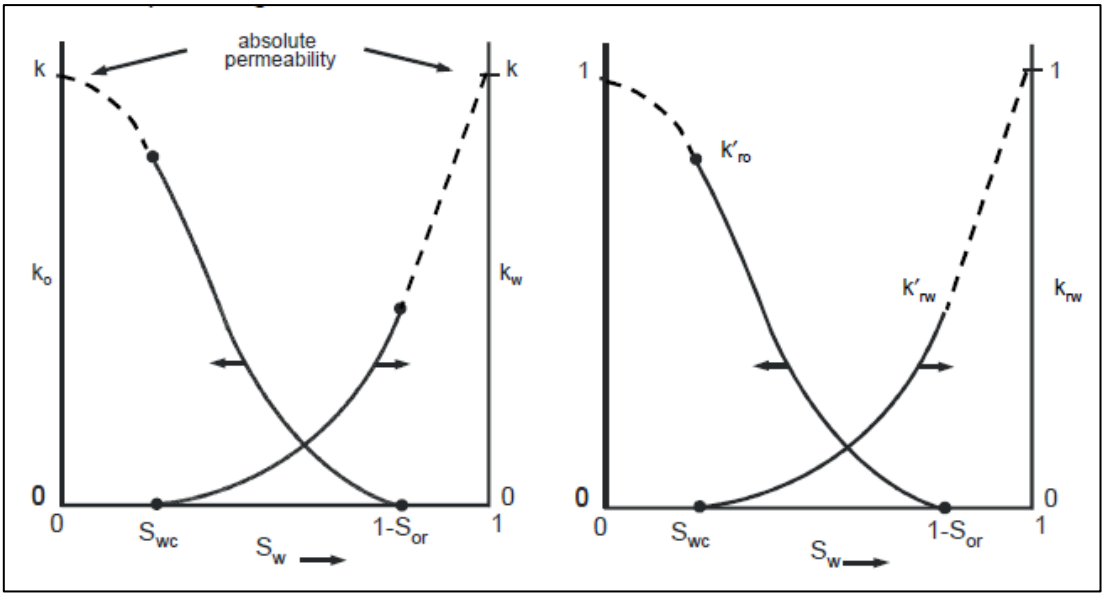

Figure 2.4: (a) Effective and (b) corresponding relative permeability, as functions of water saturation (Dake, 1978)

In order to describe the effect of saturation change on relative permeability in two-phase and three-phase systems, several relative permeability correlations have been introduced over the years. A simple correlation, generally based on the work of Corey (1954), has been applied in many studies to generate relative permeability data in a two-phase system. Although Corey's initial work was on a gas/oil system, the mathematical expression has been extended to oil/water systems as well. Therefore, for an oil/water system based on normalized saturation, the correlation can be expressed as:

$$k_{ro} = k'_{ro}\left[S_{on}\right]^{N_o} \tag{2.6}$$

$$k_{rw} = k'_{rw}\left[S_{wn}\right]^{N_w} \tag{2.7}$$

where, k_{ro} and k_{rw} are the oil and water relative permeabilities respectively, k'_{ro} and k'_{rw} are the endpoint oil and water relative permeabilities respectively, S_{on} and S_{wn} are the normalized oil and water saturations, and N_o and N_w are the respective Corey exponents for oil and water.

The normalized saturations are functions of water saturation (S_w), the residual oil saturation (S_{or}) and the irreducible water saturation (S_{wi}). They are expressed as follows:

$$S_{on} = \frac{1 - S_w - S_{or}}{1 - S_{wi} - S_{or}} \tag{2.8}$$

$$S_{wn} = \frac{S_w - S_{wi}}{1 - S_{wi} - S_{or}} = 1 - S_{on} \tag{2.9}$$

The N_o and N_w values typically range from 1 to 9 in most cases. Water-wet systems generally have higher N_w values compared to N_o and vice versa for oil-wet systems.

2.1.4 Wettability Effect on Relative Permeability in Oil Recovery

Wettability has a major effect on relative permeability because it controls the location, flow, and spatial distribution of fluids in a core (Anderson W. G., 1987). In the water-wet case, water is the preferential wetting phase. Therefore, after the initial drainage process (migration of oil into a fully water-saturated reservoir), it will essentially occupy the small pores with high capillary pressure (Abdallah, et al., 2007). Water saturation is consequently at its lowest and it can be said that the relative permeability of water is zero. Oil will in turn occupy the large pores with a high relative permeability, k_{ro} (usually equal to 1.0). During natural or induced imbibition with water, both phases flow in such a way that the displacement process takes a frontal profile as water begins to sweep oil from the larger pores. As a result, the oil relative permeability, k_{ro}, which is initially high, decreases as oil saturation behind the front decreases. The relative permeability of water, k_{rw}, starts low (mostly at zero) and begins to increase as water saturation increases behind the displacement front. This frontal displacement however is not perfect because as the water fills up both small and larger pores, it creates a bridge-like film at the pore throat of the large pores. This blocks oil flow into the pore throat since the oil would be deficient in the driving pressure required to overcome the capillary entry pressure for the now water-saturated pore throat; hence, droplets of oil are trapped within the pores (Figure 2.5(c)). The final k_{rw} is lower than the original k_{ro} because of the oil trapped in large pores (Figure 2.6).

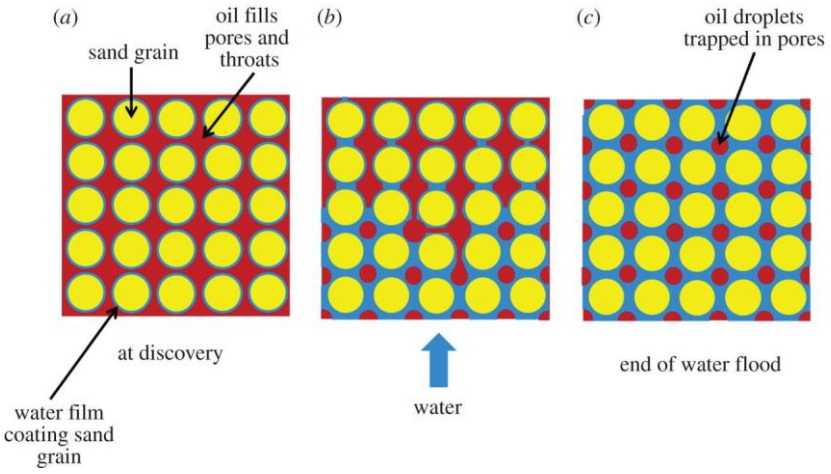

Figure 2.5: Illustration of oil trapping in a water-wet rock. (a) At discovery the sand grains are coated with a thin water film and the pores are filled with oil; (b) as water flooding progresses the water films become thicker until (c) the water films join and oil continuity is lost (Muggeridge, et al., 2014)

In a mixed-wet formation, the initial drainage process macroscopically follows the same pattern as the water-wet case. However on observation of the microscopic displacement, some of the oil occupying the large pore spaces is preferentially allowed to be in direct contact with the rock matrix. It is important to note that the water in the smaller pores still ensure that the formation is partly water-wet. During natural or induced imbibition with water, the displacement process takes a frontal profile as water begins to sweep oil from the larger pores. As a result, the oil relative permeability, k_{ro}, which is initially high, rapidly decreases as oil saturation behind the front decreases. The relative permeability to water, k_{rw}, starts low and begins to increase as water saturation increases. This displacement however is more efficient than the water-wet case as the water behind the front do not accumulate at the pore throat but remain at the centre of the pore space. Therefore, the trapping phenomenon encountered in the water-wet case is significantly reduced. As the pores become progressively filled with water, the oil begins to move out of the pores through high permeability channels; hence k_{ro} continues to speedily decrease. The k_{rw} increases as water breaks through to a producing well; however in contrast to the water-wet case, oil production continues for a long time, although the water cut increases (Abdallah, et al., 2007). Waterflooding experiments on mixed-wet (weakly water wet) cores have been shown to result in higher ultimate oil recovery in comparison to strongly water-wet core samples (Jadhunandan & Morrow, 1995).

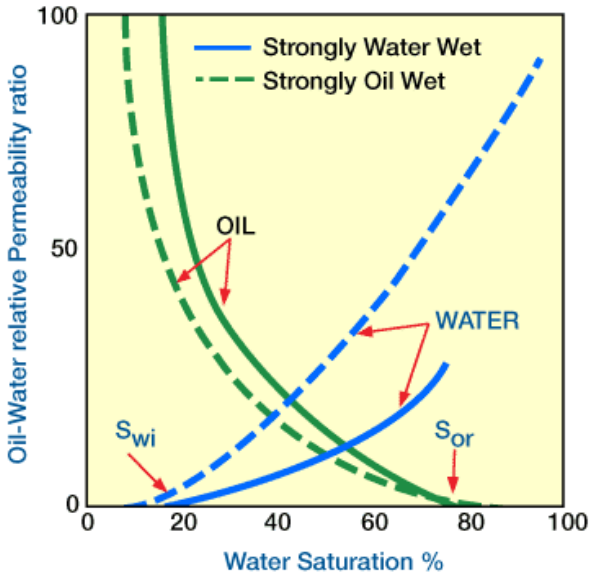

Figure 2.6: Relative permeability imbibition curves for oil-water systems (IPIMS, n.d.)

Some oil-wet reservoirs have been observed to be formed during the maturation process of a source rock in which organic carbon (kerogen) initially present in the pores is converted to oil

(Abdallah, et al., 2007). This is however a very rare phenomenon. On the other hand, some rock-types especially carbonates, although naturally water-wet, can become preferentially oil-wet. When oil first invades a water-filled pore during the drainage process, the solid surface is coated by a thick wetting film of water. When a critical capillary pressure is exceeded, the water films rupture resulting in direct contact of the crude oil with the pore wall. Surface active components of the crude, called asphaltenes, deposit on the rock surface, rendering it oil-wet (Al-Hadhrami & Blunt, 2000). Water injection through these formations results in early water breakthrough as the water speedily flows through high permeability pores/fractures; hence much of the oil remains trapped in the reservoir as shown in Figure 2.7.

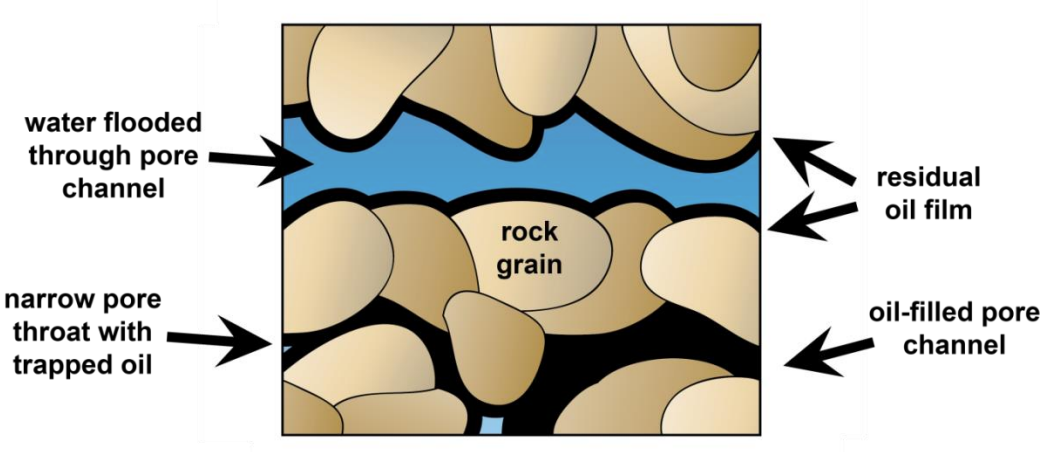

Figure 2.7: Oil-wet petroleum reservoir after water injection (Aurand, 2015)

After water breakthrough, little or no oil is produced since the capillary-affected oil in small pores and trapped oil in large pores would be immobile. Hence, k_{rw} increases speedily as water fills up the pore channels. The trapped oil remaining as residues after waterflooding in both water-wet and oil-wet reservoirs is the main target for most enhanced oil recovery methods.

2.2 Microbial Enhanced Oil Recovery (MEOR)

MEOR is a tertiary recovery process that generally entails the activation of either in-situ or injected microbes (mostly bacteria) in a reservoir that can be produced by waterflooding. The microorganisms in turn produce certain chemicals which serve as agents for mobilising residual oil. Microbial activation could be either by stimulation of indigenous microbes via nutrient injection into the reservoir (Brown, et al., 2000) or by direct injection of microbes and nutrients (Armstrong & Wildenschild, 2011). The first case would require initial

microbial analysis of the produced oil from the reservoir in order to discover the intrinsic microbes that are present within the fluid which could contribute to enhanced oil production. These microbes would then be cultured with different substrates (nutrients) in order to analyse the microbial growth and nutrient consumption. Suitable nutrients are then injected at optimal concentrations into the reservoir. In the latter case, microbes with inherent suitable properties for MEOR, which have been tested both experimentally and in the field, are injected into the reservoir together with specific nutrients that would enhance microbial growth in-situ (Jenneman, et al., 1984). In some cases, the by-products of microbial nutrient consumption called metabolites are initially separated from the microbe/substrate/metabolite solution at the surface and are thereafter injected into the reservoir (Al-Sulaimani, et al., 2012).

2.2.1 Microbes used in MEOR

Before any MEOR process is executed, it is very essential to carry out extensive analysis on the types of microorganisms that are suitable for improving the fluid and rock properties of the reservoir. Youssef et al., (2009) classified these microorganisms as either autochthonous or allochthonous. Generally, autochthonous microorganisms refer to those microbes that have been present in the oil reservoir after the deposition and accumulation process; hence they are termed indigenous. Allochthonous microorganisms are foreign (exogenous) or transient microbes that have been introduced into the reservoir in different ways. One way could be through contamination of the natural environment after drilling or during core sampling, especially in the near-wellbore region. Secondary recovery processes like waterflooding could be another way of introducing surface (exogenous) microbes as well as certain sulphates and oxides that could temporarily or permanently change the geochemical properties of the formation thereby altering the structure of the microbial community (Youssef et al., 2009).

Generally, oxygen levels in typical reservoirs are very low; therefore, indigenous microbes are mostly anaerobic or facultative. Aerobic microbes, which typically require the presence of oxygen to metabolise substrates, are usually exogenous in nature. Over the years, different classes of microbial species have been tried out in the recovery of residual oil aided by several microbe-induced mechanisms that favour increased sweep efficiency. Table 2.1 illustrates some types of species that have been proven to give acceptable results from experimental studies.

Table 2.1: Microbial species used in enhanced oil recovery **(Bryant & Burchfield, 1989)**

Scientific Name	Type of Metabolism	Products
Clostridium sp.	Anaerobic	Gases, acids, alcohols and surfactants
Bacillus sp.	Facultative	Acids and surfactants
Pseudomonas sp.	Aerobic	Surfactants and polymers; can degrade hydrocarbons
Xanthomonas sp.	Aerobic	Polymer
Leuconostoc sp.	Facultative	Polymer
Desulfovibrio sp.	Anaerobic	Gases and acids; sulphate-reducing
Arthrobacter sp.	Facultative	Surfactants and alcohols
Corynebacterium sp.	Aerobic	Surfactants
Enterobacter sp.	Facultative	Gases and acids

Products from biochemical reactions that occur during the metabolism process include; gases, acids, alcohols, biomass, surfactants and polymers (Bryant & Lockhart, 2002). These products are the active agents that enable the alteration of the fluid and rock properties of a formation which lead to better and more efficient residual oil displacement. Table 2.2 below gives a summary of the reaction products and their advantageous effects on the EOR process.

Table 2.2: Products derived from microbial metabolism and their effects for EOR **(Bryant & Lockhart, 2002)**

Product	Effect
Acids	Increase rock porosity and permeability Produce CO_2 through reaction with carbonate minerals
Biomass	Selective and nonselective plugging Emulsification through adhesion to oil Changing wettability of mineral surfaces Reduction of oil viscosity and pour point Desulphurization of oil
Gases	Reservoir repressurization Oil swelling Viscosity reduction Increased permeability caused by solubilisation of carbonates
Solvents (e.g. alcohol)	Dissolution of oil
Surfactants	Lowering interfacial tension Emulsification
Polymers	Mobility control Selective or nonselective plugging

2.2.2 Microbial EOR Displacement Mechanisms

2.2.2.1 Biogenic Gas Production

The anaerobic fermentation of sugars by microorganisms results in the formation of CO_2 and H_2 among other by-products like organic acids and polar solvents (Youssef et al., 2009). Therefore, when sugar-containing nutrients are used as substrates for indigenous or injected microbes, these gases are formed. Other gases like N_2 and CH_4 could be generated from other anaerobic processes that require nitrate reducing bacteria (NRB) and methanogens respectively. The presence of the biogenic gases results in reservoir pressurization. Additionally, gas dissolution into the oil could occur thereby reducing its dynamic viscosity. Kianipey & Donaldson (1986) reported CO_2 and N_2 production in MEOR experiments carried out on water-wet and oil-wet thin unconsolidated sandstone cells. Specifically, a species of *Bacillus licheniformis* was cultured in a solution majorly containing glucose, phosphates, sodium chloride, sulphates and nitrates. This solution was then injected into the cells and incubated at 37°C for 24 hours. The light gases introduced a third phase and resulted in an increase in oil mobility, thereby increasing recovery.

2.2.2.2 Plugging and Biofilm Production

Most reservoirs are heterogeneous in nature. As a result, flow characteristics typically defined by the permeability differ from layer to layer. Usually during waterflooding, since reservoir brine is more mobile than oil, water would tend to flow faster in regions of high permeability compared to oil. This leads to water channelling through the thief zones with very little amounts going through the low permeability zones. This eventually results into very low volumetric sweep of oil as water breakthrough is achieved much earlier. Introduction of certain microbes into a reservoir have been found to result in plugging of these thief zones.

Selective plugging of high permeability zones typically refers to the adsorption of microbes on the inner walls of the pores. This leads to a reduction in porosity as well as permeability. According to Zekri et al. (1999), plugging (or clogging as it is sometimes called) can be enhanced by either viable microbial cells or non-viable microbes (dead cells). In their laboratory tests, injection of thermophilic bacteria into limestone cores at residual oil saturation resulted in selective plugging by viable and non-viable bacteria. The viable bacteria have the ability to grow and adhere on the rock surface thereby forming a biofilm. This biofilm acts as a non-flowing phase that consists of immobile bacteria cells and/or some extracellular polymeric substances (EPS) that are heterogeneously distributed inside the

pores. Non-viable bacteria were found to act as particulates that clog fluid flow in the pores and ultimately reduce porosity.

Plugging has also been observed in field applications of MEOR (Gullapalli, et al., 2000; Brown, et al., 2000). Gullapali et al. (2000) carried out field tests in the Eunice Monument South Unit (EMSU) field, New Mexico. The field test started with the injection of a concentrated solution of bacterial spores for 16 days followed by water injection for 3 days to allow for spore clean-up in the near wellbore region. Afterwards, a highly concentrated nutrient solution was injected into the reservoir for 100 days. Normal waterflooding activities resumed after the MEOR treatment. Comparing the pre-treatment and post-treatment injection profiles confirmed that microbial growth during the nutrient injection period resulted in blocking of the thief zones, leading to the formation of a biofilm. This biofilm remained stable for more than 8 months after the MEOR treatment.

2.2.2.3 Interfacial Tension (IFT) Reduction

The interfacial tension between oil and water plays a major role in oil recovery by waterflooding. Many EOR processes aim at reducing the IFT in order to increase oil mobilisation within the pores. These processes require surface active agents called surfactants which have a hydrophilic (lipophobic) head and a hydrophobic (lipophilic) tail. As highlighted previously, microbial consumption of nutrients results in the formation of metabolites. These metabolites could be either biosurfactants or biopolymers. Biosurfactants are natural amphiphilic compounds that can reduce the oil-water IFT and also serve as oil emulsifiers during the MEOR process. Many laboratory tests have revealed that IFT reduction via biosurfactant production is a major mechanism for MEOR processes. These biosurfactants could be produced in-situ after nutrient injection into the reservoir (Wei, et al., 2013) or directly injected into the reservoir after surface separation from the microbial solution (Al-Sulaimani, et al., 2012).

Armstrong & Wildenschild (2011) carried out MEOR experiments using microbial solutions as flooding agents. In this study, active and inactive (non-viable) *Bacillus mojavensis* suspended in fresh nutrient and spent nutrient media respectively were injected in cores containing residual synthetic oil (soltrol 220). Results showed that reduction of IFT was highest when the core was flooded with inactive bacteria suspended in fresh media. This was suggested to be due to metabolic activities that resulted in the production of biosurfactants causing an IFT reduction from 54.3 mN/m to 8.7 mN/m.

Gudiña et al. (2012) isolated 58 bacterial strains from crude oil samples by enriching them with a Raymond mineral medium. The isolated strains were then suspended and grown in a mineral salt solution with a pH of 7.0. Only five of these strains (which were found to be *Bacillus subtilis*) produced extracellular biosurfactants under anaerobic conditions at 40°C. The best three strains reduced the IFT to around 30 mN/m compared to waterflooding values of 66.4 mN/m. Injection of these strains into a sand-packed column recovered between 19.8 and 35% of the trapped oil.

Direct injection of biosurfactant produced by a *Bacillus subtilis* strain was carried out by Al-Sulaimani et al. (2012). This resulted in recovery 23% of the residual oil after waterflooding. They also carried out experiments with a biosurfactant-chemical surfactant mixture in varying ratios. An optimal recovery of 50% of the residual oil was achieved with a 50-50 ratio of biosurfactant and chemical surfactant (ethoxylated sulphonates).

Hou et al. (2011) carried out microbial EOR field tests via 9 injectors and 24 producers in Block Chao 50 of the Chaoyanggou oilfield. In these tests, two bacterial strains – *Brevibacillus brevis* and *Bacillus cereus* were isolated from produced water and then injected together with carbon-rich nutrients as a solution into the reservoir. Results showed an average reduction in oil-water IFT from 46.3 mN/m to 39.8 mN/m due to the production of biosurfactants during microbial metabolism under reservoir conditions.

2.2.2.4 Biodegradation of Heavy Hydrocarbons

It is a generally-known fact that the viscosity of an organic compound is a direct function of its average molecular weight. Paraffinic hydrocarbons are mostly made up of short-chain (low molecular weight) and long chain (high molecular weight) alkanes; hence, higher amounts of long chain alkanes would lead to increase in viscosity. Biodegradation is a process that results in the conversion of long-chain hydrocarbons into short-chain hydrocarbons due to the aerobic or anaerobic metabolic action of microorganisms (Youssef et al., 2009). The mechanism of this process is quite unclear. However, Singer & Finnerty (1984) proposed the following ways in which bacteria may have direct and indirect interactions with crude oil resulting in physical and chemical degradation:

- Interaction of microbial cells with hydrocarbons dissolved in the aqueous phase
- Direct contact of microbial cells with hydrocarbon droplets much larger than the cells
- Interaction of microbial cells with solubilized, pseudo-solubilized or micro-emulsified hydrocarbons much smaller than the cells

Purwasena et al. (2010) have carried out laboratory tests entailing the use of an isolated bacteria strain, *petrotoga sp*. AR80, for the metabolic degradation of 33°API crude oil from the Yabase oilfield in Japan. They observed that most of the oil viscosity decrease occurred by selective degradation of heavier hydrocarbons during the exponential growth phase of the bacteria. The effect of salinity of the growth medium (nutrients and brine) and temperature were also investigated. Salinity reduction and temperature increase respectively resulted in higher degrees of viscosity reduction.

Asphaltenic crude oil samples taken from the Qinghai and Xingjiang oilfields in China have been incubated in a culture solution containing an effective mix of bacteria (*Bud bacillus*, *Bacillus brevis*, *pseudomonas* and *coccus*) and nutrients. This resulted in reduction of asphaltene and gum composition by values as high as 40% (Tingshan et al., 2005).

Several MEOR field tests have also been carried out in order to investigate the mechanism of biodegradation as it relates to oil viscosity reduction, oil mobilisation and additional recovery (Hou et al., 2011; Tingshan et al., 2005; Ghazali Abd. Karim et al., 2001). Tingshan et al. (2005) performed field scale microbial injection tests entailing oil mobilisation via biodegradation of heavy crude oil containing significant amount of asphaltene and gum. The average viscosity of crude oil from the two fields under investigation (the Qinghai and Xingjiang oilfields) decreased by about 15%. This resulted in additional recovery ranging from 8.53% to 35.72% from three wells in the Qinghai field. The average daily oil output from six wells in the Xingjiang oilfield increased from 2.39 ton to 14.196 ton after microbial treatment.

2.2.2.5 Increase in Water Viscosity by Biopolymer Production

Biopolymers are one of the other by-products (metabolites) derived from microbial metabolism. They basically find application in indirectly reducing water mobility by viscosity increment. Other applications like selective and non-selective plugging of high permeability channels have also been highlighted (Bryant & Lockhart, 2002).

Illias, et al. (1999) isolated certain thermophilic facultative bacteria strains from oil and water samples produced from Malaysian oil wells. The isolates were then cultured in enrichment media containing minerals salts, yeast extract and sucrose (the main carbon source). It was observed that the viscosity of culture solution of two bacteria strains (S13 and S17A) increased during the exponential growth phase as a result of biopolymer production that began just 4 hours into the incubation period. Viscosity increase from 1.01 cp to 3.763 cp (for

S13) and 3.62 cp (for S17A) were recorded at the end of this growth phase. Moving into the stationary phase, viscosity remained constant as biopolymer production ceased.

Sugai, et al. (1999) carried out laboratory MEOR tests using *Clostridium sp.* TU-15A isolated from reservoir brine of the China Jilin oilfield. The bacteria strain was first cultured in a synthetic solution containing molasses at a pH of 8.2. Maximum bacteria growth was attained in one day and viscosity increase of the culture, due to polymer production, started on second day. They discovered a linear relationship between the concentration of the molasses and viscosity of the medium despite the presence of other indigenous microorganisms. Flooding experiments carried out using two different sandpacks indicated an incremental recovery of 12% and 15% respectively after waterflooding.

2.2.2.6 Wettability Alteration

The mechanism of wettability alteration during microbial EOR processes is still quite unclear. This is due to its simultaneous occurrence with oil-water interfacial tension reduction. Another reason is that different microbes have different effects on rock wettability for various lithologies (sandstone and carbonates). Therefore, this phenomenon could be either advantageous or detrimental to the oil recovery process.

Laboratory MEOR experiments implemented by core flooding have shown changes in the wettability of sandstone cores from strongly water wet to less water wet (slightly water wet or mixed wet) characteristics (Kowalewski et al. 2006). Experiments with initially non-oil wetting (water-wet) carbonate rocks have indicated wettability alteration to more oil wetting conditions (Zekri et al., 2003; Rabiei et al., 2013). In some other cases, initially oil-wet carbonates have been found to be altered to water-wet states (Salehi, et al., 2006). In conjunction with IFT reduction, recovery of residual oil after waterflooding has been made possible by bacterial growth and biosurfactant production (Kowalewski, et al., 2005; Al-Sulaimani, et al., 2012). Wettability determination is usually done by contact angle measurements (Zekri, et al., 2003) and/or wettability index calculations (Kowalewski, et al. 2006; Al-Sulaimani, et al., 2012). Zekri, et al. (2003) suggested that wettability alteration is a function of some fluid and rock properties such as water salinity, microbial concentration, rock mineralogy, asphaltene concentration, sulphur content and reservoir temperature.

2.3 Review of Previous Works on MEOR Simulation

Most research on MEOR has been relatively focused on laboratory work and pilot testing due to the practical and physical approach taken to achieve desired results of incremental oil production. Modelling and simulation of microbial processes is quite an arduous task mostly because it entails converting complex qualitative data or phenomena into quantitative models. Chang et al. (1991) were finally able to develop a three-dimensional three-phase multiple-component homogeneous model that incorporates some of the complex physical, chemical and biological phenomena encountered during microbial EOR processes. The simulated data derived from these models were found to suitably match results from core flooding experiments and were able to account for phenomena such as diffusion, dispersion, clogging, chemotaxis, microbial growth and decay, and nutrient consumption (Bryant et al., 1992). Models for heterogeneous media have also been proposed (Khan et al., 2008). Yao et al., (2011) carried out field simulations on an existing block in the Sinopec Shengli oilfield after developing an optimized model that predicts microbial metabolism, microbial growth, component migration and changes in fluid properties.

Save for plugging/clogging aided by the biofilm effect, the aforementioned works have not been able to fully describe the mechanisms that are actually encountered during fluid displacement in microbial processes. The inherent complications and uncertainties in the prediction of these mechanisms and the limitation of conventional reservoir simulators have been major drawbacks. Very few authors have tried to describe some specific mechanisms like IFT reduction via biosurfactant production and water viscosity increase by biopolymer production using modified models (Nielsen, 2010; Behesht et al., 2008; Lacerda et al., 2012).

Bryant and Lockhart (2002) carried out a detailed analysis of microbial EOR from the perspective of reaction engineering due to the analogous nature of mainstream chemical EOR and MEOR mechanisms. This novel approach highlights important performance constraints that limit the field application of MEOR and have inadvertently not been put into proper perspective in previous studies. The analysis starts with a base case implementation of MEOR which assumes that the residual oil in the formation is the only carbon source for the microbes, and that the process will sequentially entail inoculation of injection wells with microbes, a shut-in period for incubation and waterflooding of the reservoir with a mixture of water and nutrients. In order to evaluate the feasibility of the base case, performance constraints were introduced into a microbial system represented by an isothermal plug flow

bioreactor. Results from this analysis have shown that in-situ biogenic gas production of CO_2 and CH_4 is not an effective mechanism for oil displacement. Another important outcome is that in-situ generation of biopolymers which increase water viscosity is intrinsically unstable especially in heterogeneous systems. Finally, it was recommended that future field tests should focus on increasing the volumetric sweep efficiency via plugging (permeability reduction due to biomass action) rather than the application of in-situ metabolic products which only affect the displacement efficiency.

Nielsen (2010) proposed a reactive transport model that incorporates the microbial processes of convection, bacterial growth, nutrient consumption and surfactant production. As a starting point, a one-dimensional model was initially developed for the purpose of describing two major mechanisms – fluid diversion (plugging) due to the formation of a biofilm and interfacial tension reduction attributable to surfactant production. The system comprises two flowing phases (oil and water) and a static phase (biofilm) with five components (oil, water, bacteria, nutrients and surfactant). The surfactant effect was accounted for by introducing a partitioning coefficient that controls the concentration of surfactant in both water and oil phases; which in turn affects the rate of oil mobilisation. Residual oil recovery due to surfactant formation was found to be a function of two variables: the distance from the inlet of the injector to the oil mobilisation point (the point at which the effect of the surfactant becomes significant), and the extent of IFT reduction due to surfactant action which results in the creation of an oil bank (a second waterfront). The effect of biofilm formation was accounted for by applying the Langmuir adsorption isotherm that describes the distribution of bacteria in both water and biofilm phases. Furthermore, multiple (two and three) dimensional models were created and simulated using both finite and streamline simulators to account for reservoir heterogeneity and the gravity effect (3-D only).

Amundsen (2015) replicated existing one dimensional flow models that describe the effects of the production of surfactants (Nielsen, 2010) and polymers (Lacerda et al., 2012) together with biofilm formation. These models were implemented with MRST – an open-source simulation package that has been developed as a toolbox for the purpose reservoir simulation studies that require creating new models and computational methods. The effects of IFT reduction via surfactant production and increase in water viscosity due to polymer production were compared to those derived from existing models. Although not quantitatively similar to previous works by Nielsen (2010) and Lacerda et al. (2012), the overall results qualitatively described the expected effects of these mechanisms on residual oil recovery. The models

were also tested with a simple two-dimensional heterogeneous system defined by a thief zone (high permeability channel). Results from the implementation of these models indicated that the biopolymer effect was the most efficient mechanism because it resulted in better volumetric sweep due to the reduction in water mobility.

Bültemeier et al (2014) are currently working on implementing MEOR in a commercial reservoir simulator (CMG-STARS) by developing models that incorporates chemical reaction kinetics (rather than basic Monod kinetics) in predicting the effects of polymers and surfactants for various bacteria-nutrient combinations.

3 Reservoir Modelling

In order to predict the performance of a subsurface reservoir, a model that describes its extent (size) and geometry together with the inherent rock and fluid properties is required. The prediction of this flow behaviour is based on a high degree of uncertainty in reservoir structure and geology. These uncertainties largely affect the results of reservoir simulation studies and they must be accounted for. The scope of this project is limited to modelling and simulation studies that seek to describe displacement mechanisms via deterministic modelling only; hence, uncertainty analysis will be ignored.

Ignoring flow within the wellbore to a surface facility, a petroleum reservoir model inherently comprises two major models:

- A geological (static) model that describes the geometry, grid-block size and spacing, rock and petrophysical properties of the formation.
- A dynamic (flow) model that describes the initial equilibrium distribution of fluids within the porous medium based on the fluid properties. It also considers the time-dependent flow of fluids generally expressed as a set of partial differential equations with appropriate boundary conditions that describe the conservation of mass/volume within the porous medium.

3.1 Geological (Static) Model

This model gives a dimensional, geological and petrophysical description of the reservoir. As proposed by Lie (2015), the model for this study will incorporate a macroscopic scale modelling approach that is based on a continuum hypothesis and the existence of representative elementary volumes (REV). The concept of REV is based on an averaging of petrophysical properties (like porosity and permeability) which are usually microscopic (pore scale) and heterogeneous in nature and representing them on a macroscopic scale that is independent of size. Therefore, as shown in Figure 3.1 for porosity, an REV size ranges from a lower bound, that describes the transition from a microscopic to a macroscopic scale, to an upper bound that defines the transition from a homogenous to a heterogeneous state (Al-Raoush & Papadopoulos, 2010). This concept finds its application when the principle of

conservation of mass within a defined control volume is utilised during dynamic (flow) analysis.

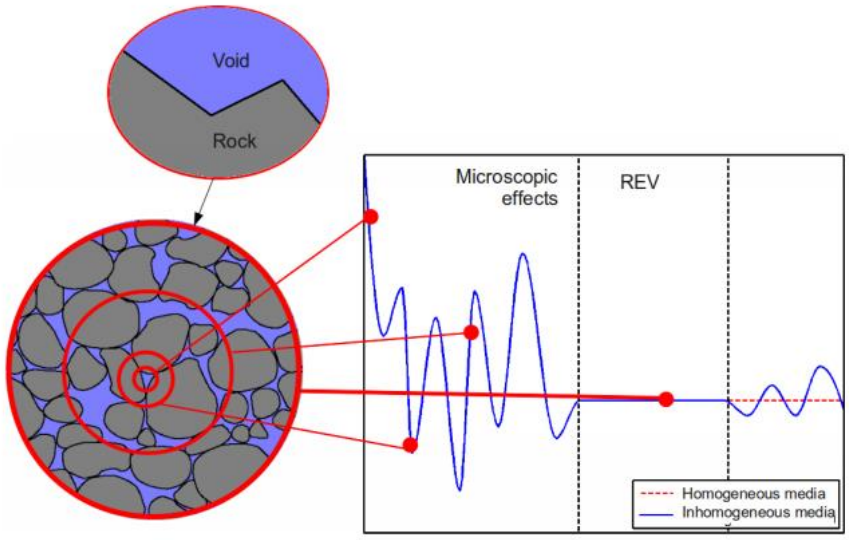

Figure 3.1: The concept of a representative elementary volume (REV) for expressing an idealized relationship between porosity on the y-axis and a measuring scale on the x-axis (Lie, 2015)

3.2 Dynamic (Flow) Model

This model incorporates equations that describe the flow of fluids within the porous medium. The rate and direction of flow is mostly affected by two major rock properties – porosity and permeability. These properties define the flow paths and the ease of fluid flow through these paths. Intrinsic fluid properties like viscosity and density which are functions of temperature and pressure also affect fluid flow. The simplest expression of multiphase fluid flow through a porous medium is given by Darcy's equation.

$$u_i = -\frac{\mathrm{K}k_{ri}}{\mu_i}.(\nabla p - \rho_i g \nabla z) \tag{3.1}$$

where u_i is the Darcy (macroscopic) flow velocity vector through the porous medium, K is the absolute permeability tensor of the formation, k_{ri} is the relative permeability with respect to a particular phase *i* (which is usually oil, water or gas), p refers to the pressure, ρ_i is the density of phase *i*, *g* is the acceleration due to gravity and *z* is the basis vector for the vertical axis. Darcy's law is valid for isothermal laminar flow with constant fluid properties.

As modest as it may be, Darcy's law alone does not adequately describe transient flow within a reservoir; hence for problems regarding transient flow – which is usually the case in hydrocarbon reservoirs – a complete governing equation is of utmost necessity (Zimmerman, 2003). This equation is premised on the law of conservation of mass applied to a control volume (in this case an REV). The following expression is derived when this law is applied to an REV characterised by multiple components and phases.

$$\frac{d}{dt}\left(\phi\sum_i c_{ji}\rho_i S_i\right)+\nabla.\left(\sum_i c_{ji}\rho_i u_i\right)=\sum_i c_{ji}q_i \tag{3.2}$$

Here, ϕ is the porosity, c_{ji} is the mass composition of component *j* in phase *i*, S_i is the volumetric fraction (saturation) of phase *i* and q_i is the phase source. The phase velocity u_i is computed as the Darcy velocity described in equation (3.1).

Equations (3.1) and (3.2) do not entirely make up the dynamic model. Other inputs such as the PVT model, phase equilibrium distribution, definition of fluid contacts etc. are required to create a complete model. For simple material balance calculations in reservoir models, the Black Oil (PVT) model is usually used to describe hydrocarbon components as a lumped species with the same properties at different temperatures and pressures. It represents hydrocarbons found in the reservoir in terms of two surface components – stock tank oil and surface gas – using PVT properties like the formation volume factor, *B* (the ratio of the volume occupied by bulk component *j* at reservoir conditions to the volume at surface conditions) and the solution gas-oil ratio, R_s (The ratio of surface volume occupied by dissolved gas to that occupied by oil).

A more robust approach is the compositional model which expresses the amounts of components in each phase by a mass or mole fraction and characterises the thermodynamic behaviour of the fluid by an equation of state. As a result, the compositional model can be applied directly to equation (3.2). Most basic reservoir simulators do not allow for compositional modelling due to its inherent computational demands; hence, it is mostly limited to surface separation of produced well streams where less and more precise calculations are required. Therefore, for the purpose of our analysis, the Black Oil approach will be taken. Equation (3.2) can then be written for a liquid phase, *i* and for gas as:

$$\begin{aligned}
&\frac{d}{dt}\left(\frac{\phi\rho_{s,i}}{B_i}S_i\right)+\nabla.\left(\frac{\rho_{s,i}}{B_i}u_i\right)=q_i \\
&\frac{d}{dt}\left(\frac{\phi\rho_{s,g}}{B_g}S_g+\frac{\phi R_{so}\rho_{s,g}}{B_o}S_o\right)+\nabla.\left(\frac{\rho_{s,g}}{B_g}u_g+\frac{R_{so}\rho_{s,g}}{B_o}u_o\right)=q_g
\end{aligned} \tag{3.3}$$

where, *i* refers to oil (*o*) or water (*w*) and *g* refers to gas.

For further simplification, the second expression in equation (3.3) will be neglected (no gas in solution at reservoir conditions) on the assumption of a strictly oil-water system that comprises one component in each phase (100% oil in oil phase and 100% water in water phase). The flux term q_i for both oil and water can also be expressed in terms of surface fluxes; $q_{s,i}=q_i.\rho_{s,i}$. Oil and water can be said to be slightly compressible; hence the density terms would be fairly constant. Therefore, we have the following set of equations for oil and water respectively:

$$\begin{aligned}
&\frac{d}{dt}\left(\frac{\phi}{B_o}S_o\right)+\nabla.\left(\frac{u_o}{B_o}\right)=q_{s,o} \\
&\frac{d}{dt}\left(\frac{\phi}{B_w}S_w\right)+\nabla.\left(\frac{u_w}{B_w}\right)=q_{s,w}
\end{aligned} \tag{3.4}$$

Equations (3.1) and (3.4) can then be combined, linearized, discretized and solved for pressure and saturation either implicitly or explicitly. The fully implicit method is most common due to its robust and unconditionally stable nature. Another important method is the Implicit Pressure, Explicit Saturation (IMPES) solution method. Here, the temporal and spatially discretized equations are solved for pressure and fluxes within each grid implicitly at a particular time step. Thereafter, these values are then updated and saturations are solved for explicitly.

4 MEOR Modelling

The MEOR model is based on a system that comprises two flowing phases (oil and water phase) and, as the case may be, a sessile biofilm phase. These phases are distinct and consist of different bulk components. Figure 4.1 shows the phase and component distribution of the MEOR model.

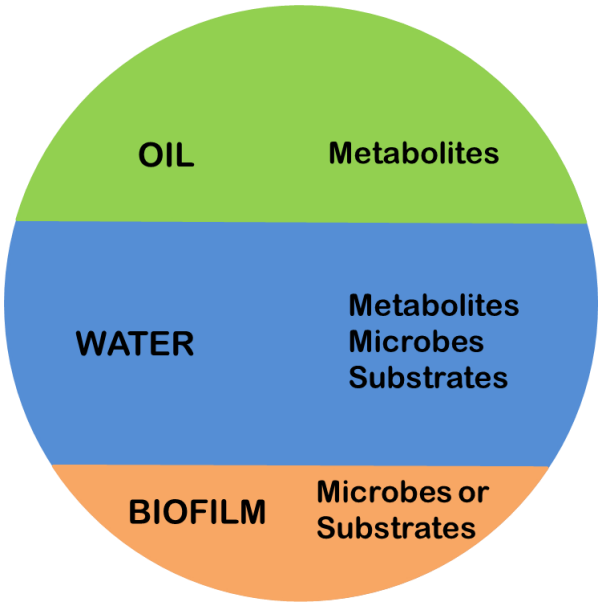

Figure 4.1: Distribution of components in each phase.

Here, the oil phase is initially composed of only oil, the water phase contains the microbes and substrates (nutrients), and the biofilm, when formed, can be composed of microbes or extracellular polymeric substances (EPS). Metabolites are produced in the water phase and can move into the oil phase over time. Since most microbial activities occur in the water phase, the reservoir model for the water phase described in the previous section will be revised in order to account for the additional components. The sub-models for the additional components will be discussed. An initial assumption is that the metabolite produced is a surfactant which is limited to the water phase and oil-water phase contact. However, as an extension of this, surfactant distribution between the oil and water phases would be incorporated for more robustness. The biofilm phase will also be initially described by bacteria adsorption and will be extended to food adsorption. EPS and metabolite adsorption will be ignored.

4.1 Microbe Modelling

When microbes are suspended in an aqueous medium in the presence of available nutrients one or both of the following occur: (a) microbial growth (b) metabolite production. For the purpose of this work, bacteria would be used to represent the term “microbes” due to their common application for MEOR purposes whether as anaerobic, aerobic or facultative microorganisms. Excluding bacteria death (decay), bacterial growth is divided into three sequential phases.

- The lag phase: The period where bacteria are freshly introduced into the nutrient-rich medium and adapt to the environment. It is characterised by no or minimal bacterial growth.
- The exponential growth phase: Cell division occurs at an exponential (logarithmic) rate and the bacteria population increases based on their genetic potential, the availability of nutrients and environmental conditions.
- The stationary phase: This occurs when cell division ceases or the rate of cell division is equal to the rate of cell death; hence, maximum population density of viable bacteria is attained. This could be due to nutrient depletion and/or changes in environmental conditions.

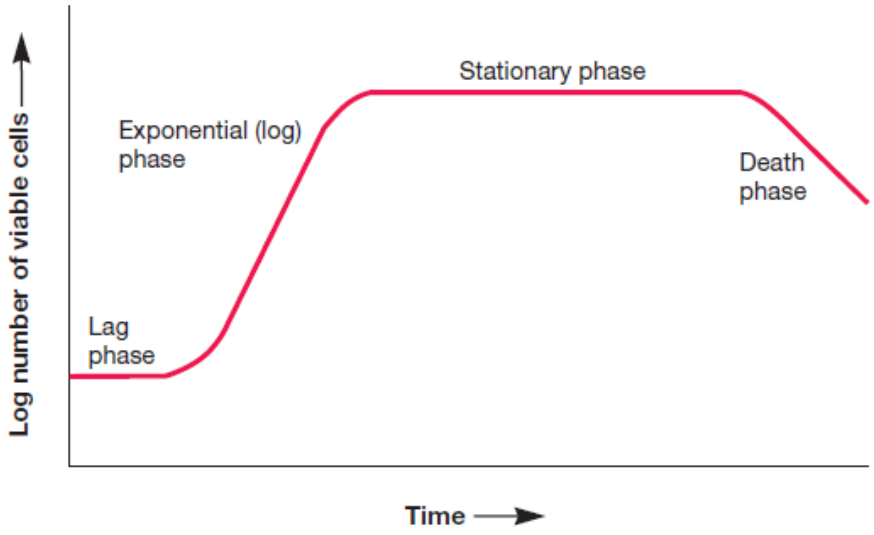

Figure 4.2: A Typical growth rate curve of a microbial system showing the sequential phases (Willey et al. 2008)

4.1.1 Microbial Feeding Process

Microbes generally feed on a consortium of substrates that are necessary for their survival in a particular habitat. These substrates range from inorganic compounds like sulphates and nitrates to organic compounds like aromatic hydrocarbons and carboxylic acids (Wolicka & Borkowski, 2012). Microbes found in or injected into crude oil require a combination of these nutrients for growth and metabolism. Figure 4.3 displays a pictorial illustration of the feeding mechanism within an oil reservoir. From the figure, it can be observed that when bacteria and nutrients are injected into the water phase of a reservoir in surface contact with an oil phase, they initially occupy the water phase where they can derive some essential nutrients, such as dissolved oxygen and nitrates (Youssef et al., 2009), required for their metabolic activities. These metabolic activities involve conversion of available nutrients into metabolites (e.g. surfactants). Metabolites in the form of surfactants have the potential to reduce the interfacial tension (IFT) between the oil and water phase. However before this can occur, a threshold surfactant concentration must be attained within the system. This could be delayed if surfactants prefer to be in the oil phase rather than in the water phase. Once this concentration is reached, the IFT between oil and water is reduced resulting in one of the following occurrences:

I. Some oil droplets may move into the water phase. The hydrocarbons contained in the oil would then be harnessed by the bacteria for feeding purposes and growth.
II. Some bacteria will move directly into the oil-water interface to get their carbon feeding requirements.
III. An oil-water emulsion could be formed such that oil globules are suspended in water. This third pseudo-phase would characteristically contain oil; hence, bacteria can move into the emulsion phase and feed on hydrocarbons in oil.

It is important to emphasize here that microbes do not have control over the metabolites they produce. Thus, the metabolite produced by one bacteria cell may take part in reducing the IFT and the released oil could be harnessed by another cell for growth.

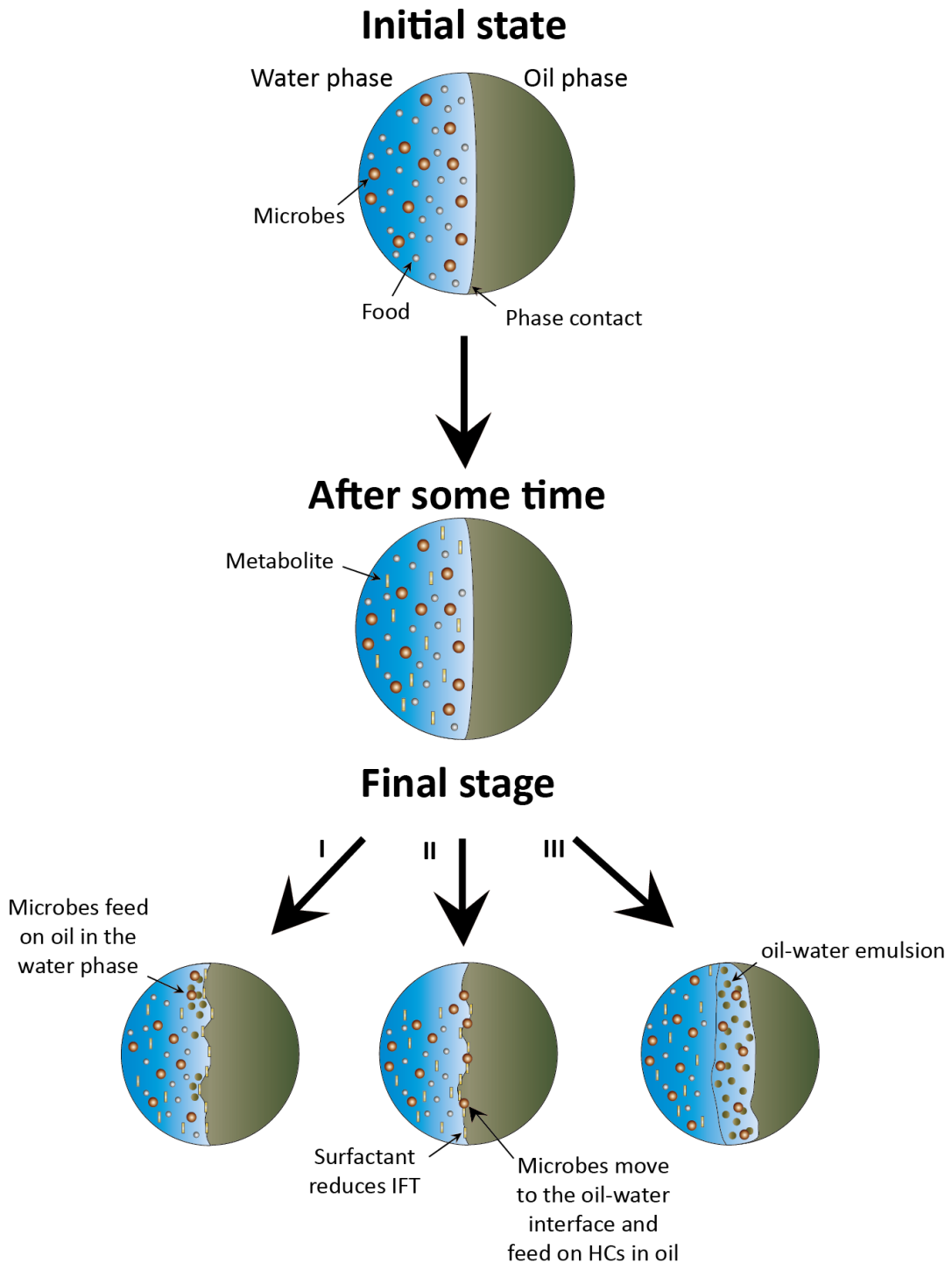

Figure 4.3: The sequential stages of microbial feeding showing nutrient consumption, metabolite production, IFT reduction and the possible resulting effects I, II and III.

4.1.2 Model definition

Several models that mathematically describe the kinetics of microbial growth have been in use for many years. Many of these models assume that nutrient ingestion and cellular growth occur consecutively. One of such models is the simplistic Monod's equation which is based on Michaelis-Menten kinetics. This model assumes that growth is mainly restricted by a

single growth limiting nutrient while other nutrients are in excess. It also describes a system where a breakeven nutrient concentration is required for cellular reproduction to commence and thereafter, bacteria concentration increases and approaches a maximum (steady) rate. According to (Tang & Wolkowicz, 1992) these breakeven concentrations depend directly on the nutrient dilution rate. Monod's equation can therefore be described by the following expression.

$$\mu_b = \mu_{b,\max} \cdot \frac{C_{nw}}{K_{bn} + C_{nw}} \tag{4.1}$$

where, μ_b is the specific growth rate of the bacteria species, $\mu_{b,\max}$ is the maximum specific growth rate, C_{nw} is the nutrient mass concentration in the water phase and K_{bn} is the half-saturation constant which is defined as the nutrient concentration at $\mu = 0.5\mu_{\max}$.

This same expression with a slight modification can be used to describe the second aforementioned phenomenon – metabolite production. According to Zhang et al. (1992), Larceda et al. (2012) and Amundsen (2015), the model can be expressed as

$$\mu_m = \mu_{m,\max} \cdot \frac{C_{nw} - C_{n,crit}}{K_{mn} + C_{nw} - C_{n,crit}} \tag{4.2}$$

Here, μ_m is the metabolite production rate, $\mu_{m,\max}$ is maximum metabolite specific production rate, $C_{n,crit}$ is the critical nutrient mass concentration (the minimum nutrient concentration required for metabolite production), and K_{mn} is the half saturation constant for metabolite production.

The biochemical reactions that take place during microbial growth and metabolite production are shown in equation (4.3) and can be assumed to follow first order kinetics. Hence, the reaction rates are direct functions of nutrient concentration.

$$\begin{aligned} nutrients &\xrightarrow{bacteria} bacteria \\ nutrients &\xrightarrow{bacteria} metabolites \end{aligned} \tag{4.3}$$

Therefore, the rate equation for bacteria growth and metabolite production respectively can be expressed as:

$$\begin{aligned} R_b &= \kappa_b C_{nw} \\ R_m &= \kappa_m C_{nw} \end{aligned} \tag{4.4}$$

where, R_b & R_m are the reaction terms for bacteria growth and metabolite production respectively, and κ_b & κ_m are the reaction rate constants for bacteria growth and metabolite production respectively.

This follows that the rate of nutrient consumption will be

$$R_n = -\kappa_b C_{nw} - \kappa_m C_{nw} \tag{4.5}$$

The reactions rate constants, κ for both equations are equivalent to the specific growth rates, μ that have been discussed previously. In order to account for the amount of nutrients ingested by the cells for the two reactions, a yield coefficient, Y is applied. This coefficient represents the fraction of the nutrient concentration that has been converted by the bacteria cells to either produce more cells or generate metabolic products. It then follows that the sum of all yield coefficients should be equal to 1. Thus, by applying these new definitions, equations (4.4) and (4.5) can be revised as follows

$$\begin{aligned} R_b &= \mu_b Y_b C_b \\ R_m &= \mu_m Y_m C_b \\ R_n &= -\mu_b Y_b C_b - \mu_m Y_m C_b = -R_b - R_m \\ Y_b &+ Y_m = 1.0 \end{aligned} \tag{4.6}$$

Here, Y_b & Y_m represent the bacteria and metabolite yield coefficients respectively, and C_b is the bacteria concentration in any phase.

For the more practical case of bacteria and nutrient injection into a reservoir with a significant population of indigenous bacteria species, the growth of all bacteria species in competition for the same limiting nutrient will depend on their relative breakeven concentrations. Therefore, only the species with the lowest value of this parameter have a greater chance of thriving (Tang et al., 1992). The models for this type of system will be discussed in Section 4.4.

4.1.3 Dynamic MEOR Model

In order to create a dynamic flow model for microbial EOR systems, component mass balances have to be made for each of the five bulk components which have been highlighted previously. These equations will be based on the mass conservation approach described in equation (3.4). The oil and water equations will remain as defined previously.

4.1.3.1 Bacteria Model

The mass balance equation for bacteria would account for bacteria species that exist both in the flowing water phase and in the sessile biofilm phase. Hence, a total bacteria concentration term C_b is assumed at this stage and is introduced into the original equation for water.

$$\frac{d}{dt}\left(\frac{\phi C_b}{B_w}S_w\right)+\nabla.\left(\frac{C_b}{B_w}u_w\right)=q_{s,b}+R_b \tag{4.7}$$

where, C_b is the total bacteria concentration, $q_{s,b}$ is the bacteria source term (flux) and R_b is the bacteria growth reaction term. Other parameters remain the same.

4.1.3.2 Metabolite Model

Metabolites are can exist in both water and oil phases. For the purpose of this study, the metabolites will be restricted to surfactants only. These surfactants exist mostly in the water phase and at the oil-water phase contact. Surfactants in the oil phase are generally regarded as being ineffective and are not included in the flow equation; nevertheless, the partitioning of surfactants between each phase will be discussed in Section 4.2. Surfactant injection will not be considered (no metabolite flux term). Adsorption of surfactants to the pore walls will also not be treated in this study. Putting all these conditions and considerations into perspective, the mass balance equation for this component will be as follows

$$\frac{d}{dt}\left(\frac{\phi C_{mw}}{B_w}S_w\right)+\nabla.\left(\frac{C_{mw}}{B_w}u_w\right)=R_m \tag{4.8}$$

where, C_{mw} is the metabolite (surfactant) concentration in the water phase and R_m is the metabolite reaction term.

4.1.3.3 Nutrient Model

The nutrients are supplied to the system via the water phase and are assumed to remain in this phase throughout the production period. For now, we will assume that nutrient adsorption to the pore walls is insignificant (i.e. $C_{nw} = C_n$). Therefore, the following equation applies

$$\frac{d}{dt}\left(\frac{\phi C_n}{B_w} S_w\right) + \nabla.\left(\frac{C_n}{B_w} u_w\right) = q_{s,n} + R_n \tag{4.9}$$

where, C_n is the nutrient concentration, $q_{s,b}$ is the nutrient source term (flux) and R_n is the nutrient depletion reaction term.

4.2 Metabolite (Surfactant) Modelling

Surfactants, also called biosurfactants as in the case of MEOR, are generally amphiphilic (lipophilic – hydrophilic) compounds with chemical properties that enable reduction of oil-water interfacial tension (IFT) and also serve as oil emulsifiers during the MEOR process. The surfactant flow model introduced in the previous section is based on the premise that surfactants found in the oil phase do not take part in the process of reducing the IFT. Although this notion is valid, it is also necessary to account for these ineffective surfactants in the MEOR model. This novel approach was proposed by Nielsen (2010). Essentially, it involves the partitioning of surfactants by defining a distribution coefficient D_i that describes the relationship between surfactant concentration within each phase and the mass concentrations of oil and water. This was revised by Amundsen (2015) to include fluid saturations and is represented by the following mathematical expression:

$$\frac{C_{mw}}{C_{mo}} = D_i \frac{\rho_w S_w}{\rho_o S_o} \tag{4.10}$$

where, C_{mw} & C_{mo} is the mass concentration of surfactants in the water phase and oil phase respectively.

From the expression for total surfactant concentration in the system represented as $C_m = C_{mw} + C_{mo}$, Amundsen (2015) derived the concentration of surfactants in the water phase (which are the major components that reduce IFT) as follows:

$$C_{mw} = \frac{C_m D_i \frac{\rho_w S_w}{\rho_o S_o}}{1 + \left(D_i \frac{\rho_w S_w}{\rho_o S_o} \right)} \tag{4.11}$$

This expression reveals that for lower values of D_i more surfactants are will preferably occupy the oil phase. However, for larger values of D_i (i.e. as $D_i \rightarrow \infty$), surfactants will typically occupy the water phase ($C_{mw} \approx C_m$) and would be readily available for IFT reduction. Therefore, the initial assumption of this study is that the distribution coefficient is large enough so that the surfactant oil phase concentration is negligible.

It has been observed that IFT reduction begins to occur after a threshold surfactant concentration has been attained. Thereafter, an increase in surfactant concentration by one order of magnitude would result in drastic reduction in IFT by several orders of magnitude. Thereafter, increasing surfactant concentration will have very little or no effect on IFT. From the example illustrated by Nielsen (2010) in the Figure 4.4, this threshold surfactant concentration is between 10^{-5} and 10^{-4} kg/m^3.

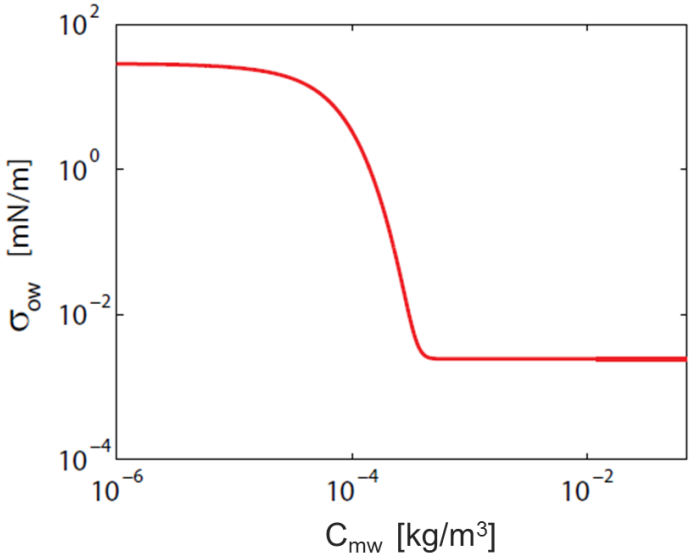

Figure 4.4: The relationship between surfactant concentration and IFT reduction showing the necessary requirement for IFT reduction – attaining a threshold surfactant concentration **(Nielsen, 2010)**

From this curve, an empirical correlation relating the decrease in IFT to surfactant concentration is expressed by the following equation:

$$\sigma_{ow}^{*} = \sigma_{ow} . \frac{-\tanh(l_3 C_{mw} - l_2) + 1 + l_1}{-\tanh(-l_2) + 1 + l_1} \tag{4.12}$$

Here, σ^{*}_{ow} & σ_{ow} are the new IFT and initial IFT respectively, and l_1, l_2 & l_3 are constants that determine the threshold concentration and the extent/limit of IFT reduction.

4.2.1 Effect on Oil-Water Relative Permeability

The reduction in oil-water IFT caused by the action of surfactants directly affects the relative permeability versus fluid saturation distribution. Three major effects have been observed to occur when this happens. The first is the reduction of the residual oil saturation (S_{or}) because initially immovable capillary-trapped oil becomes mobile. Another effect is a change in the end-point relative permeability (mostly water relative permeability) to favour lower water mobility at higher water saturations. Lastly, IFT reduction would change the shape and position of the curves rendering them less curved and shifting them mostly to the right.

In order to account for these effects in the relative permeability model, Nielsen (2010) discussed three approaches:

- Capillary number method
- Interpolation of relative permeabilities using Coats' correlation
- Interpolation of relative permeabilities using the Corey correlation

The various oil-water relative permeability curves derived from these methods are illustrated by the following plots:

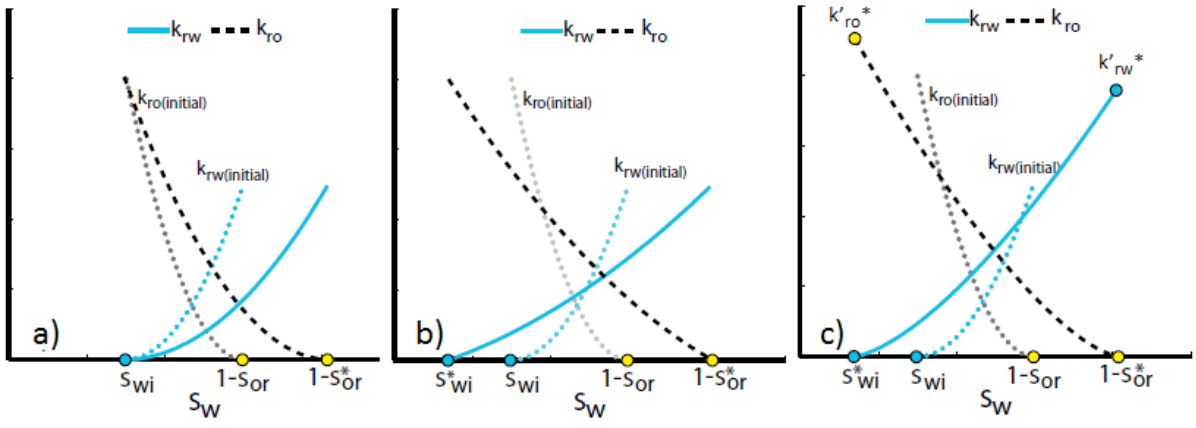

Figure 4.5: Relative permeability plots showing the possible changes in S_{or} and S_{wi} as well as the end-point relative permeabilities (a) represents the result from the Capillary Number method (b) is derived from Coats' method, and (c) is the curve generated by applying Corey's interpolation method (Nielsen, 2010)

The first plot (a) is derived from applying the capillary number method to determine a new S_{or} and then using equations (2.6) to (2.9) to generate the curves. It can be observed that the endpoint relative permeabilities for both oil and water (k_{rw} and k_{ro}) remain unchanged despite

the reduction in S_{or}; hence, the curves only stretch along the water saturation axis to the right. The second plot (b) representing the application of Coats' interpolation method results in not only a new S_{or} but also a modified initial water saturation (S_{wi}); nevertheless, the endpoint k_{rw} and k_{ro} do not change. The third plot (c) depicting the curves derived from interpolation of parameters in the Corey correlation. The curves generated by applying this approach are more straightened and span broader on the water saturation axis due to the decrease in both S_{or} and S_{wi} similar to the Coats' approach. However, the major difference is that the endpoint k_{rw} and k_{ro} are modified and assume a new (usually higher) value.

Amundsen (2015) recommends that the Corey approach best describes the change in relative permeability curves expected in physical systems. This change is characterised by an improvement on (basically an increase in) the relative permeabilities at all water saturations as compared to the base case. Coats' approach does not account for this as there are regions where decrease in relative permeabilities is encountered (typically at low water saturation for k_{ro} and at high water saturation for k_{rw}). The capillary number method is not also considered because of its limitation in only modifying the residual oil saturation. The relative permeability model derived from the Corey interpolation method for an oil-water system will now be described.

First, the interpolation function from Coats' approach is used. It is expressed as:

$$f(\sigma_{ow}^{*}) = \left(\frac{\sigma_{ow}^{*}}{\sigma_{ow}} \right)^{\frac{1}{n}} \tag{4.13}$$

where, $f(\sigma_{ow}^{*})$ is Coats' interpolation function which ranges from 1 at maximum IFT to 0 at minimum IFT, n is an adjustable exponent that ranges from 4 to 10 and is used for relative permeability curve fitting of experimental data.

To account for the change in endpoint saturations, modified initial water and residual oil saturations (S_{wi}^{*} and S_{or}^{*}) are defined and expressed by the following equations:

$$\begin{aligned} S_{wi}^{*} &= f(\sigma_{ow}^{*}) \cdot S_{wi} \\ S_{or}^{*} &= f(\sigma_{ow}^{*}) \cdot S_{or} \end{aligned} \tag{4.14}$$

Modified endpoint oil and water relative permeabilities ($k_{ro}'^{*}$ and $k_{rw}'^{*}$) are also defined and characterised by the following equations:

$$k_{ro}'^{*} = f(\sigma_{ow}^{*}) \cdot k_{ro}' + \left(1 - f(\sigma_{ow}^{*})\right) \tag{4.15}$$

$$k_{rw}'^{*} = f(\sigma_{ow}^{*}) \cdot k_{rw}' + \left(1 - f(\sigma_{ow}^{*})\right) \tag{4.16}$$

The Corey exponents for oil and water (N_o and N_w) described in Subsection (2.1.3) as part of the Corey correlation in equations (2.6) and (2.7) are also revised to account for the IFT change. The new exponents which would be generally lower in value compared to the base case (because the system approaches full miscibility) are defined by the following relation:

$$\begin{aligned} N_o^{*} &= f(\sigma_{ow}^{*}) \cdot N_o + \left(1 - f(\sigma_{ow}^{*})\right) \\ N_w^{*} &= f(\sigma_{ow}^{*}) \cdot N_w + \left(1 - f(\sigma_{ow}^{*})\right) \end{aligned} \tag{4.17}$$

Finally, equations (2.6) to (2.9) can then be applied with the modified exponents, endpoint saturations and endpoint relative permeabilites to generate the new relative permeability curves that account for the effect of IFT reduction via surfactant action.

4.2.2 Effect on Water Saturation Profile

The biosurfactants have been known to have the capacity to reduce oil-water IFT and thus mobilise more capillary-trapped oil. This causes a change in the water saturation profile during oil displacement by water. Figure 4.6 exemplifies and compares a typical saturation plot for normal waterflooding and one generated by the action of these biosurfactants. The MEOR curve (generated from results in Section 6.5.2) resembles a typical curve generated for viscous water flooding (Green & Willhite, 1998). In the viscous water flooding case, water mobility is reduced by increasing its viscosity in order to displace more oil whereas in the case of MEOR through biosurfactant action trapped oil is mobilised and displaced by water. In the MEOR curve, there is an existence of a second water front behind the primary water front. Thus, water breakthrough occurs twice and with lower impact on oil production. The second water front therefore allows for the creation of an oil bank. Part of this oil bank represents the capillary-trapped oil that has been released and mobilised by the IFT reduction effect of the surfactants. Oil production will also be more efficient with the effective combination of the two fronts. This is because the saturation at the primary water front S_{f1} is lower than that of the waterflooding front S_{fw}. Therefore, after primary water breakthrough, the water saturation behind the front will be just slightly higher than the irreducible water saturation S_{wi}. Thus water production after primary breakthrough will be limited to this

saturation and does not increase until the time of secondary breakthrough; hence less water is produced alongside the oil bank. Figure 4.6 also shows that IFT reduction reduces S_{or} to S^*_{or}; therefore at the end of microbial flooding, the system will settle at this new residual oil saturation.

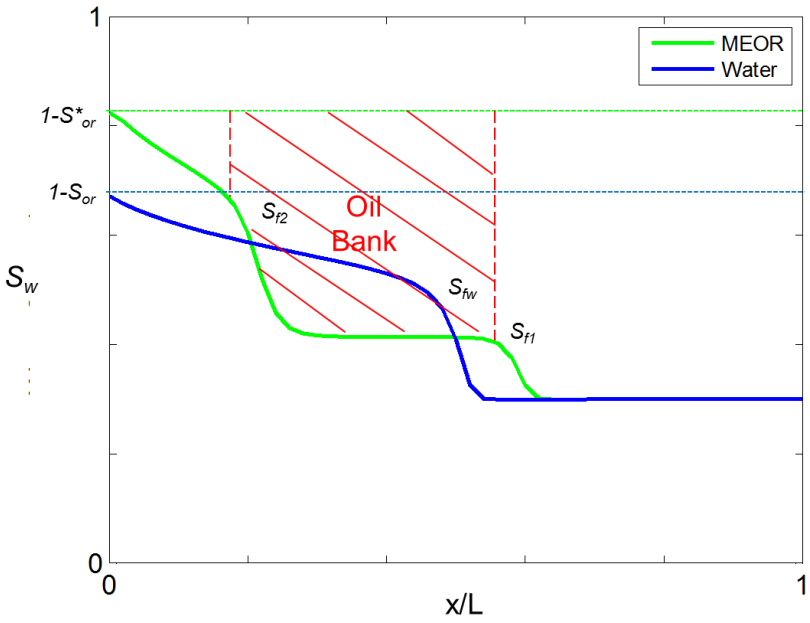

Figure 4.6: The saturation profiles for ordinary waterflooding and MEOR with surfactant effect showing the oil bank, the double water fronts and the change in residual oil saturation

4.3 Biofilm Modelling

The formation of a biofilm is usually preceded by the adsorption of bacteria, metabolites or nutrients on the pore walls. These components, which initially occupy the water phase, adhere to the rock surface and eventually cause a reduction in the pore space available for fluid flow. Therefore, two major flow parameters are affected by this phenomenon – porosity and permeability. Although, the scope of this study will cover both bacteria and food (nutrient) adsorption, the theory behind both mechanisms is the same. Thus, a generic model will be developed and then modified for each adsorption case.

Component adsorption on pore walls will be modelled by assuming equilibrium adsorption such that there is an instant partitioning between the water and biofilm phase at the commencement of adsorption. For the case of bacteria adsorption, it is assumed that the sessile bacteria continue feeding on the nutrients and grow; however, new cells are assumed to be produced into the water phase. Equilibrium adsorption will be described by Langmuir-

type isotherms based on a single layer of adsorbing components and on the assumption that water as a bulk component is absent in the biofilm phase (Nielsen, 2010). Taking all these into account, the mass of adsorbed component per unit surface area, χ_j can now be expressed as:

$$\chi_j = \frac{\omega_1 \omega_2 C_{jw}}{1 + \omega_2 C_{jw}} \tag{4.18}$$

where, ω_1 and ω_2 are Langmuir constants, C_{jw} is the water phase concentration of component *j*. The constant ω_1 has dimensions of mass per unit area and it determines the maximum adsorption level while ω_2 has dimensions of specific volume (volume per mass) determines the rate of adsorption (Amundsen, 2015). It is important to note here that Nielsen (2010) only specified ω_1 and not the product $\omega_1\ \omega_2$ in the numerator of equation (4.19). This is because ω_1 was expressed in dimensions of length as against mass per unit area.

The parameter χ_j will then be used to calculate the mass concentration of the component adsorbed on the pore walls. The amount of the adsorbed component will heavily depend on the surface area available for adsorption. This is expressed in form of specific surface area $\tilde{A}_s$, (area per pore volume) and is usually within the range of 10^5 to 10^6 m^2/m^3 of total volume. Therefore, the effective surface area available for adsorption, A_s in m^2/m^3 PV is expressed as:

$$A_s = \frac{\tilde{A}_s}{\phi} S_w \tag{4.19}$$

Therefore, the mass concentration of the adsorbed component *j* in the biofilm phase *b* expressed in kg/m^3 PV will be:

$$C_{jb} = A_s \chi \tag{4.20}$$

This fraction of the pore volume occupied by the adsorbed component which is represented by the biofilm partition is a function of the mass concentration and the density of the biofilm given by the following relation:

$$\psi = \frac{C_{jb}}{\rho_b} \tag{4.21}$$

Combining equations (4.19), (4.20) and (4.21) in order to express the concentration of the adsorbed component in the biofilm phase as a function of the flowing (water) phase concentration, the following equation is derived.

$$C_{jb} = \psi\rho_b = \left(\frac{\tilde{A}_s}{\phi} S_w\right)\frac{\omega_1\omega_2 C_{jw}}{1+\omega_2 C_{jw}} \tag{4.22}$$

As mentioned previously the formation of biofilm within the pore space will cause a reduction in porosity and permeability. The new effective porosity, ϕ^* which describes the pore space available for fluid flow will now be defined as:

$$\phi^* = \phi(1-\psi) \tag{4.23}$$

The permeability change can be approached from the perspective of absolute permeability and relative permeability; however, since we have a multiphase system, the appropriate approach will be the latter. It is also important to state here that the change in relative permeability only affects the water relative permeability because the adsorbed components are assumed to initially exist only in the water phase. This modification can be empirically described by the following version of the Kozeny-Carman relation:

$$\frac{k_{rw}^*}{k_{rw}} = \left(\frac{\phi^*}{\phi}\right)^{\gamma} \tag{4.24}$$

where, k_{rw}^* is the modified water relative permeability, γ is an exponent that lies between 2 and 5. The relation ϕ^*/ϕ is termed the relative porosity change, ϕ_{rel}.

Thullner (2010) discussed the different relations used to describe the relative permeability modification all based on the Kozeny-Carman relation. From these relations, the formula proposed by Clement et al., (1996) was chosen due to its simple approach appropriate for this study. It followed a macroscopic approach and assumes that the adsorbed components preferentially plug larger pores. It also assumes that the biofilm growth is invariant to the pore size distribution but only affects the maximum pore radius. This relation is expressed as:

$$\begin{aligned} k_{rw}^* &= k_{rw}\left(\phi_{rel}\right)^{19/6} \\ k_{rw}^* &= k_{rw}\left(1-\psi\right)^{19/6} \end{aligned} \tag{4.25}$$

Finally, the same expressions in the microbe model in Section 4.1 will require some modification in order to accommodate the effect of biofilm formation. Thus, for the case of bacteria adsorption, the bacteria flow equation (equation (4.7)) will be modified to account for only free bacteria in the water phase.

$$\frac{d}{dt}\left(\frac{\phi C_{bw}}{B_w}S_w\right)+\nabla.\left(\frac{C_{bw}}{B_w}u_w\right)=q_{s,b}+R_b \tag{4.26}$$

where, C_{bw} refers to the mass concentration of bacteria in the water phase.

The reaction terms defined in equation (4.6) and the mass of adsorbed bacteria per unit χ_b surface area will also be modified accordingly:

$$\begin{aligned}
R_b &= \mu_b Y_b\left(C_{bw}+C_{bb}\right)\\
R_m &= \mu_m Y_m\left(C_{bw}+C_{bb}\right)\\
R_n &= -\mu_b Y_b\left(C_{bw}+C_{bb}\right)-\mu_m Y_m\left(C_{bw}+C_{bb}\right)\\
\chi_b &= \frac{\omega_1\omega_2 C_{bw}}{1+\omega_2 C_{bw}}=\frac{\omega_1\omega_2(C_b-C_{bb})}{1+\omega_2(C_b-C_{bb})}
\end{aligned} \tag{4.27}$$

where, C_{bb} is the bacteria mass concentration in the biofilm phase.

Therefore, the mass conservation equation for the adsorbed bacteria will then be:

$$\frac{d}{dt}\left(\frac{\phi C_{bb}}{B_w}S_w\right)=\chi_b A_s S_w\phi \tag{4.28}$$

For the case of food adsorption, the nutrient flow equation (equation (4.8)) will be revised as follows:

$$\frac{d}{dt}\left(\frac{\phi C_{nw}}{B_w}S_w\right)+\nabla.\left(\frac{C_{nw}}{B_w}u_w\right)=q_{s,n}+R_n \tag{4.29}$$

where, C_{nw} refers to the mass concentration of nutrients in the water phase. All reaction terms remain the same as defined in equation (4.6) and the mass of nutrients adsorbed per unit surface area χ_n will be expressed as:

$$\chi_n=\frac{\omega_1\omega_2 C_{nw}}{1+\omega_2 C_{nw}}=\frac{\omega_1\omega_2(C_n-C_{nb})}{1+\omega_2(C_n-C_{nb})} \tag{4.30}$$

Finally, the mass conservation equation for the adsorbed nutrients is derived as:

$$\frac{d}{dt}\left(\frac{\phi C_{nb}}{B_w} S_w\right) = \chi_n A_s S_w \phi \tag{4.31}$$

Where, C_{nb} is the mass concentration of adsorbed nutrients.

4.4 Microbial Competition Modelling

It is a well-known notion that some reservoirs harbour resident indigenous microbes which derive their feeding requirements from the reservoir environment and alter the chemical properties of the reservoir oil (Youssef et al., 2009). By injecting new microbes via MEOR into the reservoir, a change in the existential balance of the indigenous microbial system occurs and microbial competition will become significant. From the perspective of enhanced oil recovery, the presence of these indigenous microbes will affect the performance of the MEOR process in one way or another. This aspect of MEOR modelling is seldom studied and available literature specific to this process is quite rare. Delshad et al. (2002) proposed a model for implementing MEOR with several microbial species in UTCHEM; however, the model did not account for microbial competition because a high concentration of nutrients was assumed. Nonetheless, from a microbiological standpoint, models can be created for microbial competition within a chemostat (Tang et al., 1992; Ballyk, et al., 2001; Pavlou, 2006). A chemostat is a type of bioreactor that is characterised by a continuous supply of feed, allows for sufficient mixing of feed components and ensures a constant reactor volume via an effluent stream containing unused nutrients, metabolites and microbes. Therefore, a chemostat can be said to be a special type of continuous stirred-tank reactor (CSTR). Models for microbial competition for a system described as a plug flow reactor have also been created (Ballyk et al., 2001; Wang, 2010). Plug flow reactors are more representative of the conditions within an ideal reservoir such that there is no mixing or backflow of components. However, these reactors can be characterised by adsorption of components on the pore walls especially at low flow rates (Ballyk et al., 2001). For the case of simplicity and understanding of displacement mechanisms, the chemostat model will be applied. This model assumes that there is rapid diffusion of nutrients as soon as they enter into the bioreactor. It also assumes high microbial mobility within the reactor; thus reducing the chances of bacteria adsorption. Systems involving two or more microbial species in these biochemical reactors have been studied (Tang et al., 1992). However for the purpose of this project, pure and simple

interaction of two bacteria species will be investigated. By "pure and simple", we mean the pattern of microbial competition is not considered and that only one limiting nutrient affects the growth rates of the competing species (Fredrickson & Stephanopoulos, 1981). According to Pavlou (2006), there are four possible scenarios that can play out in a competitive system. They are outlined as follows:

- Total washout of microbes: This happens when competition leads to no growth in the population of both bacteria species; hence with time all bacteria cells will be discharged via the effluent stream without reproducing.
- Growth of only indigenous bacteria: Occurs when indigenous bacteria concentration increases with time due to access to food
- Growth of only exogenous bacteria: Here, injected bacteria concentration increases with time as they diffuse and access more nutrients compared to the other species
- Coexistence of both bacteria species within the chemostat

Therefore, for two bacteria species within a reservoir modelled as a chemostat, the following modified equations represent the rates of reaction for the biochemical reactions that take place within the system:

$$\begin{aligned}
\frac{dC_{b_1}}{dt} &= R_{b_1} = -\delta C_{b_1} + \mu_{b_1} C_{b_1} Y_{b_1} \\
\frac{dC_{b_2}}{dt} &= R_{b_2} = -\delta C_{b_2} + \mu_{b_2} C_{b_2} Y_{b_2} \\
\frac{dC_m}{dt} &= R_{m,c} = \left(\mu_m C_{b_1} + \mu_m C_{b_2}\right) Y_m \\
\frac{dC_n}{dt} &= R_{n,c} = -R_{b_1} - R_{b_2} - R_{m,c}
\end{aligned} \tag{4.32}$$

Here, δ is called the dilution rate expressed in day^{-1}. It describes C_{b_1} and C_{b_2} are the concentrations of the indigenous and exogenous bacteria respectively, R_{b_1} and R_{b_2} are the rates of reaction for the indigenous and exogenous bacteria respectively, $R_{m,c}$ and $R_{n,c}$ are the rate terms for metabolite production and nutrient consumption respectively during microbial competition; and all other variables remain the same as defined in Section 4.1. As applied in the one-species case, Monod's equation will be used to describe the specific growth rates of the bacteria species and metabolite.

$$\mu_{b_1} = \mu_{\max,b_1} \cdot \frac{C_n}{K_{bn} + C_n}$$
$$\mu_{b_2} = \mu_{\max,b_2} \cdot \frac{C_n}{K_{bn} + C_n} \tag{4.33}$$

In this model describing bacteria competition, several assumptions will be made. The first is that all indigenous bacteria are free to move from one part of the reservoir to another in order to source for available nutrients. Another assumption is that the yield coefficients, the maximum growth rate and the half-saturation constants of both indigenous and exogenous (foreign) bacteria are the same. As an initial base case, the dilution rate is assumed to be equal to the maximum growth rate Pavlou (2006). Finally, it is assumed that both bacteria species produce biosurfactants as metabolites. By taking all these into consideration, the following equations will be used to describe the MEOR model for bacteria competition:

Indigenous Bacteria
$$\frac{d}{dt}\left(\frac{\phi C_{b_1}}{B_w} S_w\right) + \nabla.\left(\frac{C_{b_1}}{B_w} u_w\right) = R_{b_1} \tag{4.34}$$

Exogenous Bacteria
$$\frac{d}{dt}\left(\frac{\phi C_{b_2}}{B_w} S_w\right) + \nabla.\left(\frac{C_{b_2}}{B_w} u_w\right) = q_{s,b} + R_{b_2} \tag{4.35}$$

Nutrients
$$\frac{d}{dt}\left(\frac{\phi C_n}{B_w} S_w\right) + \nabla.\left(\frac{C_n}{B_w} u_w\right) = q_{s,n} + R_{n,c} \tag{4.36}$$

Metabolites
$$\frac{d}{dt}\left(\frac{\phi C_m}{B_w} S_w\right) + \nabla.\left(\frac{C_m}{B_w} u_w\right) = R_m \tag{4.37}$$

It is important to highlight here that nutrient and bacteria adsorption is not considered when the chemostat model is applied. Therefore, all bacteria and nutrients are assumed to occupy the water phase.

5 Model Implementation and Simulation

The reservoir and MEOR models developed in the preceding chapters will be implemented by a solution procedure that involves model definition, discretization and automatic differentiation (AD). The reservoir model will be used for strict waterflooding as a base case oil recovery scenario; hence this model will comprise two flowing phases with two bulk components – oil and water. The MEOR model will be used for the scenario of injecting an aqueous solution consisting of bacteria and nutrients into a reservoir limited by a residual oil saturation of 30%. It is assumed that after waterflooding takes place, the reservoir attains a new equilibrium state and the fluids are redistributed accordingly. All models and scenarios will be implemented and simulated with a reservoir simulation package called the MATLAB Simulation Toolbox (MRST).

5.1 MATLAB Reservoir Simulation Toolbox (MRST)

Most reservoir simulation studies require the use of powerful simulators due to the tremendous computational demands that accrue to these projects. Conventional simulation packages like ECLIPSE by Schlumberger, STARS by CMG etc. have been commercialised and used widely for many of these projects with good acceptability. These simulation packages have strengths and weaknesses depending on the purpose for which they are applied. For example, ECLIPSE finds immense application in simulation of polymer flooding, WAG injection, etc., while CMG-STARS has been proven to best tackle problems involving thermal and chemical (alkaline, low salinity water) flooding due to its entirely compositional approach in treating reservoir fluid streams. Another simulator worth mentioning is UTCHEM developed as an in-house reservoir simulator by the University of Texas at Austin. Although not commercialised, it has been used for many research applications in the field of surfactant/polymer flooding, chemical flooding and microbial EOR. Studies have been carried out in comparing this simulator with other conventional simulation packages and it has been proven to give acceptable (and sometimes better) results (Goudarzi et al., 2013). The aforementioned software packages have one major limitation; they cannot be modified by the end-user. Consequently, studies that require slight modifications of models to suit specific purposes cannot be implemented. MRST compensates for this lack of flexibility due to the fact that new models can be developed for

almost any new fluid displacement technique as long as they can be mathematically described by sets of equations.

This novel simulation package was developed for the sole purpose of reservoir simulation studies by SINTEF Applied Mathematics, in Oslo, Norway as a free open-source software package, which can run in MATLAB. Initially, it was developed to support research on consistent discretization and multi-scale solvers on unstructured polyhedral grids. However, it has evolved into an efficient platform for rapid prototyping and efficient testing of new mathematical models and simulation methods (Lie, 2015). Just like the MATLAB software, MRST consists of a core module that houses routines and data structures used for creating and manipulating grids and physical properties. This module also contains utilities for performing automatic differentiation as well as a few routines for processing input files and plotting quantities defined over cells and interfaces. For more robustness, MRST has been reinforced with a set of add-on modules that can be applied together with the core modules for additional reservoir modelling studies as shown in the illustration below:

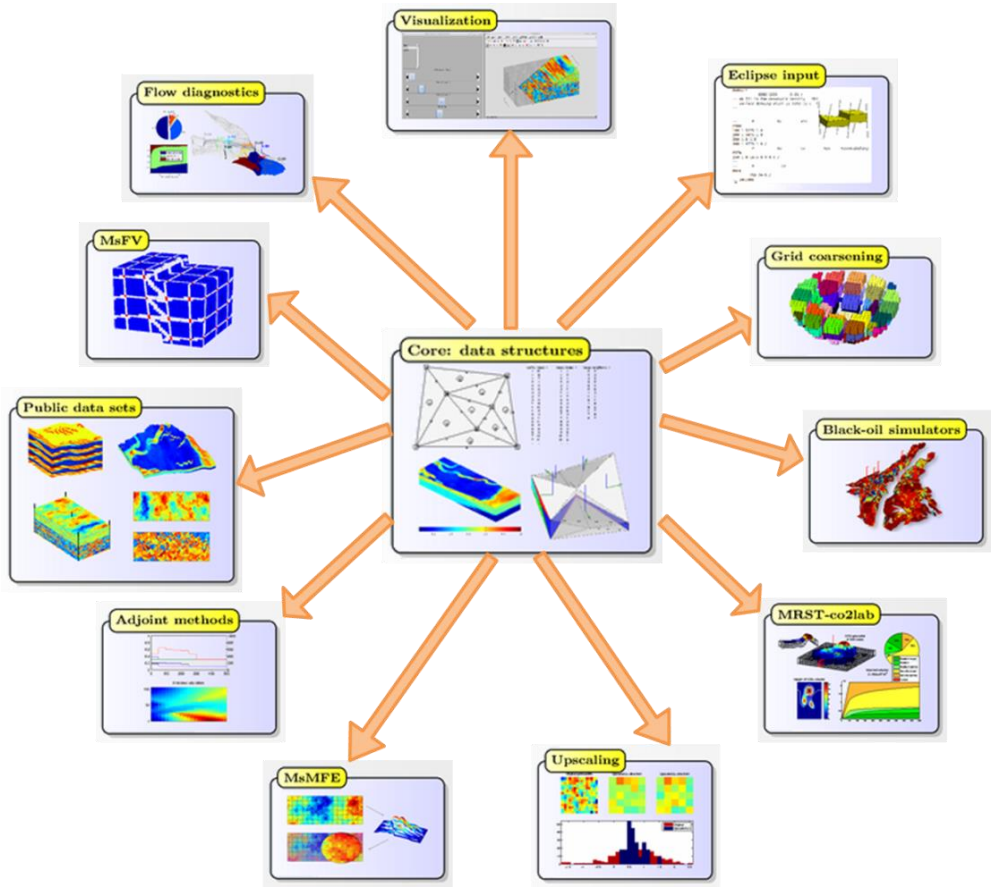

Figure 5.1: Major components of the MRST simulator with the core modules (at the centre) and the sets of add-on modules (Adapted from Lie, 2015)

For simple dynamic flow modelling with MRST, the first step is to set up the computational domain (i.e. reservoir geometry) with grid sizes and dimensions. Next, rock properties like permeability and porosity are assigned to each grid cell. Afterwards, petrophysical data are incorporated into geological model and thereafter, boundary conditions of pressures and/or fluxes are set. At this point, the model can be discretized (independent of specifying a flow model) by computing the transmissibilities for each grid cell. The next step involves defining fluid properties from an add-on module. Before this step, data structures from the core module have been used in defining the model; however, they have not been applied here because fluid property specification is dependent on the mathematical and numerical formulation of the flow equations (Lie, 2015). Finally, the discretized flow model represented is solved for pressures, fluxes and fluid saturations by automatic differentiation.

Amundsen (2015) discusses the simulation procedure as one that follows a series of sequential steps. First, it starts with setting a schedule by specifying the total simulation time, the length of time steps and all other intermediate steps as required for the specific fluid production scenario. Pressures, fluxes and saturations are updated for all grid cells after each time step in order to solve for values in future time steps. Amundsen (2015) expresses the discretized form of the oil and water flow equations (equation (3.4)) together with Darcy's equation (equation (3.1)) as follows:

$$\frac{\left(\frac{\phi\rho_{s,i}S_i}{B_i}\right)^{n+1}-\left(\frac{\phi\rho_{s,i}S_i}{B_i}\right)^{n}}{\Delta t^{n}}+\mathtt{div}\left(\frac{\rho_{s,i}u_i}{B_i}\right)^{n+1}-q_i^{n+1}=0 \tag{4.38}$$

$$u_i^{n+1}=-\frac{\mathrm{K}k_{ri}}{\mu_i^{n+1}}\left(\mathtt{grad}(p^{n+1})-g\rho_i^{n+1}\mathtt{grad}(z)\right) \tag{4.39}$$

Here, μ is viscosity (should not be confused with specific growth rate), n is the current time step, Δt is the time step length, i represents oil or water, and `grad` and `div` are the discrete forms of the gradient and divergent operators respectively. The mapping of the `div` operator is from faces to cells (Lie, 2015); hence, it is used to evaluate the fluid flux at the shared boundaries between a cell and its neighbours and then maps this value into the neighbouring cells (Amundsen, 2015). The mapping of the `grad` operator is from cells to faces; hence, it is defined as the negative adjoint of the `div` operator (Lie, 2015). Therefore, pressure derived from applying this operator is mapped from a particular cell to its shared boundaries.

Next, the discretized form of the flow equations for all cells and faces are defined as a system of nonlinear equations which must be solved implicitly for pressure, fluxes and saturation at each time step. Typical solvers utilise Jacobian matrices to compute the first derivatives of the nonlinear system of equations while applying the Newton-Raphson iterative procedure to find the solution. However, for oil-water (and other multiphase) systems that are computationally demanding, this approach has been found to be time-consuming and may be characterised by numerical errors especially when the Newton iteration does not converge to a solution. For better computational efficiency, MRST uses automatic differentiation to construct Jacobian matrices. This technique is used to numerically evaluate the derivatives of complex functions using a program that computes elementary MATLAB functions (e.g. sine, power, exp) to reduce computational requirements (Lie, 2015).

5.2 MEOR Model Implementation

The MEOR model developed by Amundsen (2015) follows the hierarchical system of class definition that is unique to MRST. This ensures that there is no repetition of line of codes and for better synchronisation of new models with existing ones. The hierarchical tree starts with *PhysicalModel*. It is the super class that implements the physical models for use with automatic differentiation. The next class is *ReservoirModel*. It is basically an addendum to the *PhysicalModel* that contains the fluid and rock models as well as commonly used phases and variables. Following this class is *ThreePhaseBlackOilModel*. It is a Black Oil model that allows for definition of three flowing phases with extra abilities to account for dissolved gas and gas condensates. The main class used for this oil-water modelling study is *TwoPhaseOilWaterModel*. It is a subclass of *ThreePhaseBlackOilModel* that does not account for dissolution of gas in the oil (and/or water) phase. Amundsen's MEOR model tagged *MEORaModel* is a subclass of *TwoPhaseOilWaterModel* that contains additional structures and equations for general microbial growth, metabolite production and biofilm formation (via bacteria adsorption only). For the purpose of this study, Amundsen's model has been modified to allow for food (nutrient) adsorption. Another model has been developed to include the effect of the presence of indigenous bacteria on injected bacteria growth. This new model will be tagged *MEORIndaModel*. A modified MRST model hierarchy for MEOR modelling is illustrated in Figure 5.2.

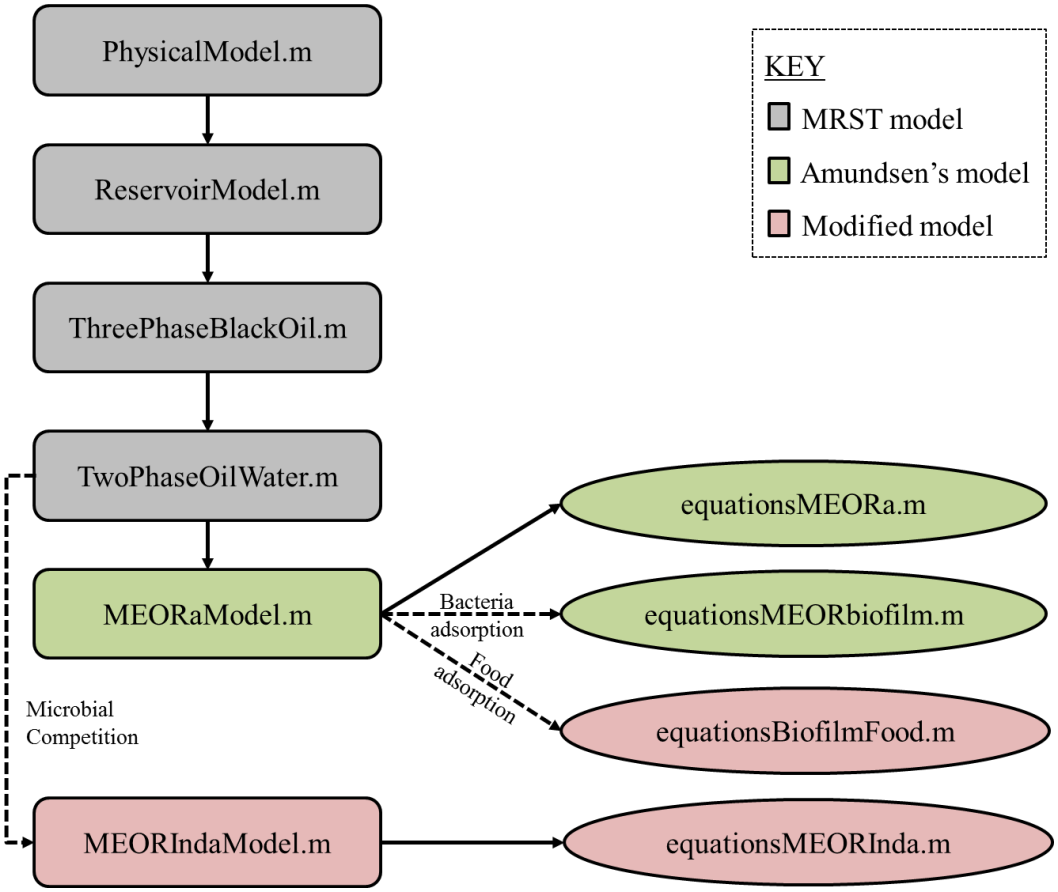

Figure 5.2: Modified class hierarchy for MEOR modelling with MRST

The solution procedure follows that of Amundsen (2015) with some slight modifications (see Figure 5.3). The procedure starts with the definition of the reservoir geometry (i.e. the computational domain). This is then followed by the providing other user-defined inputs such as the rock properties, petrophysical properties and fluid properties. All these define the initial equilibrium state of the reservoir; hence, the reservoir model is created. Thereafter, the boundary conditions are set – in this study we assume a producer (sink) and an injector (source) on either side of the boundaries. The simulation step is actuated by first defining the simulation schedule to cover for the entire production period. The model is then simulated using the pre-defined MEOR equations for the particular area of investigation. Simulation results are then plotted and analysed. In this study, biosurfactants are the only metabolites produced.

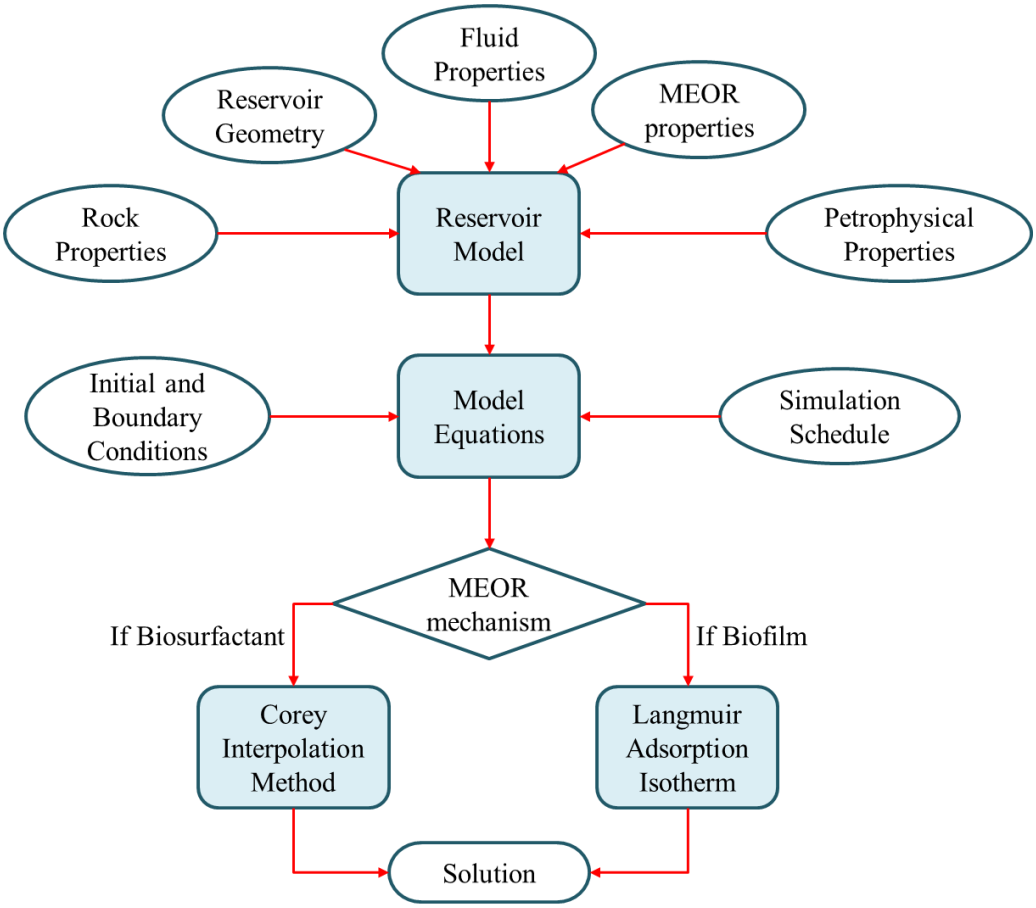

Figure 5.3: Model implementation methodology for MEOR with effects of biosurfactants and biofilm

5.3 Running the MEOR codes in MRST

Due to some initial challenges encountered in running the MEOR codes, the author discusses the following high-level procedures aimed to serve as a simple guide to future users of MRST for MEOR modelling. Steps for downloading and initialising MRST in MATLAB can be found in the MRST guide book (Lie, 2015).

- Four compressed folders containing all MEOR codes created by Amundsen were downloaded from the repositories found in a secure portal called "Bitbucket". These folders contain all essential files (scripts, functions, models etc.).
- The folders were then uploaded into the existing MATLAB folder.
- In order to activate MRST in MATLAB, the *startup.m* file was run. This file is located in the *mrst-master-aleksander-testing-and-explanation* folder. Apart from loading MRST, Amundsen's codes will also be loaded into the current directory.

- Next, the simulation script for MEOR tagged *aTest.m* and located in the *mrst-master-aleksander-testing-and-explanation* folder was opened. This is an editable script containing information about the input parameters (reservoir geometry, rock and fluid properties), MEOR model selection, boundary conditions, and simulation schedule. During the course of this work, this script was edited to suit the purpose of this study.
- All MEOR models and equations are found in the *ad-blackoil* subfolder of the *mrst-master-aleksander-meor-autodiff* folder. New models and equations were developed and added to this subfolder.

In summary, the process starts with downloading and initialising MRST, followed by running the start-up program, which then allows for running the test cases with the MEOR models.

6 One-Dimensional MEOR Simulations

The scope of this project covers only one-dimensional reservoir modelling. This definition should not be mistaken as a one-dimensional (straight-line) reservoir because the actual reservoir dimension is volumetric with areal and depth characteristics. Taking this approach helps to better understand the distribution of components and properties along a streamline of cells from the injector to the producer. This is sufficient for studying the MEOR mechanisms under investigation. The mechanisms will be limited to biosurfactant production, bacteria adsorption and food adsorption. The effect of microbial competition on the system will also be discussed. Several assumptions in the model definition, parameters and states have been made and will be explicitly outlined. The input parameters to the model are derived from both Nielsen (2010) and Amundsen (2015) with a few changes and will be categorised accordingly.

6.1 One-Dimensional MEOR Model Definition

For a one-dimensional flow model, the spatial vector is reduced to a linear scale; hence assuming horizontal flow in the *x*-direction (across reservoir length), the flow equations for all components defined in Chapter 4 will be modified as follows:

Oil
$$\frac{d}{dt}\left(\frac{\phi}{B_o}S_o\right)+\frac{\partial}{\partial x}\left(\frac{u_o}{B_o}\right)=q_{s,o} \tag{4.40}$$

Water
$$\frac{d}{dt}\left(\frac{\phi}{B_w}S_w\right)+\frac{\partial}{\partial x}\left(\frac{u_w}{B_w}\right)=q_{s,w} \tag{4.41}$$

Free Bacteria
$$\frac{d}{dt}\left(\frac{\phi C_{bw}}{B_w}S_w\right)+\frac{\partial}{\partial x}\left(\frac{C_{bw}}{B_w}u_w\right)=q_{s,b}+R_b \tag{4.42}$$

Adsorbed Bacteria
$$\frac{d}{dt}\left(\frac{\phi C_{bb}}{B_w}S_w\right)=\chi_b A_s S_w \phi \tag{4.43}$$

Free Nutrients
$$\frac{d}{dt}\left(\frac{\phi C_{nw}}{B_w}S_w\right)+\frac{\partial}{\partial x}\left(\frac{C_{nw}}{B_w}u_w\right)=q_{s,n}+R_n \tag{4.44}$$

Adsorbed Nutrients $$\frac{d}{dt}\left(\frac{\phi C_{nb}}{B_w}S_w\right)=\chi_n A_s S_w \phi \tag{4.45}$$

Metabolites $$\frac{d}{dt}\left(\frac{\phi C_{mw}}{B_w}S_w\right)+\frac{\partial}{\partial x}\left(\frac{C_{mw}}{B_w}u_w\right)=R_m \tag{4.46}$$

From the discretization of this model using finite difference approximations, we get the following sets of equations to be solved for pressure, saturation, bacteria concentration, nutrient concentration and metabolite concentration using the AD method.

Oil $$\frac{1}{\Delta t^n}\left(\left(\frac{\phi S_o}{B_o}\right)^{n+1}-\left(\frac{\phi S_o}{B_o}\right)^{n}\right)+\mathtt{div}\left(\frac{u_o}{B_o}\right)^{n+1}-q_{s,o}^{n+1}=0 \tag{4.47}$$

Water $$\frac{1}{\Delta t^n}\left(\left(\frac{\phi S_w}{B_w}\right)^{n+1}-\left(\frac{\phi S_w}{B_w}\right)^{n}\right)+\mathtt{div}\left(\frac{u_w}{B_w}\right)^{n+1}-q_{s,w}^{n+1}=0 \tag{4.48}$$

Free Bacteria $$\frac{1}{\Delta t^n}\left(\left(\frac{\phi C_{bw}S_w}{B_w}\right)^{n+1}-\left(\frac{\phi C_{bw}S_w}{B_w}\right)^{n}\right)+\mathtt{div}\left(\frac{u_w C_{bw}}{B_w}\right)^{n+1}-q_{s,b}^{n+1}-R_b=0 \tag{4.49}$$

Adsorbed Bacteria $$\frac{1}{\Delta t^n}\left(\left(\frac{\phi C_{bw}S_w}{B_w}\right)^{n+1}-\left(\frac{\phi C_{bw}S_w}{B_w}\right)^{n}\right)-\left(\chi_b A_s S_w \phi\right)^{n+1}=0 \tag{4.50}$$

Free Nutrients $$\frac{1}{\Delta t^n}\left(\left(\frac{\phi C_{nw}S_w}{B_w}\right)^{n+1}-\left(\frac{\phi C_{nw}S_w}{B_w}\right)^{n}\right)+\mathtt{div}\left(\frac{u_w C_{nw}}{B_w}\right)^{n+1}-q_{s,n}^{n+1}-R_n=0 \tag{4.51}$$

Adsorbed Nutrients $$\frac{1}{\Delta t^n}\left(\left(\frac{\phi C_{nw}S_w}{B_w}\right)^{n+1}-\left(\frac{\phi C_{nw}S_w}{B_w}\right)^{n}\right)-\left(\chi_n A_s S_w \phi\right)^{n+1}=0 \tag{4.52}$$

Metabolites $$\frac{1}{\Delta t^n}\left(\left(\frac{\phi C_{mw}S_w}{B_w}\right)^{n+1}-\left(\frac{\phi C_{mw}S_w}{B_w}\right)^{n}\right)+\mathtt{div}\left(\frac{u_w C_{mw}}{B_w}\right)^{n+1}-R_m=0 \tag{4.53}$$

When considering the case of microbial competition, equation (6.10) will be modified to account for the two bacteria species as follows:

Indigenous Species $$\frac{1}{\Delta t^n}\left(\left(\frac{\phi C_{b_1} S_w}{B_w}\right)^{n+1}-\left(\frac{\phi C_{b_1} S_w}{B_w}\right)^{n}\right)+\mathrm{div}\left(\frac{u_w C_{b_1}}{B_w}\right)^{n+1}-R_{b_1}=0 \quad (4.54)$$

Exogenous Species $$\frac{1}{\Delta t^n}\left(\left(\frac{\phi C_{b_2} S_w}{B_w}\right)^{n+1}-\left(\frac{\phi C_{b_2} S_w}{B_w}\right)^{n}\right)+\mathrm{div}\left(\frac{u_w C_{b_2}}{B_w}\right)^{n+1}-q_{s,b_2}^{n+1}-R_{b_2}=0 \quad (4.55)$$

Since all nutrients will be available in the water phase, the nutrient equation for microbial competition will be expressed as:

Nutrients $$\frac{1}{\Delta t^n}\left(\left(\frac{\phi C_n S_w}{B_w}\right)^{n+1}-\left(\frac{\phi C_n S_w}{B_w}\right)^{n}\right)+\mathrm{div}\left(\frac{u_w C_n}{B_w}\right)^{n+1}-q_{s,n}^{n+1}-R_{n,c}=0 \quad (4.56)$$

Metabolites will be produced by both species; hence, equation (6.14) will be modified as follows:

$$\frac{1}{\Delta t^n}\left(\left(\frac{\phi C_{mw} S_w}{B_w}\right)^{n+1}-\left(\frac{\phi C_{mw} S_w}{B_w}\right)^{n}\right)+\mathrm{div}\left(\frac{u_w C_{mw}}{B_w}\right)^{n+1}-R_{m,c}=0 \quad (4.57)$$

6.2 Assumptions

In the process of developing this model, several assumptions were made in order to reduce complexities but still maintain the model's robustness. They will now be highlighted as follows:

1. One dimensional horizontal fluid flow.
2. Laminar (low velocity) flow regime; therefore, Darcy's law is applicable.
3. Fluids (oil and water) are slightly compressible. Hence oil and water densities are weak functions of pressure and are said to be approximately constant.
4. Isothermal reservoir conditions.
5. Homogeneous system; hence, porosity and absolute permeability are constant for all cells.
6. Capillary and gravity effects are negligible.
7. Piston-like fluid displacement such that only movable oil flows ahead of the primary waterfront.
8. Black Oil fluid model is used for hydrocarbon property definition.

9. Constant dynamic viscosity for reservoir fluids. This is based on the initial assumption of isothermal conditions and also on the supposition that there is no dissolved gas in oil.
10. Reservoir is in an initial equilibrium state with distinct fluid contacts.
11. Continuous bacteria and nutrient injection into the water phase of the reservoir.
12. The only by-products (metabolites) produced from bacteria feeding are biosurfactants
13. Biosurfactant partitioning between oil and water phases is instantaneous. However, biosurfactants in the oil phase do not take part in IFT reduction.
14. Metabolites do not adsorb on the pore walls and therefore cannot form a biofilm.
15. Only one component gets adsorbed at any given instance. Biofilm formation is characterised by equilibrium partitioning. Multicomponent (bacteria and food) simultaneous adsorption has been neglected.
16. In the case of bacteria biofilm, sessile bacteria continue feeding on the nutrients and grow; however, new cells are assumed to be produced into the water phase.
17. In the case of food adsorption, adsorbed nutrients cannot be used up by bacteria cells as a food source. Therefore, only nutrients in the water phase can be accessed.
18. Injected nutrients do not enter into the oil phase.
19. The major carbon source for bacteria feeding is found in oil.
20. Bacterial growth as well as metabolite production can be described by Monod kinetics.
21. The growth rate definition according to Monod's equation is such that there is one growth limiting nutrient while others are in excess.
22. No bacteria decay (i.e. no death parameter in Monod's equation). Growth is only restricted by the maximum growth rate. Once this rate is attained, bacteria growth enters the stationary phase ad infinitum.
23. There is no change in volume during the biochemical reactions because it is assumed that all components in the water phase are of the same density (as water).
24. Indigenous bacteria are all free to move from cell to cell in any direction.
25. During microbial competition, all species are capable of producing biosurfactants as metabolites.

6.3 Definition of Input Parameters

Model input parameters will be composed of those specified by Nielsen (2010) and Amundsen (2015) however, some changes and additions have been made to suit the purpose of this study. A summary of all parameters and their sources can be found in the following table:

Table 6.1: Input parameters for simulation of MEOR model for single bacteria species

Parameter	**Value**	**Source**
K	100 mD	Amundsen (2015)
p_{bh}	100 bara	
$\mu_{max,b}$	$0.2\ day^{-1}$	Nielsen (2010)
$\mu_{max,m}$	$0.2\ day^{-1}$	
K_{bn}	$1\ kg/m^3$	
K_{mn}	$1\ kg/m^3$	
Y_b	0.82	
Y_m	0.18	
σ	29 mN/m	
l_1, l_2, l_3	$\{10^{-4}, 0.2, 1.5 \times 10^{-4}\}$	
A_s	$3 \times 10^5\ m^2/m^3$ total volume	
ω_1, ω_2	$\{10^{-3}\ kg/m^2\ ,\ 1.7 \times 10^{-3}\ m^3/kg\ \}$	
μ_o	3cp	
μ_w	1cp	
ρ_w, ρ_b, ρ_n	$1000\ kg/m^3$	
N_o, N_w	2	
$q_{s,b}$	$0.5 \times 10^{-2}\ kg/m^3$	
$q_{s,n}$	$10^{-2}\ kg/m^3$	
k'_{rw}	0.5	
k'_{ro}	0.8	
S_{wi}	0.3	
S_{or}	0.3	Newly Defined
ϕ	0.35	
ρ_o	$850\ kg/m^3$	
Water Injection Rate	$265\ m^3/day$	
Reservoir Dimensions	1000 m × 100 m × 100 m	
Grid dimensions	1 m × 100 m × 100 m	

6.3.1 Reservoir Geometry and Rock Properties

The reservoir under study is assumed to be of rectangular dimensions with a length of 1km and an equal width and depth of 100m. Each cell will have grid dimensions of 1m x 100m x 100m to represent one dimensional flow. The reservoir is assumed to be homogeneous with a porosity of 35% and an absolute permeability of 100mD (Nielsen, 2010).

6.3.2 Fluid Properties

The oil is assumed to be light oil with a density of 850 kg/m^3 and a dynamic viscosity of 3 cp. The oil formation volume factor is set at 1.065 m^3/Sm^3. The water density will follow that of pure water with a density of 1000 kg/m^3 and viscosity of 1 cp. The water formation volume factor has been assumed to be 1.002 m^3/Sm^3. The densities specified here are measured at surface condition (i.e. 15.56°C and 1 atm).

6.3.3 Bacteria and Metabolites

It is presumed that bacteria and metabolite maximum growth rates $\mu_{b,max}$ and $\mu_{m,max}$ are both equal to a value of 0.2 day^{-1} (Nielsen, 2010). The same goes for the half saturation constants for both components specified as 1 kg/m^3. The bacteria yield and metabolite yield for the case of no indigenous bacteria will be 82% and 18% respectively. For the special case of bacteria competition, the yields will be distributed as 40% for each bacteria species and 20 % for metabolites. The amount of bacteria to be injected in both cases will follow that specified by Amundsen (2015) expressed in terms of mass concentration as 0.005 kg/m^3.

6.3.4 Nutrients

Nutrients will be composed of an assortment of substances necessary for metabolite production and growth. It is also expected that bacteria derived their carbon feeding demands from the oil. Amundsen (2015) specified a nutrient concentration of 0.01 kg/m^3 in the injector stream; this will also be used as the basis for nutrient injection in this study.

6.3.5 Biosurfactant Effect

The change in the relative permeability curves due to IFT reduction will follow the Corey interpolation method discussed in Section 4.2. The initial IFT σ will be equal to 29 mN/m and the l_1, l_2, *and* l_3 parameters that affect the strength of the surfactant will be according the *Surfactant A* type specified by Nielsen (2010) as 1×10^{-4}, 0.2 and 1.5×10^{-4} respectively. The

endpoint oil relative permeability will be equal to 0.8 at an initial water saturation of 30 %. The water relative permeability at a residual oil saturation of 30 % will be 0.5. The Corey exponents for both oil and water (N_o and N_w) will be equal to 2.

6.3.6 Biofilm Effect

Nielsen (2010) specified constants ω_1 and ω_2 for biofilm modelling according to the Langmuir adsorption isotherm as 1×10^{-3} kg/m^2 and 1.7×10^{-3} m^3/kg respectively. These will be used to calculate the mass of the component adsorbed per unit surface area. The value of the first constant ω_1 ensures that up to 75 % of the pore volume can be occupied by the biofilm while the value of ω_2 specifies that the concentration of the adsorbed component forming the biofilm is about half of the total amount of the injected component (Amundsen, 2015). The specific surface area available for adsorption will be equal to 3×10^5 m^2/m^3 total volume. These parameters will then be used in the biofilm mass conservation equations to determine the concentration of adsorbed components per time.

6.3.7 Simulation Schedule and Others

The dynamic flow simulation for both waterflooding and MEOR cases will follow a 30-year production period. Therefore the simulation time will be a total of 10,950 days with a time step of 10 days. Water injection will commence at the start of production at one end of the reservoir at a rate of 280 m^3/day and would sweep oil into the producer at the opposite end of the reservoir. Thus, with a reservoir pore volume of 3,500,000 m^3 approximately 0.88 PV of water will be injected. A constant pressure boundary of 100 bara at the producer end was specified by Amundsen (2015). This will be incorporated into this work as the pressure controlling mode for the producer. The base case for MEOR will be such that typical water injection would lead to water breakthrough after 10 years of oil production. The water imbibition process has been assumed to result in a residual oil saturation of 30%. The goal of MEOR will be to reduce this value by biosurfactant action and mobilise capillary-trapped oil.

6.4 Preliminary Simulations

Initially, two simulations were carried out. The first was the basic case of only water injection while the second case entailed bacteria and nutrient injection without bacteria growth and metabolite production. This was implemented as a quality check on the performance of the simulator.

6.4.1 Reservoir Pressure Profile

The first parameter of importance is the pressure distribution across the reservoir. Apart from displacing oil from pore spaces in the reservoir, water injection also serves the purpose of pressure maintenance within the reservoir. The following plot shows the changes in reservoir pressure at specific production periods.

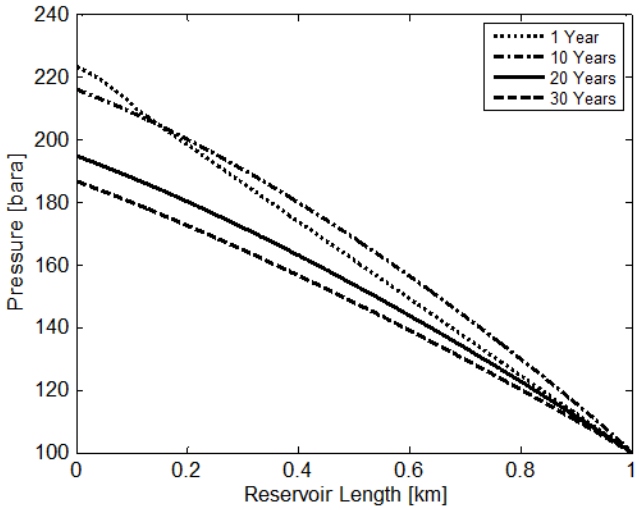

Figure 6.1: Pressure profile of across the reservoir showing convergence at the producer bottomhole pressure

As expected, the pressure profile is such that the pressure at the injector is higher than the specified bottomhole pressure of the producer (100 bara). This situation is maintained throughout the time of production; hence water injection at a volumetric rate of 280 m^3/day is sufficient for pressure maintenance within the reservoir.

6.4.2 Saturation Profile

Figure 6.2 reveals that both microbes and nutrients are carried through the reservoir, as water displaces the oil in a stable front, because the saturation curves for pure waterflooding and microbial flooding overlap. A final oil recovery of 49.28 % was achieved in both cases. Bacteria and nutrient concentrations begin to increase from the injector end of the reservoir until water breakthrough is achieved.

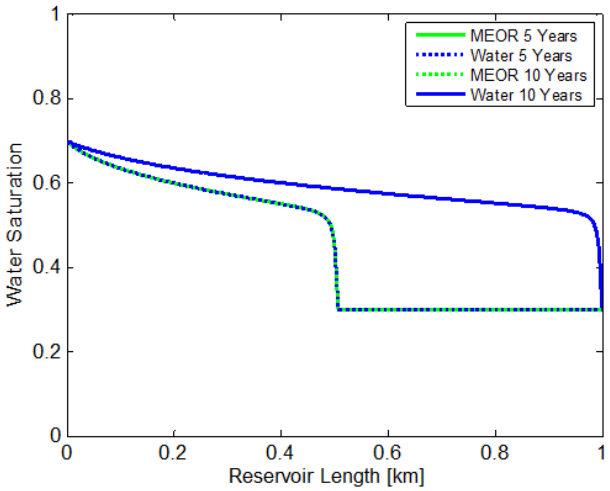

Figure 6.2: Water saturation profile for pure waterflooding and MEOR without microbial growth, metabolite production or adsorption

Bacteria and nutrient breakthrough both occur after 10 years of production – the same time as water breakthrough. After breakthrough, their respective concentrations continue to increase across the entire length of the reservoir until a constant value approximately equal to their injection concentrations (0.005 kg/m^3 for bacteria and 0.01 kg/m^3 for nutrients) is attained at the end of production. This reveals that the simulator works flawlessly and can assume frontal displacement by waterflooding when microbial growth and metabolite production options are disabled.

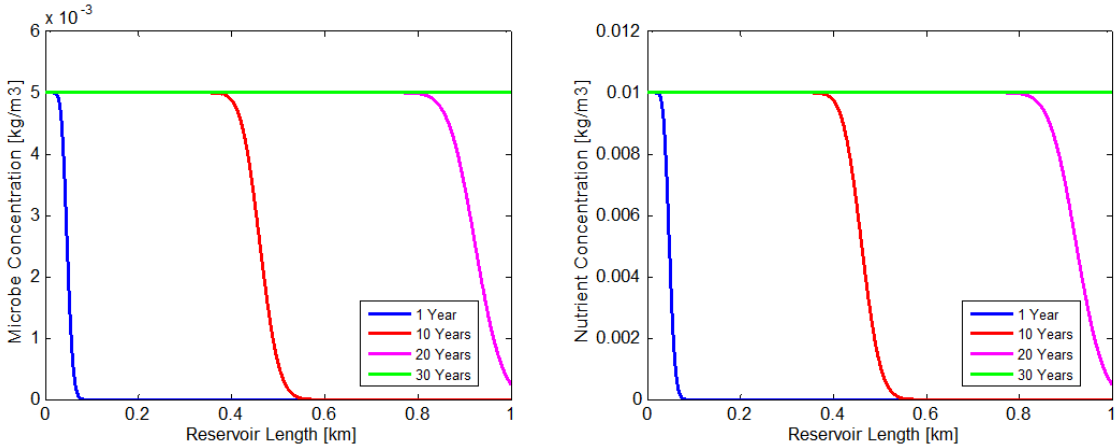

Figure 6.3: Plots of (a) microbe concentration and (b) nutrient concentration as these components are carried across the reservoir.

6.5 Single Bacteria Species

This section covers simulation studies for an idealized reservoir lacking an indigenous bacteria population. Therefore, microbial flooding of bacteria and nutrients in fixed concentrations was investigated. Several simulation cases were run to understand the singular influence of bacteria growth, biosurfactant production, and biofilm formation on oil recovery. Further investigations include a combination of these factors and the impact of certain input parameters on simulation results.

6.5.1 Bacteria Growth

Studying the effect of bacteria growth without metabolite production assumes that bacteria get all their feeding (organic and inorganic) requirements for growth from the injected nutrients. Thus, there is a 100 % yield of bacteria cells from nutrient consumption (i.e. Y_b = 1 and Y_m = 0). The following saturation profile was generated for the waterflooding and MEOR with microbial growth only:

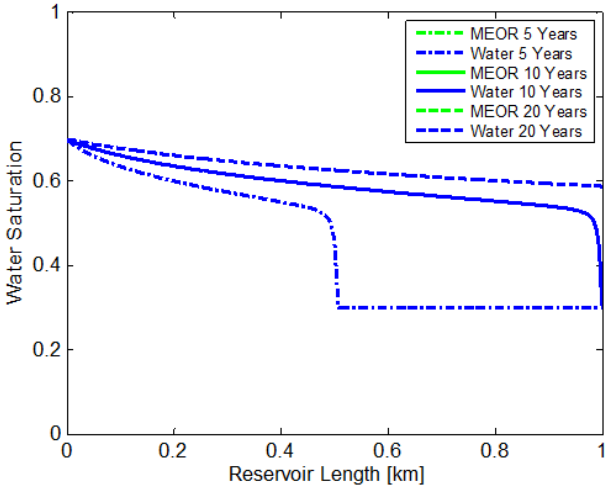

Figure 6.4: Saturation profile for the MEOR growth-only case showing a total overlap of the MEOR and the pure waterflooding saturation curves.

The saturation profile for MEOR follows that of normal water flooding because of the absence of biosurfactants. New and existing microbial cells all occupy the water phase and are carried on in the water front to the producer. Oil recovery also follows the same pattern; hence, this suggests that bacteria growth alone does not improve oil production in any way.

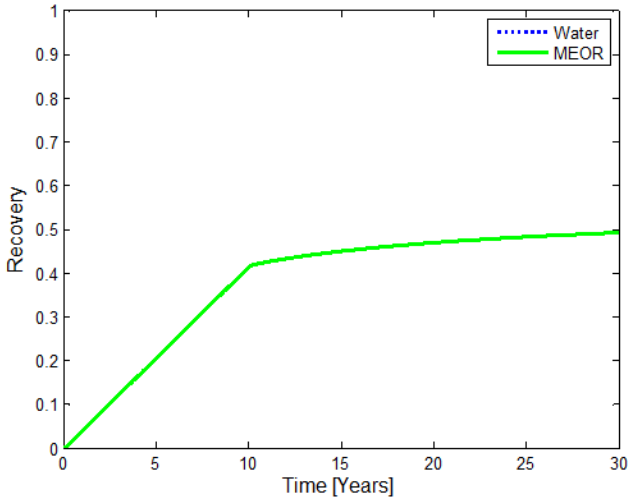

Figure 6.5: Oil recovery for the growth-only case. This coincides with the pure waterflooding curve.

The bacteria population continues to increase as they grow and move towards the producer end of the reservoir (Figure 6.6) and as a result, nutrients are mostly limited to the injector end. A maximum bacteria concentration of about 0.015 kg/m^3 is already attained after 10 years of oil production and persists until production ceases.

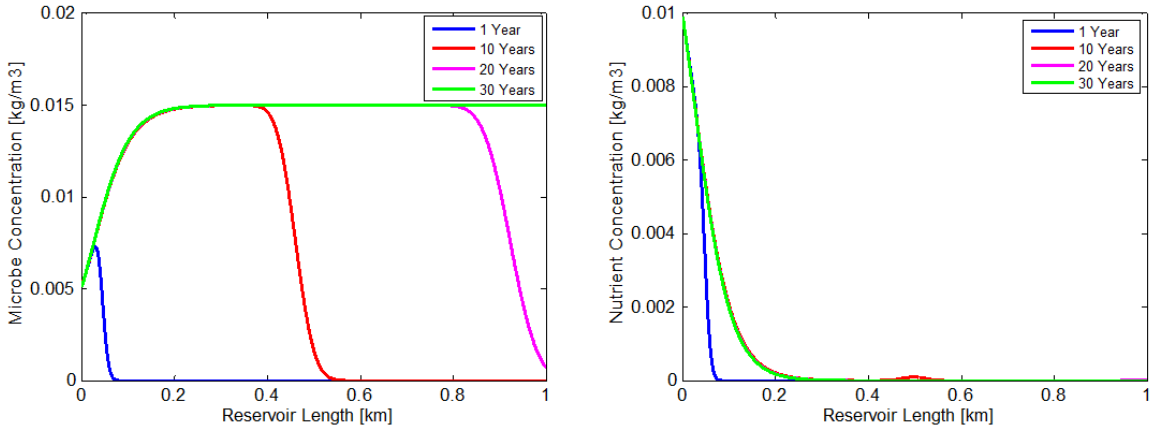

Figure 6.6: (a) Microbial and (b) nutrient concentration across the reservoir length for the growth-only case.

6.5.2 Biosurfactant Production without Bacteria Growth

The production of biosurfactants has been implied to be a precursor for bacteria growth since most bacteria are supposed to derive their carbon requirements from oil. This same assumption is used in this scenario. Bacteria ingest nutrients and produce by-products called metabolites (biosurfactants) which in turn act as emulsifying agents that introduce some oil into the water phase for bacteria feeding. In this case, it is assumed that bacteria do not get access to these carbon-based nutrients; hence, there is no cell growth.

In order to understand what is happening in the reservoir. The concentration profile of each bulk component will be discussed. First, bacteria and nutrients are introduced into the reservoir from the injector end. As time goes on, nutrients are used up by the bacteria which in turn produce biosurfactants (metabolites) that alter the surface properties of the fluids in contact. From Figure 6.7(b), it can be observed that these nutrients are mostly restricted to the injector and very small amounts get to the producer. This implies that most of the metabolites are formed close to the injector as metabolic products of newly injected bacteria cells and are then carried on by water to other parts of the reservoir alongside the bacteria. From Figure 6.7(a), it is confirmed that bacteria growth is non-existent and as production progresses, the concentration of bacteria species increases across the reservoir to the initial injection concentration (0.005 kg/m^3).

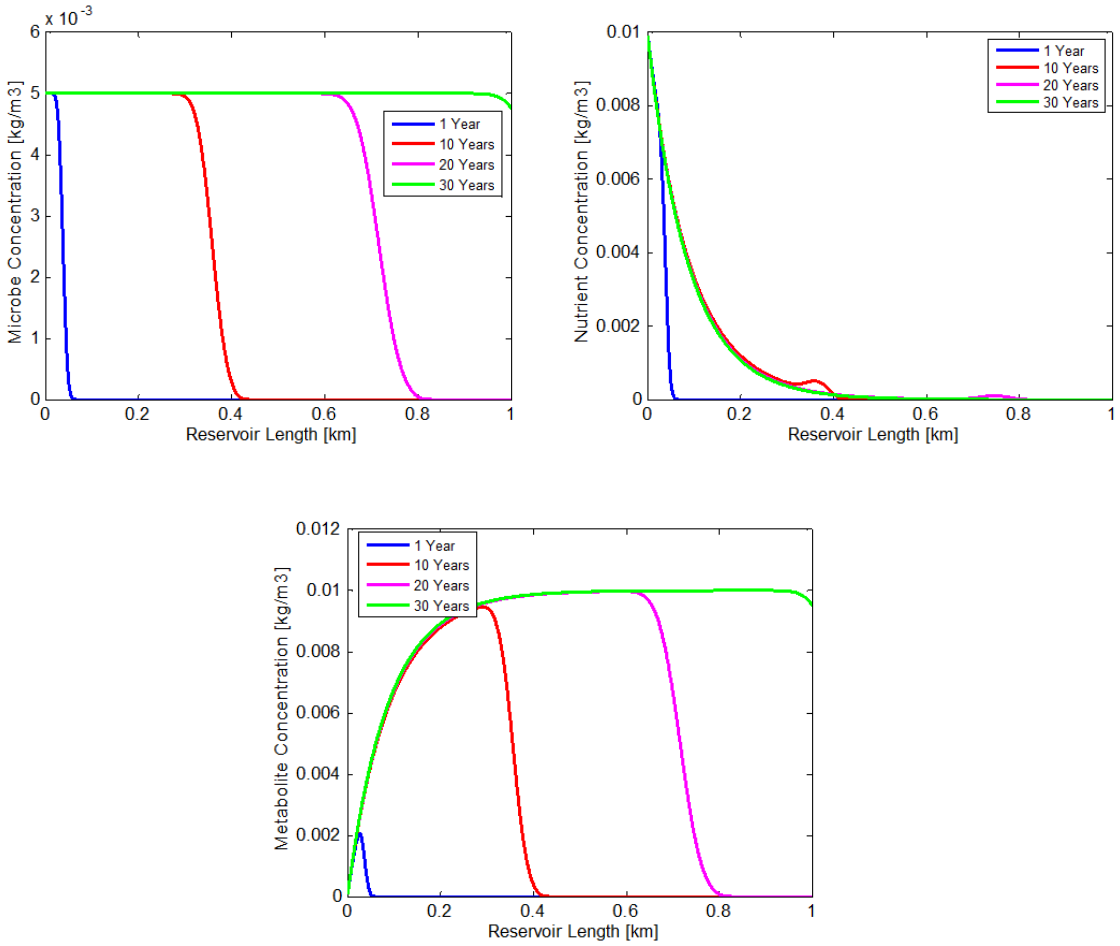

Figure 6.7: Plots showing the distribution of (a) microbes, (b) nutrients, and (c) metabolites across the reservoir length for the MEOR case of metabolite production without growth.

Simulation results for the saturation profile across the reservoir length are found in Figure 6.8. From this plot, it can be observed that microbial flooding with the production of biosurfactants results in a peculiar saturation profile. This is evidenced by the formation of

two displacement fronts. Therefore, apart from the main displacement front, there is a secondary displacement front that depicts displacement of extra oil as residual oil saturation S_{or} is reduced. This implies that capillary-trapped oil is mobilised and represented as a travelling oil bank which is expected to result in additional oil recovered by the action of the biosurfactant. Water breakthrough is slightly delayed as compared to the pure waterflooding case; hence the displacement process is more efficient. From the plot, the residual oil saturation due to biosurfactant action decreases from 30% to approximately 8% creating an avenue for more oil to be displaced as water injection progresses.

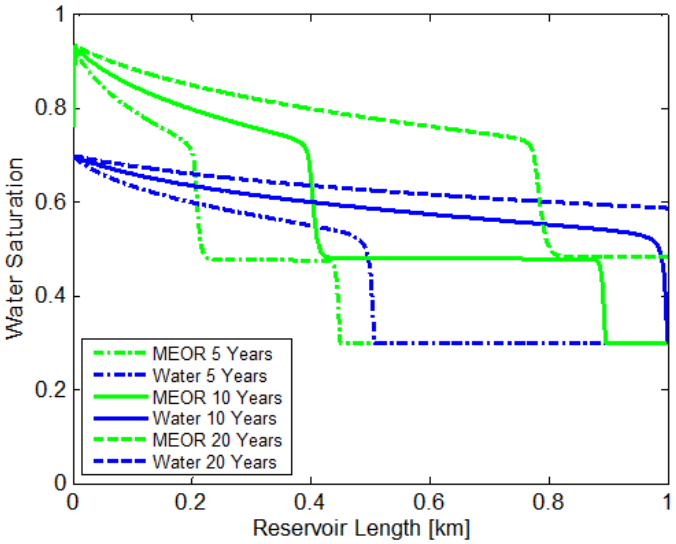

Figure 6.8: Water saturation profiles for pure waterflooding and MEOR with the biosurfactant-only option at different production times.

The oil recoveries for basic waterflooding and microbial flooding follow the pattern illustrated in Figure 6.9. Initially, they coincide before water breakthrough revealing that the displacement front is stable. Water breakthrough occurs first in the pure waterflooding case and the water curve starts to flatten out, due to increasing water production, to a final value of 49.28%. Whereas in the MEOR case, after primary breakthrough, the curve continues to monotonically increase in value until the second breakthrough is attained (i.e. the oil bank has been produced). Thereafter, the curve starts to flatten out to a value of about 74.29%. Therefore, incremental recovery from the effect of only biosurfactant production in the absence of microbial growth is 25.01%.

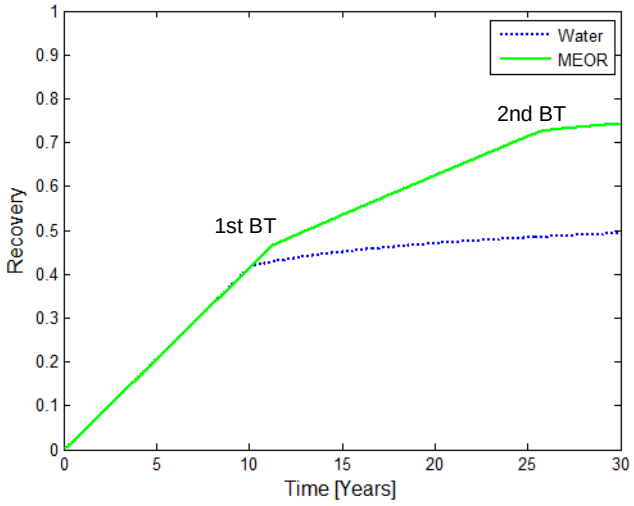

Figure 6.9: Oil recovery plot showing the flattening out of the pure waterflooding curve after breakthrough. The MEOR curve continues to monotonically rise after primary breakthrough (1st BT) until secondary breakthrough (2nd BT) is attained.

6.5.3 Bacteria Growth and Biosurfactant Production

This scenario covers the simultaneous effect of bacteria growth and biosurfactant production on oil recovery. The model however does not account for the time lapse between metabolite production and bacteria growth. Therefore, it is assumed that growth is only affected by a single limiting nutrient.

Injection of both bacteria and nutrients into the reservoir affects the fluid displacement process. From the plot of microbial concentration against production time, the bacteria cells initially occupy areas close to the injector as they consume more nutrients to simultaneously produce metabolites and grow. After one year of production, the maximum bacteria concentration is just around 0.007 kg/m^3 at the inlet section of the reservoir. As the bacteria population increases, they tend to spread out across the reservoir and eventually attain a maximum concentration of about 0.013 kg/m^3 in the inner sections of the reservoir. This maximum value is slightly less than the maximum concentration obtained in the case of only bacteria growth which was 0.015 kg/m^3. Therefore, the effect of the specified yield coefficient can be seen here. On observing Figure 6.10(b), it can be inferred that nutrients do not spread out as such because they are mostly used up before arriving at the producer end. Therefore, the highest nutrient concentration at any given time is always the concentration at the injector. Surfactants follow the same trend as bacteria as they spread out and attain a maximum concentration of 1.8×10^{-3} kg/m^3 within the reservoir as shown in Figure 6.10(c).

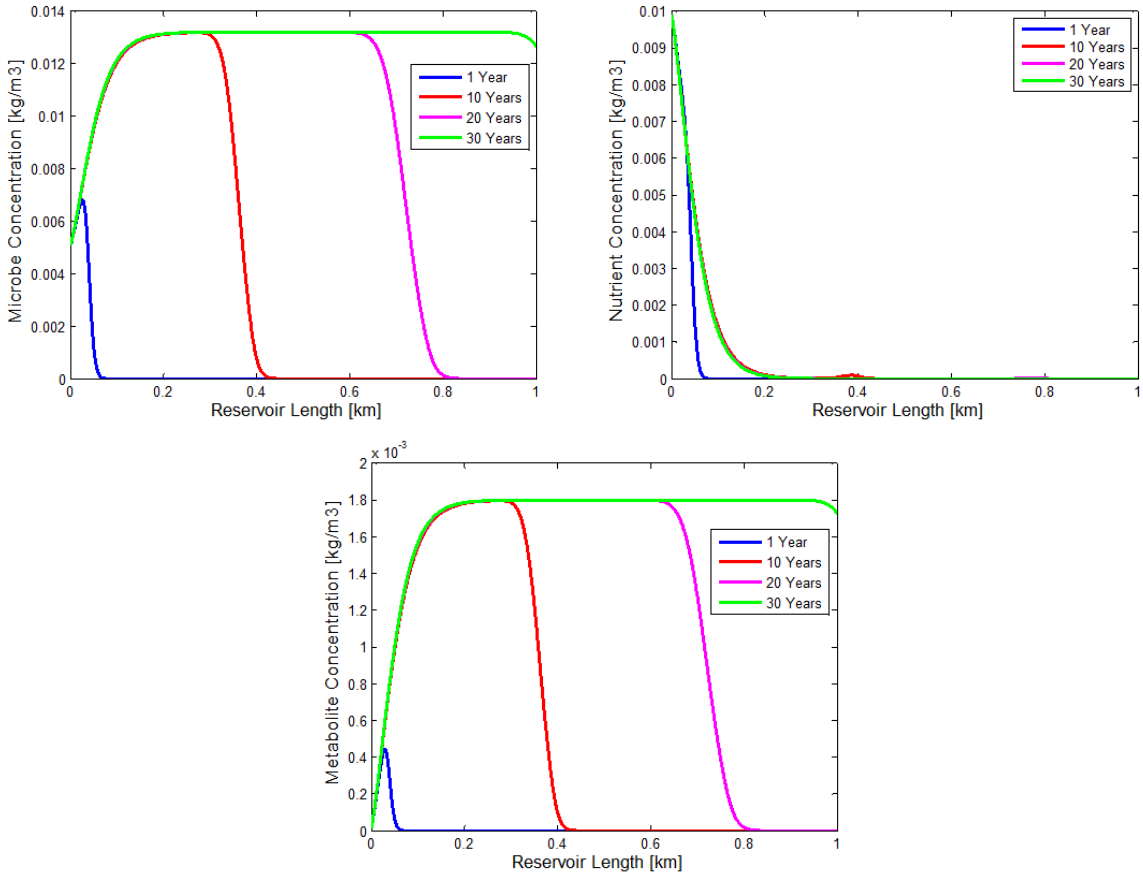

Figure 6.10: (a) Microbe, (b) nutrient, and (c) metabolite concentration across the reservoir at specific times for oil recovery with microbial flooding.

The saturation profile derived from the MEOR simulation with MRST is presented in Figure 6.11. This profile follows that of the biosurfactant-only case treated previously with the existence of an oil bank. This travelling oil bank never catches up with the pure waterflooding front; therefore primary breakthrough is delayed leading to more oil being displaced for the same time period compared to the waterflooding case. This apparent delay could be due to the reason that the pure waterflooding front has higher water saturation at the front (therefore higher water relative permeability) compared to the primary MEOR front. Consequently, the waterflooding front will move faster. After the primary water breakthrough of the MEOR front, the water saturation behind the primary front remains constant at about 50%. This means that only an additional 20% saturation of water is produced together with the oil bank. This is in contrast to the waterflooding case as the saturation behind the waterfront keeps rising until residual saturation is attained. Finally in late time, it can be observed that the residual oil saturation is significantly reduced from the initial 30% to some minimum value slightly less than 10%.

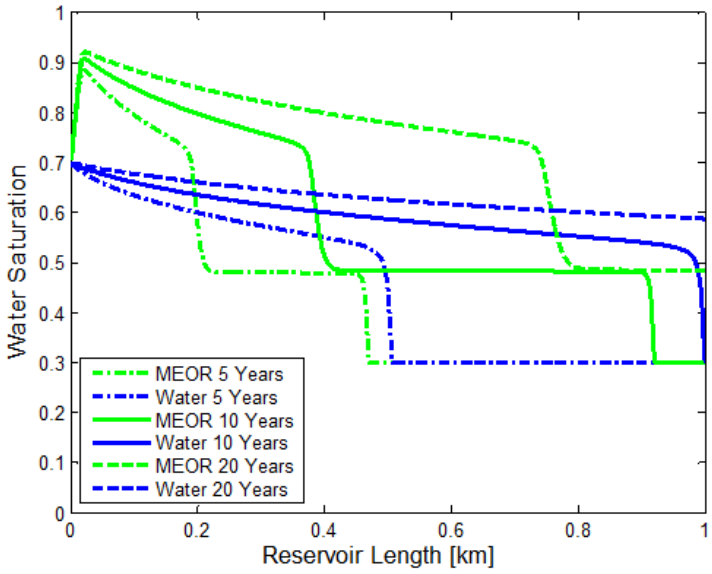

Figure 6.11: Saturation plots for pure waterflooding (blue) and MEOR with biosurfactant effect and microbial growth (green) showing the travelling oil bank and the existence of two waterfronts for the MEOR case.

The relative permeability curve shown below reveals the change in residual oil saturation S_{or} and the oil and water relative permeability endpoints as a result of IFT reduction. As expected both, curves shift to the right of the original and higher cross-point water saturation is observed. This depicts increasing water-wetness; therefore, water would begin to fill up pore spaces initially occupied by capillary-trapped oil. The new residual oil saturation S_{or}^{*} is approximately 7 % representing a decline of 23 %.

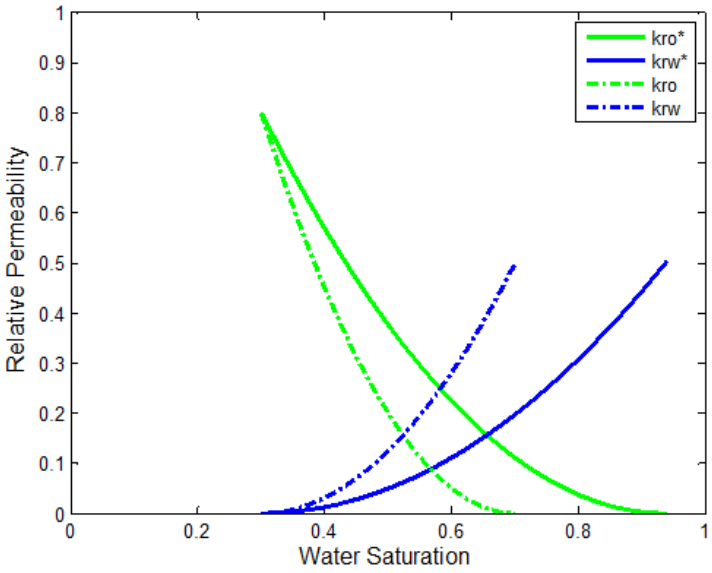

Figure 6.12: Oil and water relative permeability curves before and after the effect of the biosurfactant reducing S_{or} from 30% to approximately 7%.

The final oil recovery from the plot shown below is about 74.02 % of original oil in place. This is value is 0.27 % lower than that obtained in the biosurfactant-only case but follows the same trend. Therefore, bacteria growth slightly affects recovery because the surfactant concentration reaches the threshold concentration earlier in the biosurfactant-only case. Therefore, the trapped oil immediately after the injector end is mobilised. This oil is missed in the growth plus surfactant production case (represented by the space behind the hump of the saturation curve in Figure 6.11).

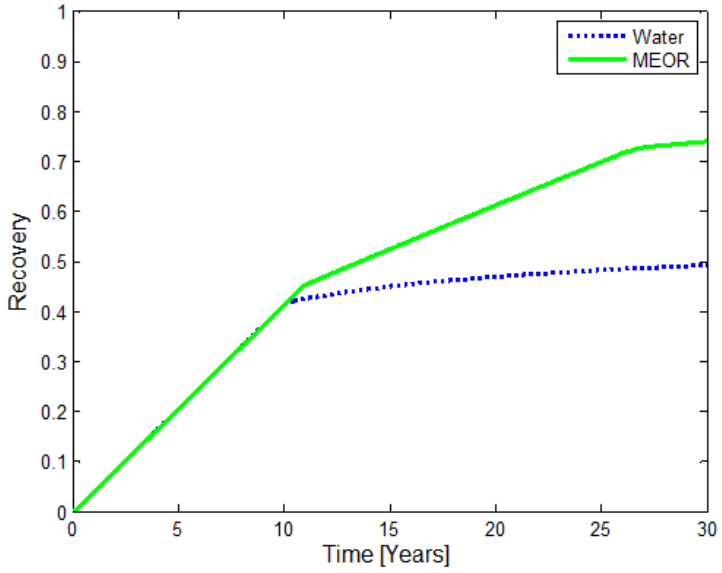

Figure 6.13: Oil recovery plots for pure waterflooding and MEOR showing better oil production after primary water breakthrough and a late secondary breakthrough for the MEOR case.

6.5.4 Biofilm – Bacteria Adsorption

Adsorption of bacteria on the pore walls resulting in the formation of biofilm is based on the Langmuir adsorption isotherm. This scenario investigates the effect of biofilm formation on fluid displacement, distribution of components across the reservoir per time, and overall oil recovery. The following plots describe the distribution of bacteria in the water phase per time across the reservoir for cases with and without biofilm formation.

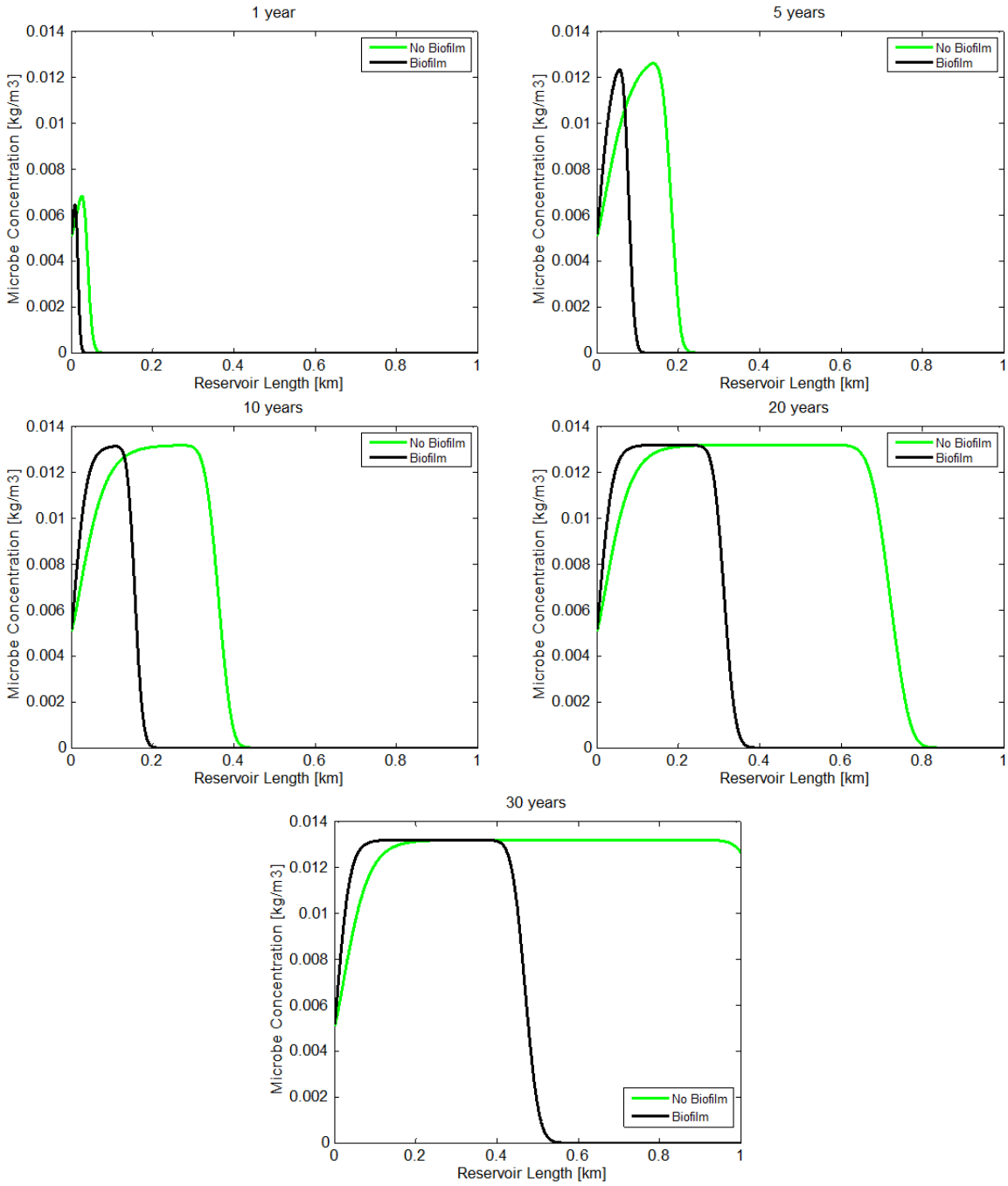

Figure 6.14: Variation in microbial concentration for the ordinary MEOR case (green) and MEOR with bacteria adsorption (black) across the reservoir length at different production times.

As we move from 1 year to 30 years of production, there is a lag in movement of bacteria when both cases are compared; hence the flowing microbes spread faster in the case of no biofilm formation than in the other case. In the former case, free bacteria attain maximum concentration before the bacteria in the latter case as shown in the *20 years* and *30 years* plots. It is suggested that some bacteria are being adsorbed on the pore walls; hence the lag in microbial movement.

Variation in the nutrient concentrations per time for both MEOR cases can be seen in Figure 6.15. Generally, nutrients seem to be concentrated at the injector end because they are mostly used up by microbes at the inlet of the reservoir.

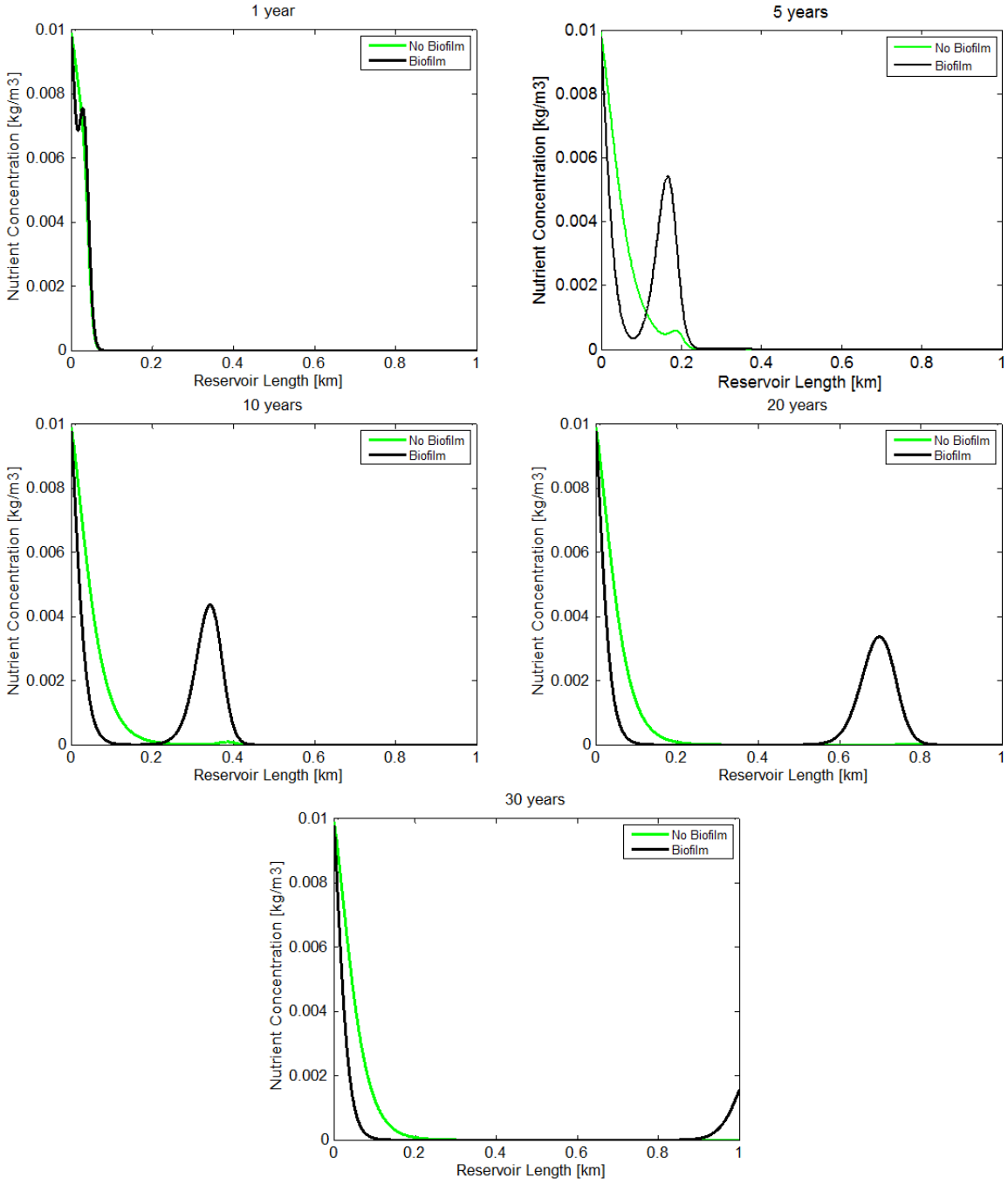

Figure 6.15: Changes in nutrient concentration across the reservoir with time. A distinct bump can be seen for the biofilm case after 5 years of production. This represents unused nutrients bypassed due to initial partitioning of bacteria between the water and the biofilm phase.

At early time of production, there is no significant difference between the two curves as they overlap quite well. However after 5 years of production, a lag in movement can be observed for the biofilm case. Additionally, for the case of biofilm formation, there is a noticeable

bump (increase) in nutrient concentration between the 100 m and 250 m section of the reservoir. This is carried on to other sections of the reservoir and eventually breaks through in late time. This bump is presumed to be what is left of the ideal nutrient curve in Figure 6.3(b) after nutrient attrition by the increased number of microbes behind the nutrient front. An illustration of this can be found in Appendix A.

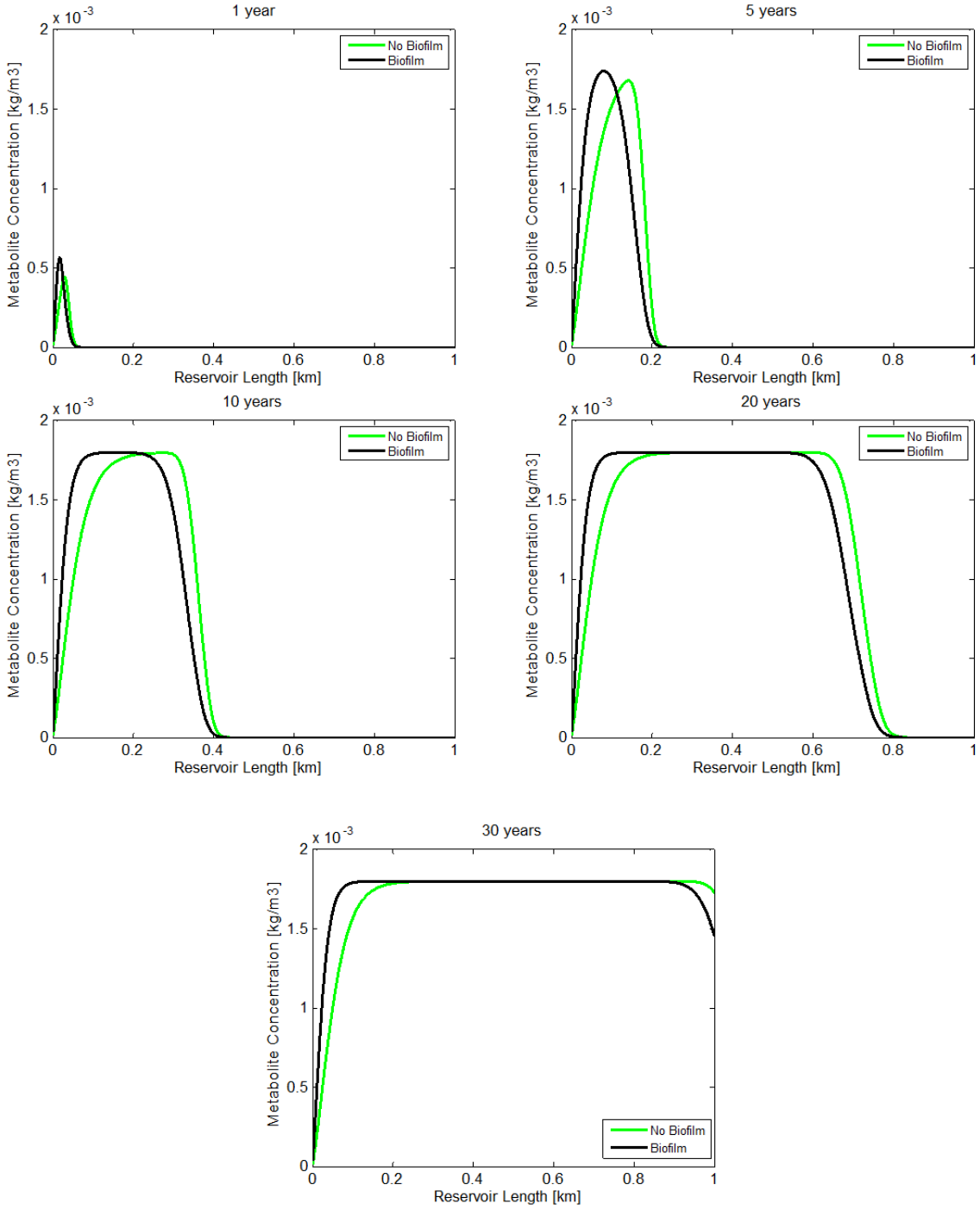

Figure 6.16: Five plots representing the change in biosurfactant concentration across the reservoir due to the effect of bacteria adsorption.

Production and movement of biosurfactants with time are shown in Figure 6.16. From the plots, it can be observed that higher concentrations of surfactants are produced per time at the reservoir inlet section for the biofilm case compared to the case of no biofilm. This would mean that more surfactants are available for IFT reduction. However, at this juncture, we cannot conclude on the efficacy of the surfactants in improving oil recovery. Moving from middle time to late time, a maximum surfactant concentration is achieved in the inner cells of the reservoir and spreads out towards the producer end. Finally, after 30 years, high concentrations of surfactants are produced at the reservoir outlet.

The water saturation plots representing fluid displacement during pure waterflooding, MEOR without biofilm and MEOR with biofilm formation are shown in Figure 6.17. Oil banks are observed in both MEOR cases. The surfactant effect is also evident in the MEOR cases as the residual oil saturation decreases with time. One major difference is the breakthrough period for all cases. Generally, water breakthrough would occur later in the MEOR cases than in the basic water flooding case since the primary MEOR fronts are behind the waterflooding front. Similar to the previous MEOR cases, water saturation behind the primary front after breakthrough is just about 15% above the initial water saturation; hence not much water is produced after the first breakthrough. This gives room for more oil represented by the oil bank to be produced. Comparing the two MEOR cases, the primary front of the biofilm case is observed to be ahead of the ordinary MEOR case; however the secondary front of the former lags behind that of the latter. Therefore, the disadvantage of an earlier breakthrough in the biofilm case is compensated for in the secondary front. The late secondary breakthrough in the biofilm case is as a result of the movement of surfactants which typically accumulate at the inlet section of the reservoir in early time and then spread out at later times. The accumulation is caused by the decrease in pore space which in turn slows down surfactant movement and allows for a wider oil bank. A wider oil bank is however not synonymous with higher recovery as shown on the recovery plot (the last plot in Figure 6.17). This is because after the primary breakthrough, water saturation behind the front in the ordinary MEOR case is slightly lower compared to the biofilm case; hence, there is more available oil to be displaced.

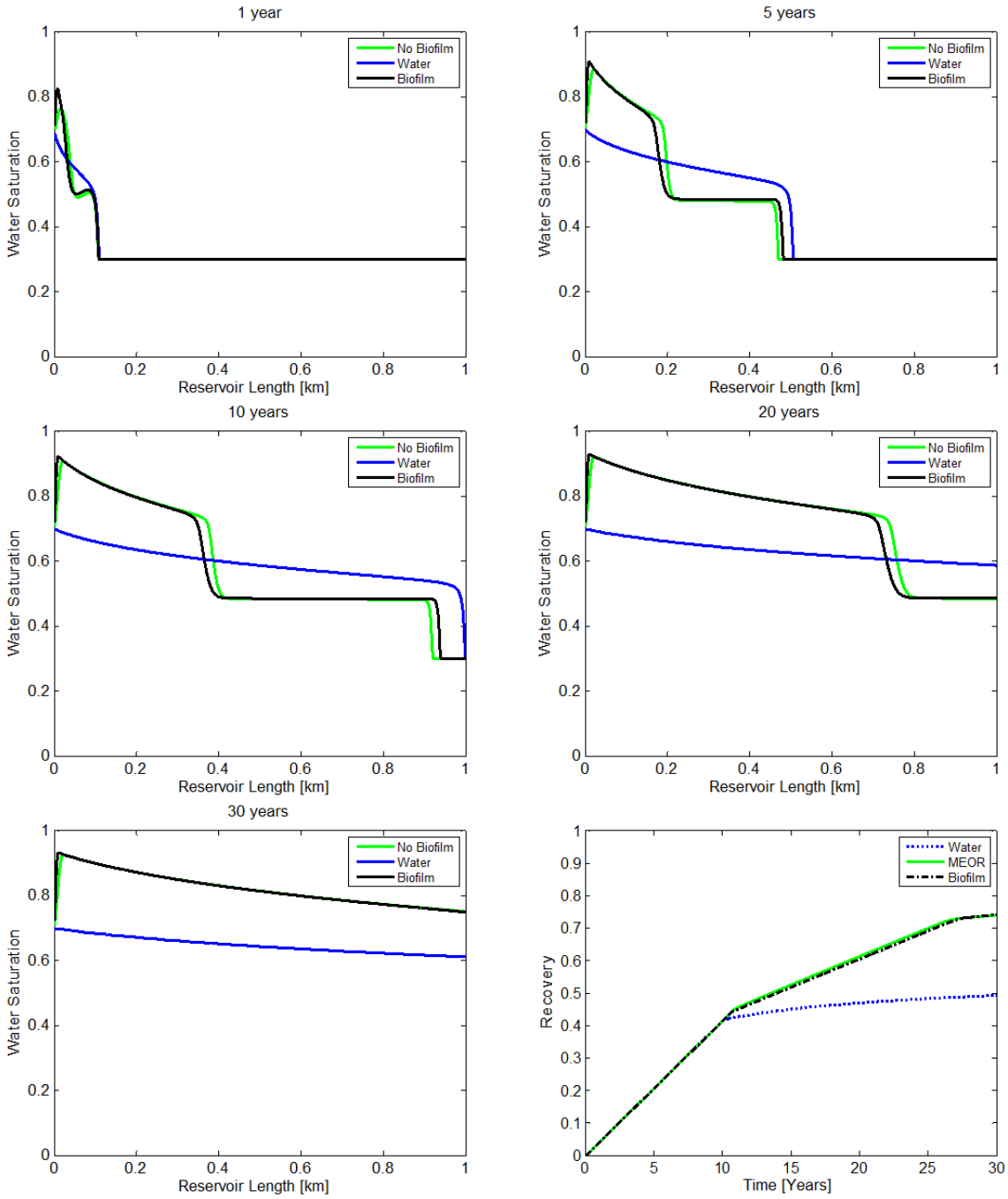

Figure 6.17: The first five plots show the saturation profiles for pure waterflooding, and MEOR with and without biofilm. Early oil mobilisation is the key difference between both MEOR cases. The sixth plot represents the variation in oil recovery with time for all cases.

Additionally, from the oil recovery plot, higher recoveries are achieved after the primary breakthrough for the case of ordinary MEOR. This advantage however is cancelled out due to the early secondary breakthrough observed for this case. As expected in late time, the biofilm recovery equals the recovery for the ordinary MEOR case and slightly surpasses it due to the latter's early secondary breakthrough. Consequently, a final recovery of 74.13 % is achieved when the biofilm effect as a result of bacteria adsorption is accounted for.

6.5.5 Biofilm – Food Adsorption

Another way in which biofilm can be formed is through the process of food adsorption. Here, some nutrients get adsorbed on the pore walls and would tend to occupy this new phase as time progresses. The effects on bacteria growth, surfactant formation and the eventual oil recovery have been investigated via reservoir simulation. Results of simulations considering this effect are quite similar to those of the bacteria adsorption case, with a few exceptions.

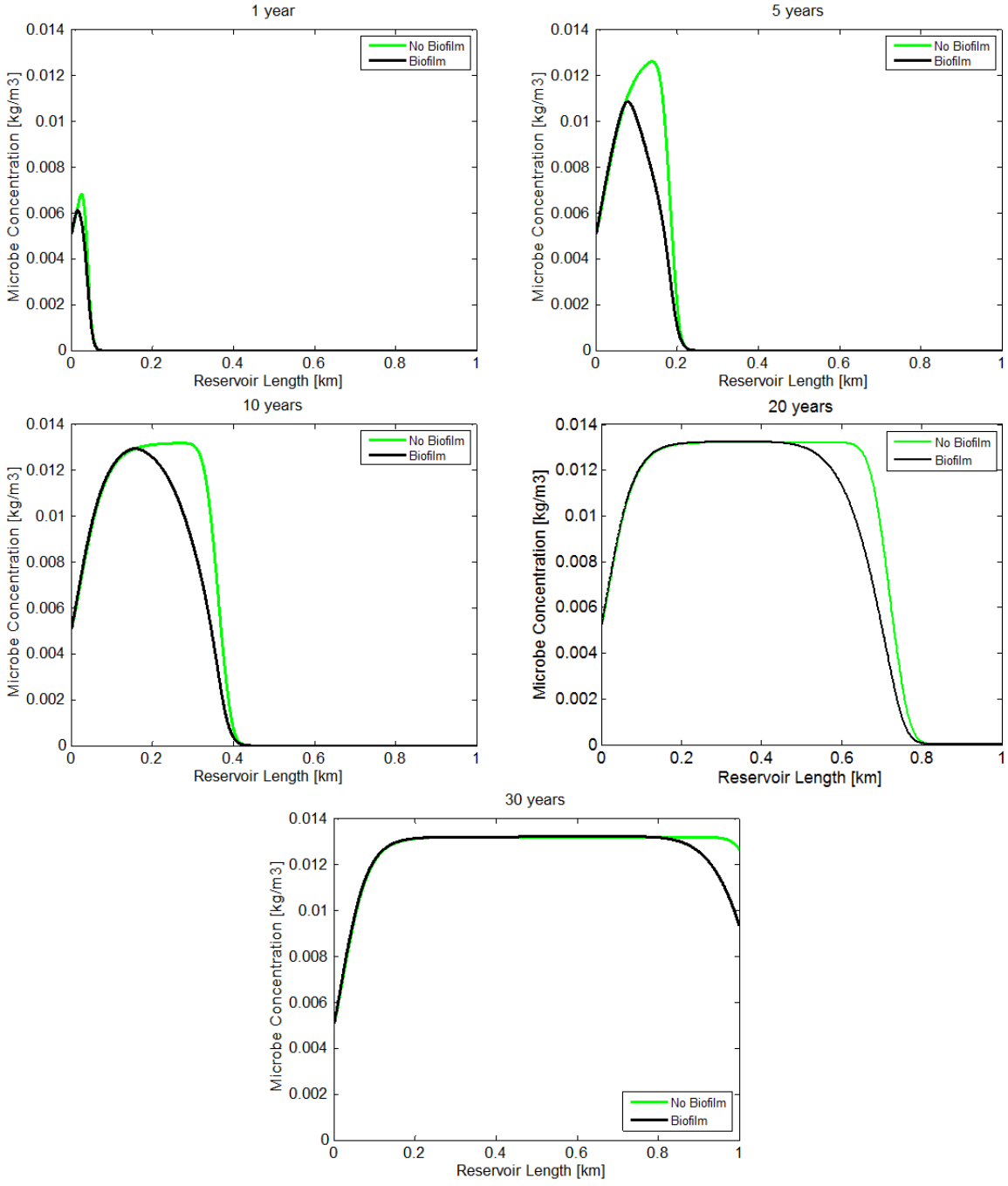

Figure 6.18: Bacteria concentration distribution for the MEOR case with (black) and without (green) food adsorption

Figure 6.18 shows an array of plots that describe the change in bacteria concentration for the ordinary MEOR case and the case of MEOR with nutrient adsorption. From this plot, it can be observed that the lack of nutrients in the flowing phase initially affects bacteria growth and population expansion. However, after bacteria breakthrough and as more nutrients are injected, the bacteria cells attain a maximum concentration within the reservoir just like in the case of ordinary MEOR.

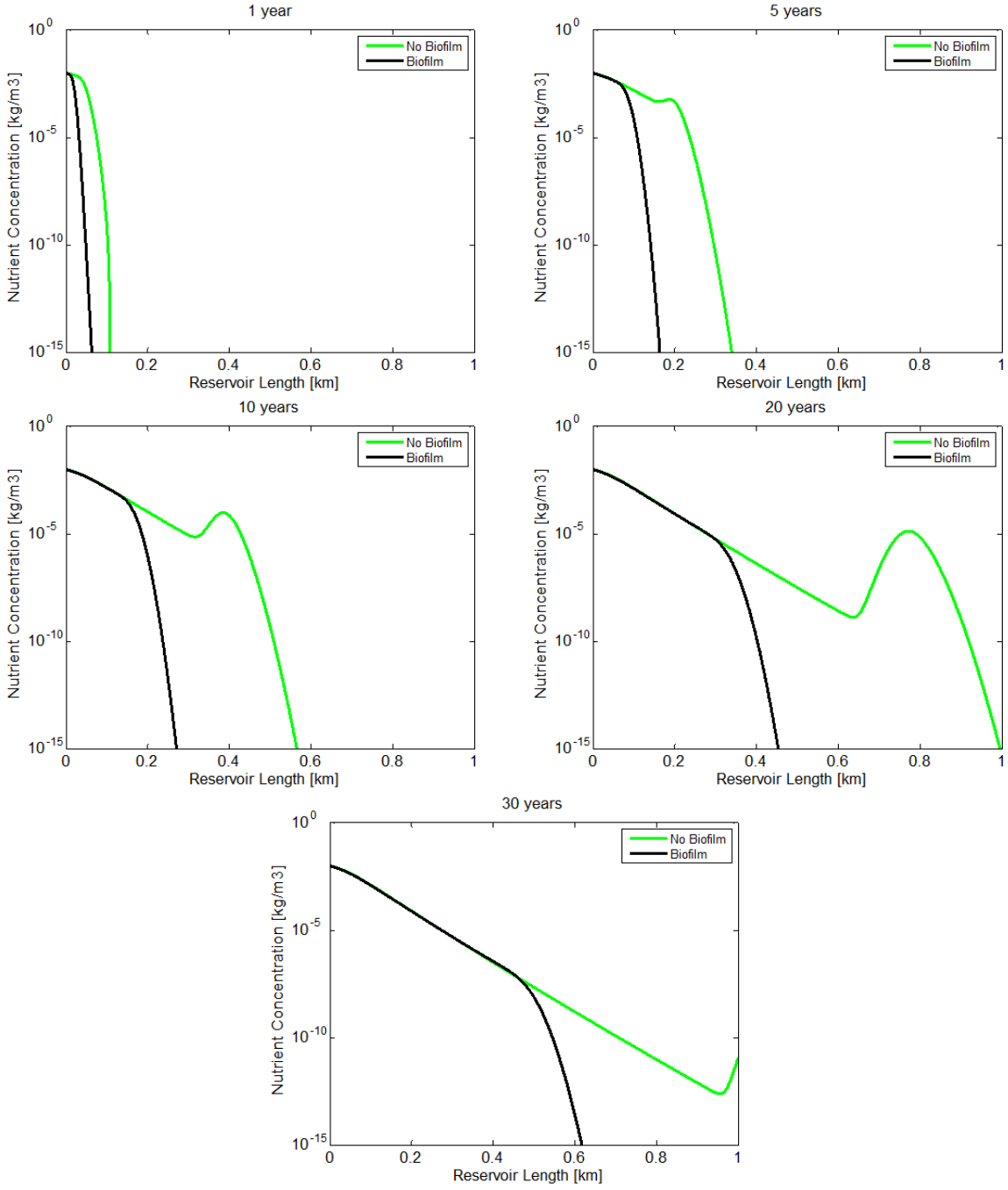

Figure 6.19: Comparison of the nutrient concentration in the water phase for MEOR cases with (black) and without (green) nutrient biofilm

A comparison of nutrient concentration for both cases is best illustrated with the semi-log plots shown in Figure 6.19. They represent the concentration of nutrients in the water phase at certain periods during oil production. After a year of production, most of the nutrients are concentrated at the inlet section of the reservoir but they spread out faster in the case of no biofilm. After 5 years, it is evident that the biofilm is being formed because the biofilm curve does not spread as fast as the ordinary MEOR curve. This difference in spread increases over time. The water phase nutrients never reach the producer end of the reservoir even after 30 years of production. They are used up as more bacteria are being injected or continue to adsorb on the pore walls. A certain dip is observed in the nutrient curve for the case of no biofilm. This becomes obvious after about 10 years of production and continues to late time. This dip could be as a result of late utilisation of nutrients by bacteria behind the nutrient front resulting in a sudden decrease in nutrient concentration behind the front. Plots depicting the amounts of adsorbed nutrients per time compared to the total number of nutrients within the reservoir (sessile + free floating) can be found in the Figure A.2 in Appendix A. The main approach to food adsorption as well as in the bacteria adsorption case is that there is an almost equal distribution of these components between the water and biofilm phases (Nielsen, 2010).

Interestingly, more surfactants are produced in the case of food adsorption as compared to ordinary MEOR (see Figure 6.20). To explain this, we start by mentioning that smaller amounts of nutrients will be swept by the moving water front in the case of biofilm formation than in the ordinary MEOR case because some nutrient get adsorbed. This retardation in nutrient flow to the producer will enable the bacteria to harness more available nutrients for metabolite production. The main question to answer is whether the availability of more surfactants will lead to a greater effect on IFT reduction accompanied by reduction in residual oil saturation. To answer this question, we take a look at the saturation profiles represented by the plots in Figure 6.21. First, it is observed that biofilm formation retains the oil bank phenomenon witnessed in the ordinary MEOR case. Secondly, after 5 years of production, it evident that the residual oil saturation at the reservoir inlet for the biofilm case is lower than that of the ordinary case due to the accumulation of surfactants which causes an early mobilisation of oil at the inlet section.

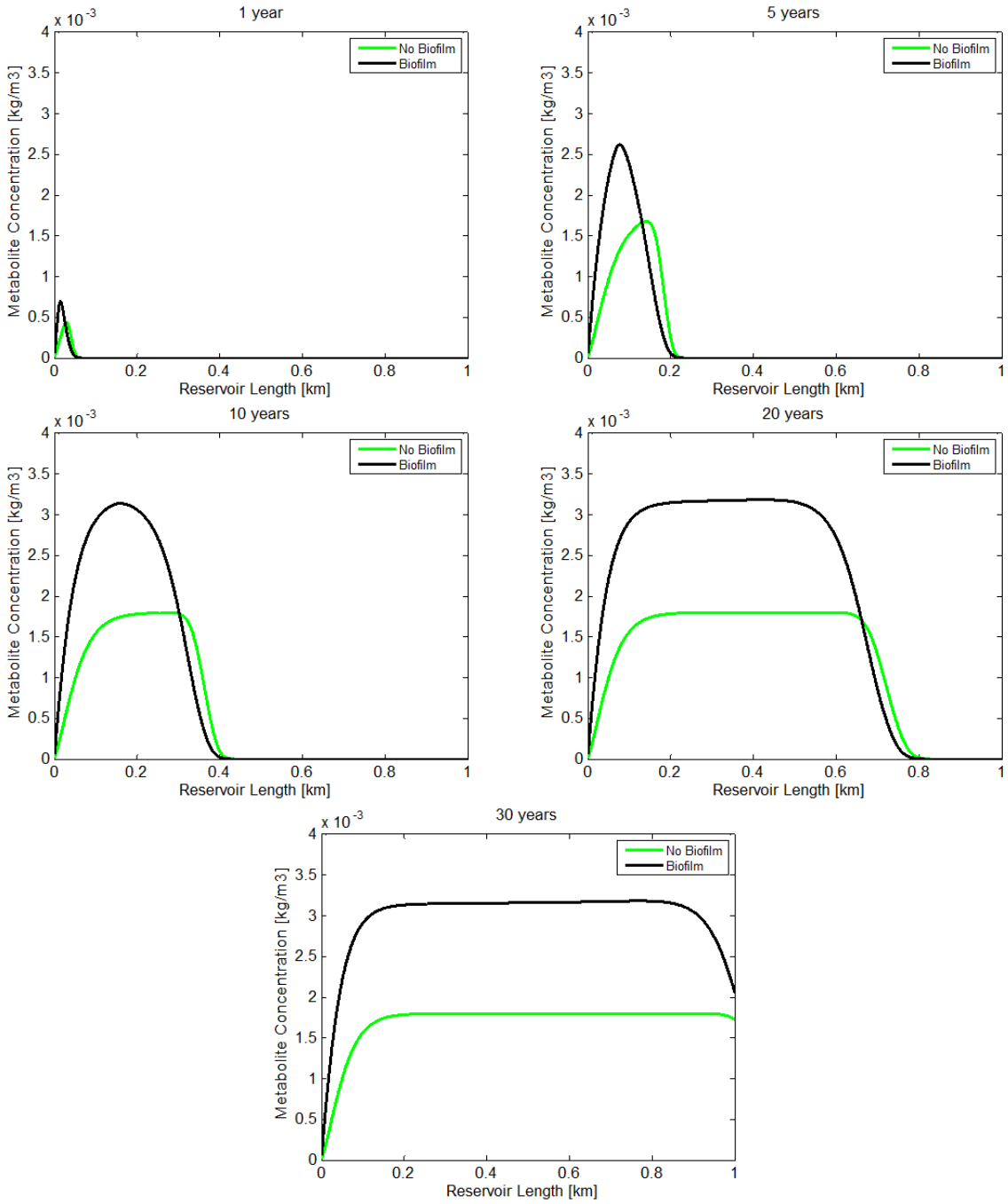

Figure 6.20: Surfactant concentration distribution across the reservoir for the MEOR with and without nutrient adsorption showing. A significant difference in concentration between both cases can be observed.

The water saturation profile follows the same trend as in the case of bacteria adsorption with a relatively early primary breakthrough for the biofilm case and a relatively early secondary breakthrough for ordinary MEOR case. The trend in oil recovery shown in Figure 6.21 is similar to that of bacteria adsorption. This biofilm case resulted in an additional recovery of about 0.16% when compared to the ordinary MEOR case. It is important to mention here that if production time is extended and as more nutrients are injected, the recovery from the case of biofilm formation will significantly exceed that of the ordinary MEOR case as a result of

the occurrence of microscopic fluid diversion due to pore throat blockage which typically commences when the biofilm phase occupies about 20% or more of the pore space (Nielsen, 2010). Hence, previously bypassed oil will be swept by the injected water. However in an economic sense, the case without biofilm may suffice because more oil will be produced at middle production time (11 to 26 years) as shown on the recovery plot.

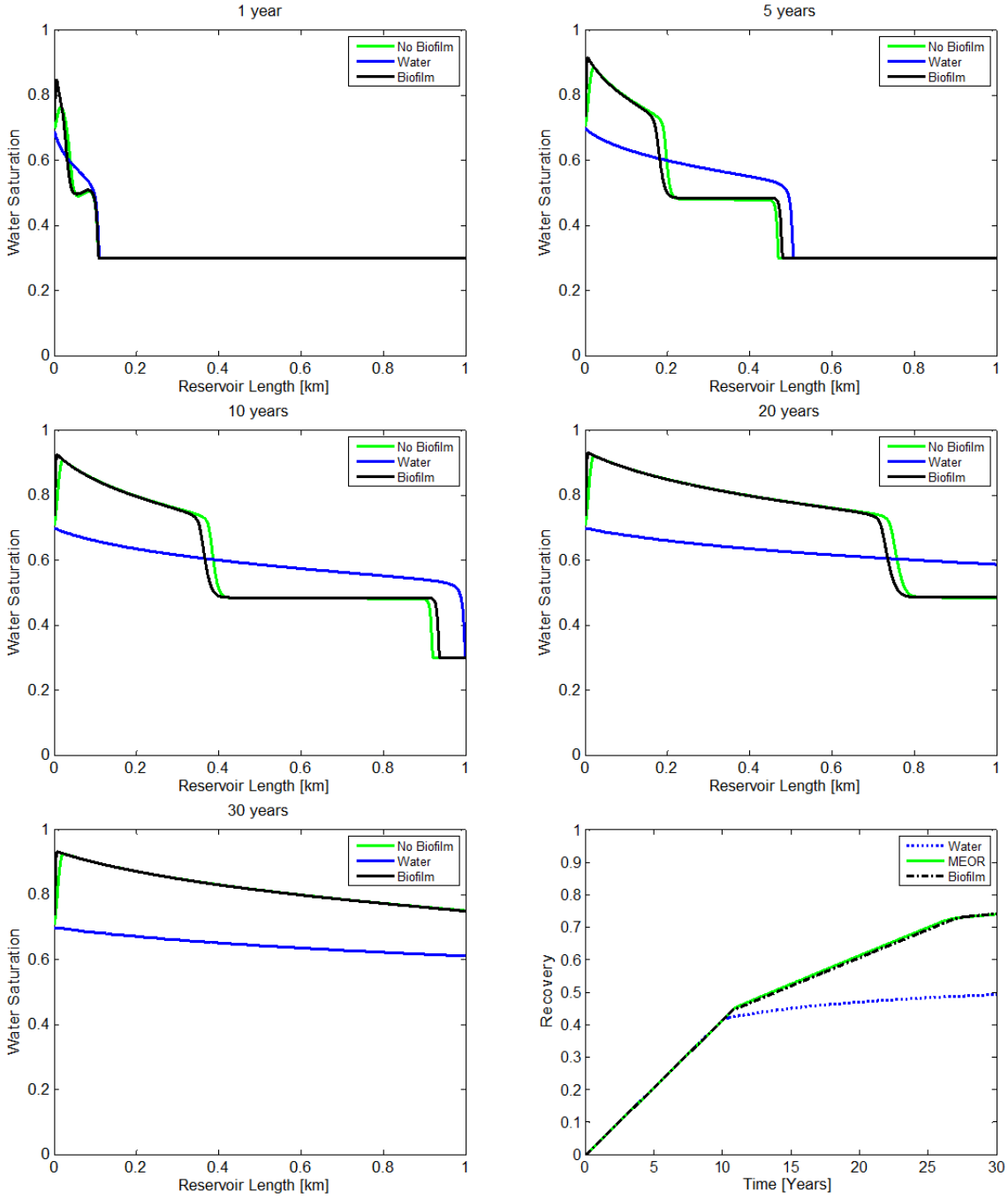

Figure 6.21: The first five plot show a comparison of the water saturation profiles during pure waterflooding, and MEOR with and without biofilm adsorption. The last plot illustrates the oil recovery associated with the three cases.

6.6 Sensitivity Analysis – Single Bacteria Species

The choice of values of variables that directly or indirectly affect the efficiency of the microbial EOR displacement process is a very important aspect of reservoir simulation. The sensitivity of simulation results to the range of values that these variables can be assigned has been analysed. The impact of parameters such as microbe and nutrient concentrations in the injection stream, the maximum specific growth rate for both microbes and metabolites ($\mu_{max,b}$ and $\mu_{max,m}$), and the Langmuir constants (ω_1 and ω_2) on oil recovery via MEOR have been studied.

6.6.1 Bacteria and Nutrient Injection Concentration

The concentrations of the components in the injection stream have been varied between the ranges of 5×10^{-5} kg/m^3 to 5 kg/m^3 for bacteria and 10^{-5} kg/m^3 to 10 kg/m^3 for nutrients as highlighted in Nielsen (2010). Several simulations involving different combinations of these parameters were run. Increments of one order of magnitude were used. The results of this analysis can be found in Table A.1 in Appendix A.

The results from this table show that an optimal combination of nutrient and bacteria concentration via MEOR without biofilm formation is attained with a nutrient concentration of 0.1 kg/m^3 and a 0.05 kg/m^3 bacteria concentration. This would lead to a final recovery of about 74.35 % of the oil in place (OIIP). It should be stated here that results for simulations with bacteria and nutrient concentrations of 5 and 10 kg/m^3 respectively could not be generated by MRST because a solution could not be found. Another important comment on this investigation is that this analysis should be subject to economic considerations because a slight increase in recovery due to extra amounts microbes and nutrients may or may not lead to a disproportionate increase in cost. In order to understand the reason for an incremental recovery of 0.33 % compared to the base case. The saturation and oil recovery plots for both cases were compared as shown Figure 6.22.

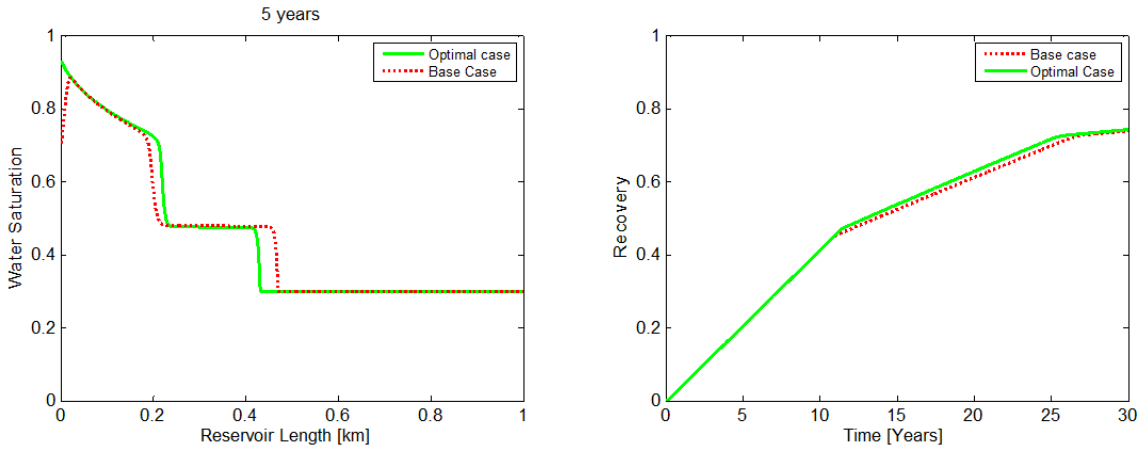

Figure 6.22: Comparison of the resulting water saturation profiles and oil recovery curves from simulations with nutrient and bacteria concentration specifications for the base case and the optimal case.

From the saturation plot, it can be seen that higher feed concentrations of bacteria and nutrients characteristic of this optimal case result in early mobilisation of oil right from the inlet of the reservoir. The high inlet concentrations allow for instant surfactant production which results in early oil mobilisation. Hence, S_{or} at the inlet is already around 7 % for the optimal case. This early creation of an oil bank means that more oil will be produced after primary breakthrough as shown on the recovery plot.

Since bacteria and nutrients contribute to the formation of biofilm, sensitivity analyses on their concentrations during MEOR with adsorbed bacteria and adsorbed nutrients respectively were carried out. The results can be found in Tables A.2 and A.3 in Appendix A. The trend is the same as that observed in the case of no biofilm.

6.6.2 Maximum Growth Rate

The maximum growth rate of bacteria cells is a major factor in determining the increase in bacteria concentration in conjunction with the production of metabolites as by-products of the biochemical reaction that takes place during feeding. From a base value of μ_{max} = 0.2 day^{-1} for both components used in the main study, a range of values spanning 0.02 to 20 day^{-1} was used. MRST could not arrive at a physical solution for μ_{max} = 20 day^{-1}; hence, this value was discarded. Table 6.2 shows the results of the simulation cases.

Table 6.2: Results from the sensitivity analysis on the effect of bacteria and metabolite maximum growth rates.

$\mu_{max,b}$ [day^{-1}]	$\mu_{max,m}$ [day^{-1}]	Oil Recovery [%]
0.02	0.02	71.28
	0.20	63.08
	2.00	50.33
0.20	0.02	74.00
	0.20	74.02
	2.00	64.16
2.00	0.02	74.32
	0.20	74.32
	2.00	74.31

Two combinations of $\mu_{max,b}$ and $\mu_{max,m}$ resulted in a maximum oil recovery of 74.32 % this is a 0.30 % improvement on the base case oil recovery. Therefore, a combination of either $\mu_{max,b}$ = 0.02 day^{-1} and $\mu_{max,m}$ = 2 day^{-1} or $\mu_{max,b}$ = 0.2 day^{-1} and $\mu_{max,m}$ = 2 day^{-1} would be most appropriate. Keeping all other variables constant, the saturation and recovery plots derived from the former set of values are shown below:

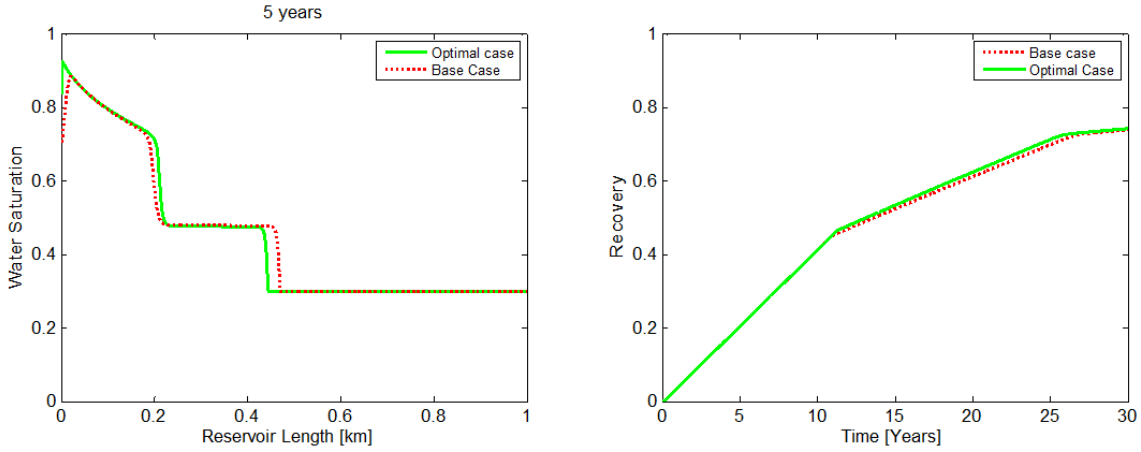

Figure 6.23: Comparing saturation profiles and oil recovery curves derived from base case and optimal maximum growth rate specifications.

These plots are very similar to the optimal feed concentration results. Early oil mobilisation occurs when metabolite growth rate is highest. This means that surfactants get to be produced at the inlet of the reservoir at very early time.

6.6.3 Surfactant Partitioning

Nielsen (2010) proposed an innovative approach to surfactant partitioning using a distribution coefficient D_i that allows for dispersal of metabolites between the oil and water phase. This constant controls, and therefore, determines the amounts of biosurfactants in the water phase that would be available for IFT reduction. The base value used in this study is unity. An analysis has been done on the overall effect of this constant on oil recovery, by taking a range of two orders of magnitude forward and backwards. The results are shown below:

Table 6.3: Final oil recoveries derived from different distribution coefficients.

D_i	Oil Recovery [%]
0.01	51.93
0.1	73.21
1	74.02
10	74.09
100	74.10

From this result, it is confirmed that higher values of the distribution coefficient will result in additional recovery as more surfactants will be able to occupy the water phase. Maximum recovery is achieved with D_i equal to 100 which gives an additional recovery of 0.08% with respect to the base case (D_i = 1). The difference from the base case is not very substantial and going by the trend in oil recovery, increasing the maximum D_i by one more order of magnitude would not cause any significant change in recovery.

6.6.4 Effect of Langmuir Constants

The Langmuir adsorption isotherm constants ω_1 and ω_2 were varied within a range of two orders of magnitude. Therefore, a set of $\omega_1 = \{10^{-5}, 10^{-4}, 10^{-3}, 10^{-2}, 10^{-1}\}$ was used for the first constant while the following set; $\omega_2 = \{1.7 \times (10^{-5}, 10^{-4}, 10^{-3}, 10^{-2}, 10^{-1})\}$ was used for the second constant. The effect of these constants on oil recovery via MEOR with biofilm formation (both bacteria and nutrient adsorption) was studied. Results from the analysis with different combinations of ω_1 and ω_2 revealed that these constants do not have an impact on simulation results. Oil recovery remained at its base case value of 74.13 % for bacteria adsorption and 74.18 % for food adsorption. This is due to the limitation of the biofilm model developed by Amundsen (2015) which does not account for heterogeneity in porosity and permeability that occurs during biofilm formation. Therefore according to the model, for a

particular instantaneous water phase bacteria (or nutrient) concentration, the adsorbed bacteria (or nutrient) concentration remains unchanged and is invariant to the Langmuir constants.

6.7 Microbial Competition

Bacteria competition within a reservoir has been modelled with the assumption that the indigenous microbes are free to move to sections where they can get necessary nutrients. Initial parameters for single-species modelling have been modified; these can be found in the following table.

Table 6.4: Revised parameters used for the scenario of microbial competition

Parameter	Value
$\mu_{max,b1}$, $\mu_{max,b2}$	0.2 day^{-1}
$\mu_{max,m}$	0.2 day^{-1}
K_{bn} (for both species)	1 kg/m^3
K_{mn}	1 kg/m^3
Y_{b1}	0.4
Y_{b2}	0.4
Ym	0.2
$C_{b2,initial}$	5×10^{-4} kg/m^3
δ	0.2 day^{-1}

Since this model has not been built and applied previously, the results could not be compared with other studies but have been analysed based on basic scientific principles. First the effect of the presence of indigenous bacteria on the microbial distribution with time will be discussed. Afterwards, the nutrient concentration across the reservoir will be analysed to determine whether bacteria competition will affect the metabolic activities that require nutrient ingestion. Moving on, the saturation profiles for the completion case and the single species case will be compared. The contrasts and similarities will also be highlighted. Oil recovery is expected to be affected by the presence of indigenous species. This will also be discussed.

6.7.1 Discussion of Microbial Competition Simulation Results

The following figure shows an array of plots that describe the distribution of indigenous and exogenous bacteria across the entire length of the reservoir for different production periods.

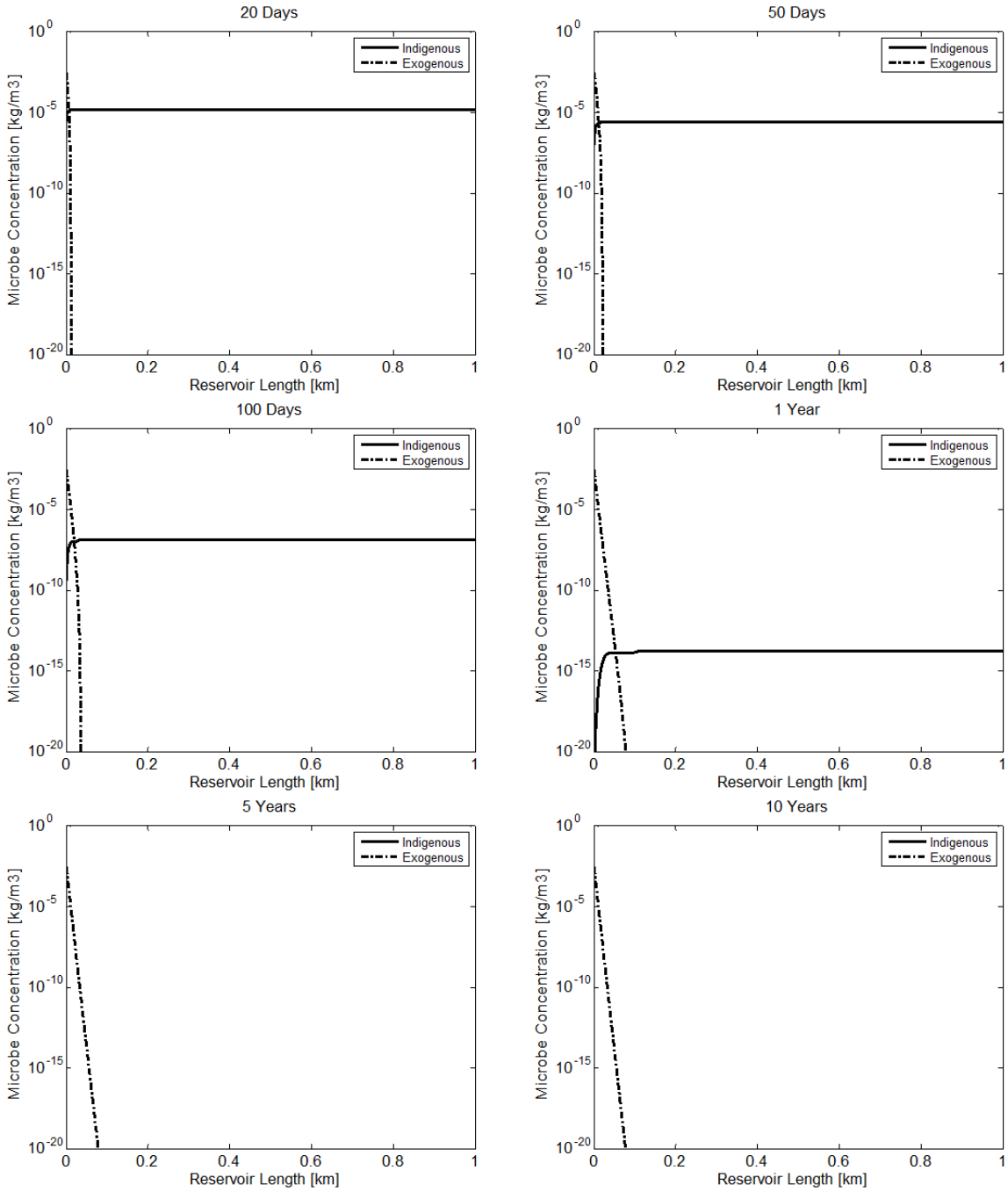

Figure 6.24: Indigenous and exogenous bacteria concentration distribution at different production times.

From these semilog plots, it can be observed that both bacteria populations do not grow but decline with time. The high concentration of exogenous bacteria at the inlet section of the reservoir is due to the continuous injection of new species into the reservoir. Hence, it can be inferred that both species flow towards the producer without any meaningful effect on oil displacement. At this juncture, it can be inferred that microbial competition inhibits the growth of both bacteria species leading to a total washout of microbes.

Figure 6.25 shows the nutrient concentration at specfic periods. From this plot, it can be observed that at early time, nutrient concentration increases but the nutrients are restricted to the inlet section. Comparing this with the plots in Figure 6.24 indicates that the competition between the microbial species does not allow for sufficient movement of nutrients as well as foreign microbes further into the reservoir. However, at later periods, when the indigenous microbes have been washed out, the nutrient concentration reaches a maximum and starts to spread out across the reservoir.

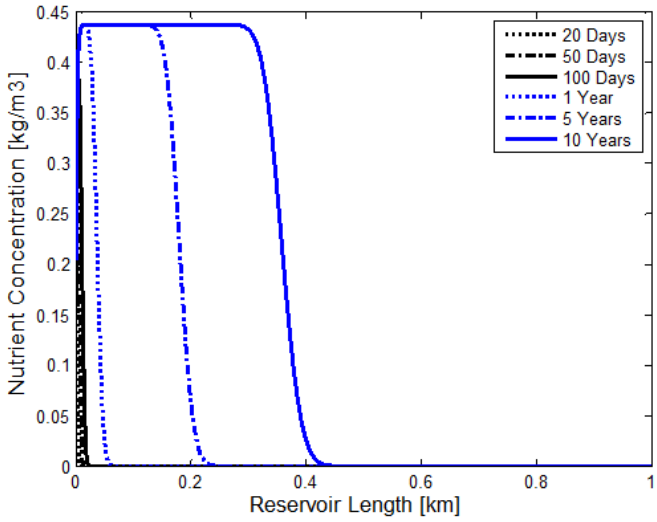

Figure 6.25: Nutrient concentration across the reservoir from early time to mid-production time for the case of microbial competition.

The model for microbial competiton allows for surfactant production by both bacteria species. Taking a look at Figure 6.26, the trend in surfactant production can be observed over time. From the start of production, bacteria are able to produce metabolites in small amounts. These metabolites in the form of biosurfactants tend to spread across the reservoir over time. Therefore it means that both species use up some nutrients for metabolism alone and not for growth. This might be because certain nutrient requirements for growth have not been met according the limiting nutrient approach used in Monod kinetics. This implies that the use of surfactants in lowering IFT between oil and water will not be effective. This could happen if the surfactant concentration is not up the threshold concentration required for the commencement of IFT reduction. In Section 4.2, it has been identified that this threshold surfactant concentration for *Surfactant A* type is between 10^{-5} and 10^{-4} kg/m^3. Therefore comparing this value to the maximum surfactant concentration on the plot, it can be observed that the threshold concentration could be attained in late time. At this point, it can be inferred

that this situation would also affect oil recovery because the IFT reduction effect of surfactants would be minimal.

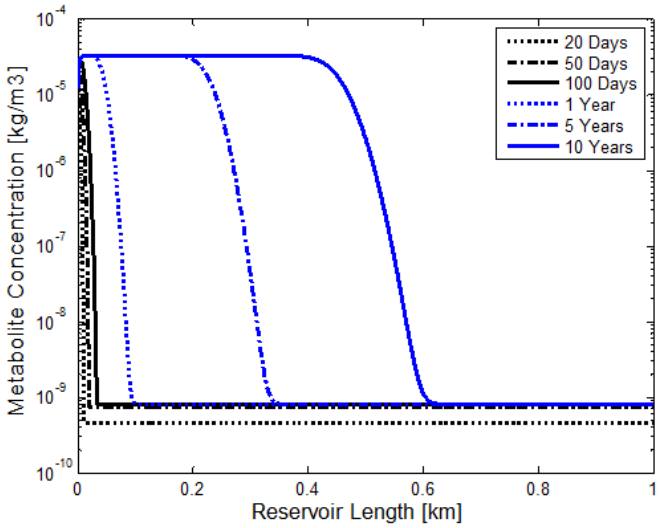

Figure 6.26: Surfactant concentration profile across the reservoir from early time to mid-production time for MEOR with microbial competition.

Taking a look at the saturation plots for pure waterflooding, the single-species MEOR system and the competitive MEOR system at different production periods (Figure 6.27), it is initially observed that the oil bank created in the single-species case is virtually non-existent in the microbial competition curve. However, after five years, there is a slight dip in the part of the curve behind the front. This could be the oil bank that should have been more evident in the absence of microbial competition. The dip is carried on until it breaks through at the producer end and as such, it is expected that there would be a slightly higher oil production compared to pure waterflooding. Another interesting feature of the saturation profile is that the water breakthrough times for the bacteria competition case and pure waterflooding are approximately the same. This means that bacteria growth which allows for lower water mobility is non-existent as the bacteria species get washed out without reproducing. In late production time, as shown on the *30 years* plot, the saturation profile for the two-species system becomes unstable as the water saturation increases at the producer end. This could be better explained if a 2-D or 3-D scale was used. Unstable fronts during water floods could happen as a result of viscous fingering; however this has been ruled out because the oil viscosity specified is that of light oil (μ_o = *3cp*) and this would have been noticed at early production times. The most likely explanation for this is that the surfactant effect does not commence until very late in production time; hence there is a decrease in residual oil at the exit of the reservoir. A final recovery of about 50.94 % of the OIIP was achieved due to the

adverse combination of early water breakthrough, minimal surfactant effect and bypassing of producible oil (last plot in Figure 6.27). Comparing this result with the one-species case, there is a decline of about 23.08 % when the effect of indigenous bacteria is considered.

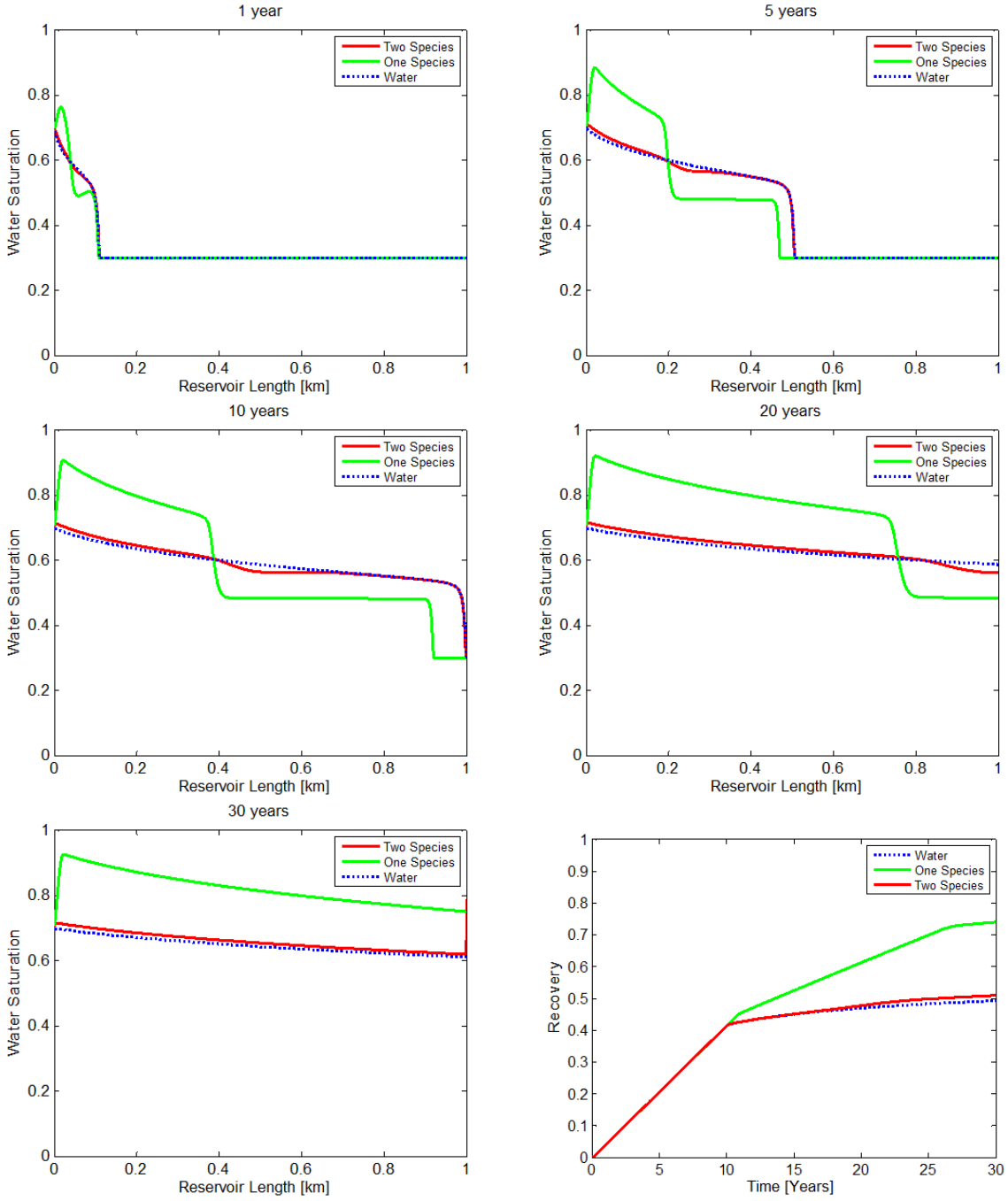

Figure 6.27: Water saturation profiles for the base MEOR case (green) and MEOR with microbial competition (red). The final plot is the oil recovery curves for pure waterflooding and the two MEOR cases.

In the next section we will discuss the sensitivity of the choice of input parameters used in this model and their influence on the simulation results for oil displacement via MEOR.

6.8 Sensitivity Analysis – Microbial Competition

The choice of input parameters is very important in simulation studies. Simulation results from microbial competition modelling have been observed to be sensitive to some input parameters like the dilution rate, the concentration of injected bacteria and nutrients, the initial concentration of indigenous microbes and the maximum specific growth rate of both bacteria species.

6.8.1 Initial Concentration of Indigenous Microbes

In the base case simulation of the microbial competition model, an initial concentration of 5×10^{-5} kg/m^3 of indigenous microbes was specified. This value was chosen such that the effect of these species would be as minimal as possible on oil recovery so that they do not overly inhibit the MEOR process. For the sensitivity analysis, a set of indigenous bacteria concentrations were applied to the model to investigate its effect on simulation results. The following table summarizes the several simulation cases that were run:

Table 6.5: Variation in final oil recovery for different initial indigenous bacteria concentrations

Indigenous Bacteria Conc. [kg/m^3]	Oil Recovery [%]
5×10^{-6}	50.94
5×10^{-5}	50.94
5×10^{-4}	50.94
5×10^{-3}	50.95

The table reveals that the initial concentration of the indigenous bacteria is not a major determining factor that affects oil recovery. In the end, the highest physically allowable value of indigenous bacteria concentration (5×10^{-3} kg/m^3) did not result in a significant increase in recovery. Therefore, it can be implied that the very existential presence of these microbes is what inherently affects the ease of diffusion of the injected microbes within the reservoir.

6.8.2 Exogenous Bacteria and Nutrient Concentration

Keeping all other input parameters constant, the nutrient and bacteria injection concentrations were varied similar to the case of the one-species system. Base case values used in the initial simulation were 0.005 kg/m^3 for exogenous bacteria and 0.01 kg/m^3 for nutrients. A range of values spanning six orders of magnitude were used resulting in 36 possible combinations of

nutrients and bacteria injection concentrations. A summary of simulation results can be found in Table A.4 in Appendix A.

From the table, it is observed that at higher concentrations of exogenous bacteria and nutrients, oil recovery increases to values approaching and even higher than single bacteria system values. It is also evident that the bacteria concentration mostly affects the simulation calculations and results. This is because for a certain value of nutrient concentration, an increase or decrease in the exogenous bacteria concentration results in a corresponding increase or decrease in final oil recovery. The maximum obtainable oil recovery therefore is dependent on the highest physically permissible exogenous bacteria concentration (i.e. 0.5 kg/m^3 in this case). This means that there will be higher amounts of exogenous bacteria available to produce biosurfactants necessary for improved oil recovery. Microbial competition can therefore be said to be virtually non-existent at high concentrations of exogenous bacteria.

Results from the injection combination 0.5 kg/m^3 of bacteria and the base case amount of nutrients (i.e. 0.01 kg/m^3) resulted in the plots shown in Figure 6.28. The saturation profile for the two-species case now seems to assume the normal MEOR case with the occurrence of two water fronts and therefore, an oil bank. The residual oil saturation at the reservoir inlet is already reduced at early time leading to an early mobilisation of trapped oil. The base case residual oil saturation does not change significantly due to the minimal biosurfactant effect. Water breakthrough for the optimal case comes much later than the base case of microbial competition. This implies that there is a more efficient primary sweep of oil by the first water front. This scenario depicts the third eventuality highlighted in Section 4.4 such that exogenous bacteria dominate and gain access to the available nutrients causing indigenous bacteria population to be washed out without growing. A final oil recovery of 74.35 % was achieved with this optimal scenario.

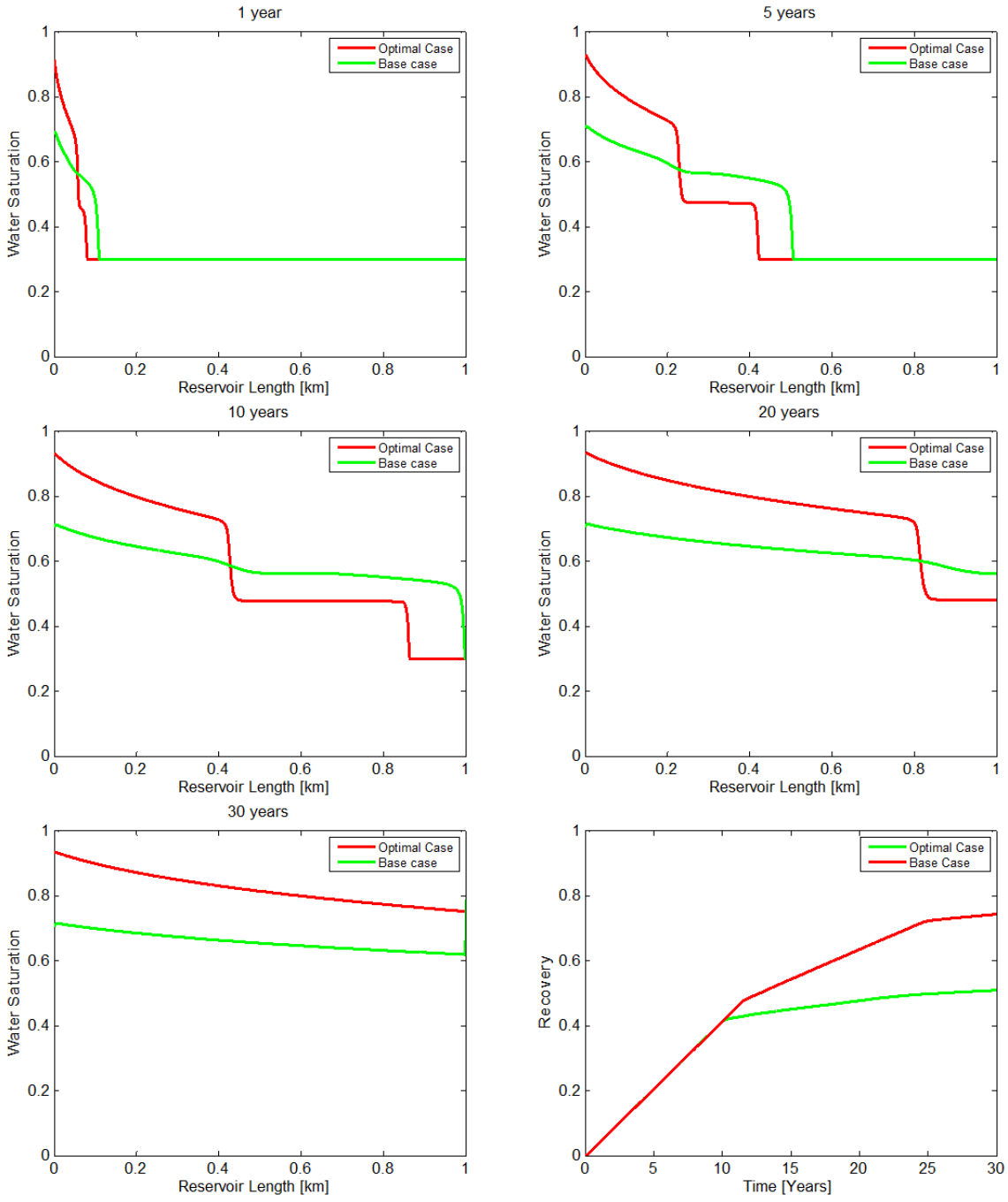

Figure 6.28: Saturation profiles and oil recovery plots for the base and optimal cases of microbial competition. The optimal case assumes the form of the single species case such that the exogenous bacteria are dominant.

6.8.3 Dilution Rate Effect

The dilution rate determines the ease at which feed components disperse within the reservoir. For the base case simulation and as an initial starting point, it was assumed that the dilution rate is equal to the maximum growth rate for both bacteria species. This however resulted in high dispersion of bacteria species such that they could not interact and produce enough metabolites for growth. In order to determine the effect of this parameter on oil displacement,

seven simulations were implemented using a range of values from $\delta = 2\times10^{-5}$ day^{-1} to $\delta = 20$ day^{-1}. The results are tabulated below:

Table 6.6: The effect of the dilution rate on final oil recovery

δ [day^{-1}]	Oil Recovery [%]
2×10^{-5}	74.04
2×10^{-4}	74.04
2×10^{-3}	74.03
2×10^{-2}	70.70
2×10^{-1}	50.94
2	49.44

Due to physical constraints, MRST could not arrive at a solution for the last simulation case with $\delta = 20$ day^{-1}. From the tabulated results, it can be observed that lower values of the dilution rate result in higher oil recovery. This is because at lower dilution rates, injected microbes would have more time to get dispersed in the reservoir and not get washed out before they feed on the nutrients. However, at 2×10^{-4} day^{-1}, a maximum recovery has already been attained; therefore decreasing δ further would result in no significant change in recovery. Interestingly, the maximum recovery is almost equal to the oil recovery value obtained for the single bacteria species case. It would have been the same if the yield coefficient for metabolites was 18% as used in the one-species case. This means that the system approaches no competition (i.e. a single bacteria species) as the dilution rate approaches zero. This was confirmed by using a value of zero for the dilution rate, using the same yield coefficients as the base case, and eliminating the initial state of indigenous microbial concentration in the model. The results were the same as those derived for a single bacteria system.

6.8.4 Maximum Growth Rate Effect

As a base case specification, the maximum growth rate for both species was assumed to be the same. In order to determine the effect of these parameters on oil recovery, other values were specified with increasing and decreasing orders of magnitude from the base values. Results from this analysis are shown in the table below:

Table 6.7: The sensitivity of oil recovery to indigenous and exogenous maximum growth rates

$\mu_{max,b1}$ [day^{-1}]	$\mu_{max,b2}$ [day^{-1}]	Oil Recovery [%]
0.02	0.02	50.92
	0.20	50.94
	2.00	51.20
0.20	0.02	50.92
	0.20	50.94
	2.00	51.20
2.00	0.02	50.92
	0.20	50.94
	2.00	51.20

Keeping all other input parameters constant, there seems to be not much of a change in oil recovery with several combinations of maximum growth rate values. However, it can be observed that the oil recovery is sensitive to a change in the value of the $\mu_{max,b2}$ irrespective of the value of $\mu_{max,b1}$. Actually, this makes practical sense because the exogenous bacteria are the major contributors to metabolite production that help to improve oil recovery due to their high concentration. Consequently, simulation results can be described as being invariant to the maximum growth rate of the indigenous bacteria.

7 Conclusion and Recommendations

This work has been implemented by investigating important mechanisms encountered during one-dimensional flow in a reservoir produced by the action of microbial enhanced oil recovery. Bacteria and nutrient injection into the water phase of an oil reservoir has been studied. Two major scenarios have been investigated – the first involving a single bacteria species and the other involving microbial nutrient competition between injected (exogenous) and indigenous bacteria species. This chapter highlights the salient deductions drawn from the project results and proposes suggestions for further studies.

7.1 Conclusion

MRST was used as a tool for one-dimensional simulations of both waterflooding and MEOR models. Simulation results in the form of plots have been elaborately discussed. On the basis of these results, it is acceptable to state that MRST is a suitable simulation tool that provides the flexibility required for MEOR simulations. New MEOR scenarios can be modelled and simulated using this tool without any compromise on the software's performance.

The change in the interfacial tension between oil and water due to the production and effect of biosurfactants is a major MEOR mechanism for oil displacement by water. This results in the mobilisation of capillary-trapped oil and therefore the creation of a travelling oil bank in the water saturation profile across the reservoir. This effect alone leads to incremental recovery of about 25.01 % over results from pure waterflooding. Combining metabolite production with growth slightly reduces this value to about 24.74 % because nutrients would be expended for the dual purpose of growth and metabolism.

Bacteria adsorption on the pore walls resulting in the formation of a biofilm has shown to have a significant effect on oil recovery due to very early oil mobilisation right at the inlet of the reservoir. The model for nutrient adsorption also follows the trend of bacteria adsorption but gives slightly higher recoveries due to an advantageous combination of the biofilm effect and the availability of more bacteria in the water (flowing) phase.

The presence of an indigenous bacteria population within the reservoir can limit the performance of the MEOR process. This could lead to the worst case of a total washout of microbes when injection concentrations of exogenous bacteria are low. Oil recovery in this

case would almost assume that of pure waterflooding. However, at high concentrations of injected microbes, competition becomes non-existent as indigenous bacteria cells are unable to harness nutrients and are therefore washed out. Oil recoveries for this best case assume base case figures for a single bacteria population within the reservoir.

Like most reservoir simulation studies, results are sensitive to specific input parameters and variables. The first is the injection concentration of the feed components. Higher injection concentrations lead to higher recoveries. However, there are physical limits to the definition of values for these parameters. Generally, bacteria injection concentrations above 0.5 kg/m^3 and injection concentration above 1 kg/m^3 for nutrients do not give any physical solution with MRST. Other variables like the maximum growth rates for bacteria and metabolites, the surfactant distribution coefficient and the dilution rate of bacteria species within the reservoir have varying degrees of effect on the simulation results. Specifications for the Langmuir constants do not affect the simulation results because the biofilm model does not account for a porosity and relative permeability modification which would lead to a change in surface area available for biofilm formation.

7.2 Recommendations for Future Work

Several assumptions have been made to suit the purpose of this thesis work. These have resulted in the creation of idealistic models. Going further, studies should be more focused on creating practical models by incorporating actual reservoir geometries and properties. This will go a long way in helping to identify the deficiencies in these models thereby creating room for more robustness.

Two- and three-dimensional MEOR modelling and simulation should be investigated specifically for the microbial competition scenario. This would enable a better view of the distribution and dispersion of the individual microbial species within the reservoir in order to derive a better understanding of the competition mode.

The MEOR model describing biofilm formation to be simulated with MRST should be beefed up to account for porosity and relative permeability changes according to the Kozeny-Carman relation. This would lead to better results – higher incremental oil recoveries – because the effect of microscopic fluid diversion, resulting from reduction in porosity and permeability in some grid cells would be evident. Therefore, production of initially bypassed oil at later production time will be accounted for.

This work has assumed a reservoir with only oil and water and no dissolved gas in any of the liquid phase. Future work can be implemented to accommodate gas miscibility with oil and/or water with the introduction of a third flowing phase when the pressure in the reservoir falls below bubble-point pressure.

Laboratory MEOR experiments and/or field tests should be executed and the results should be compared to those obtained using the models described in this report to evaluate the efficiency of these models in predicting actual displacement processes.

A final suggestion for further studies would entail creating models that accommodate variable bacteria and nutrient concentrations at different production periods. This should not be confused with variable rate flow that can be achieved by conventional models. It implies that for a constant water injection rate, schedules for injected microbes and nutrients concentrations can be created for specific production periods. This would be a basis for optimization of the injection process leading to more efficient fluid displacement and to arrive at better oil recovery values.

References

Abdallah, W., Buckley, J. S., Carnegie, A., Edwards, J., Herold, B., Fordham, E., et al. (2007). Fundamentals of Wettability. *Oilfield Review*, 44-61.

Ahmed, T. (2010). Chapter 4 - Fundamentals of Rock Properties. In T. Ahmed, *Reservoir Engineering Handbook* (4th ed., pp. 189-287). Boston: Gulf Professional Publishing.

Al-Hadhrami, H. S., & Blunt, M. J. (2000). Thermally Induced Wettability Alteration to Improve Oil Recovery in Fractured. *2000 SPE/DOE Improved Oil Recovery Symposium.* Tulsa,Oklahoma: SPE.

Al-Raoush, R., & Papadopoulos, A. (2010). Representative Elementary Volume Analysis of Porous Media using X-ray Computed Tomography. *Powder Technology*, *200*(1-2), 69-77.

Al-Sulaimani, H., Al-Wahaibi, Y., Al-Bahry, S., Elshafie, A., Al-Bemani, A., & Joshi, S. (2012, April). Residual-Oil Recovery Through Injection of Biosurfactant, Chemical Surfactant, and Mixtures of Both Under Reservoir Temperatures: Induced-Wettability and Interfacial-Tension Effects. *SPE Reservoir Evaluation & Engineering*, 210-217.

Amundsen, A. (2015). *Microbial Enhanced Oil Recovery - Modeling and Numerical Simulations.* Master Thesis, Norwegian University of Science and Technology (NTNU), Department of Mathematical Sciences.

Anderson, W. G. (1987). Wettability Literature Survey - Part 4: Effects of Wettability on Capillary Pressure. *Journal of Petroleum Technology*, *39*(10), 1283-1300.

Anderson, W. G. (1987, November). Wettability Literature Survey - Part 5: The Effects of Wettability on Relative Permeability. *Journal of Petroleum Technology*, 1453-1468.

Armstrong, R. T., & Wildenschild, D. (2011). Decoupling the Mechanisms of Microbial Enhanced Oil Recovery. *SPE Annual Technical Conference and Exhibition.* Denver: Society of Petroleum Engineers.

Aurand, K. (2015, May 3). *Using nanofluids to enhance oil recovery*. Retrieved November 27, 2015, from NTNU Tech Zone: http://www.ntnutechzone.no/en/2015/05/using-nanofluids-to-enhance-oil-recovery/

Awan, A. R., Teigland, R., & Kleppe, J. (2008, June). A Survey of North Sea Enhanced-Oil-Recovery Projects Initiated During the Years 1975 to 2005. *SPE Reservoir Evaluation & Engineering*, 497-512.

Ballyk, M., Jones, D., & Smith, H. (2001). Microbial Competition in Reactors with Wall Attachment: A Mathematical Comparison of Chemostat and Plug Flow Models. *Microbial Ecology*, *41*, 210-221.

Beckman, J. (1926). The Action of Bacteria on Mineral Oil. *Industrial and Engineering Chemistry, 4*, 23–26.

Behesht, M., Roostaazad, R., Farhadpour, F., & Pishvaei, M. R. (2008). Model Development for MEOR Process in Conventional Non-Fractured Reservoirs and Investigation of Physico-Chemical Parameter Effects. *Chemical Engineering Technology, 31*(7), 953-963.

Brown, L., Vadie, A., & Stephens, J. (2000). Slowing Production Decline and Extending the Economic Life of an Oil Field: New MEOR Technology. *SPE/DOE Improved Oil Recovery Symposium.* Tulsa, Oklahoma: Society of Petroleum Engineers.

Bryant, R. S., & Burchfield, T. E. (1989, May). Review of Microbial Technology for Improving Oil Recovery. *SPE Reservoir Engineering*, 151-154.

Bryant, R. S., Bertus, K., Stepp, A., Chang, M.-M., & Chase, K. (1992). Laboratory Studies of Parameters Involved in Modeling Microbial Oil Mobilisation. *SPE/DOE 8th Symposium on Enhanced Oil Recovery.* Tulsa, Oklahoma: Society of Petroleum Engineers.

Bryant, S. L., & Lockhart, T. P. (2002, October). Reservoir Engineering Analysis of Microbial Enhanced Oil Recovery. *SPE Reservoir Evaluation & Engineering*, 365-374.

Bültemeier, H., Alkan, H., & Amro, M. (2014). A New Modeling Approach to MEOR Calibrated by Bacterial Growth and Metabolite Curves. *SPE EOR Conference at Oil and Gas West Asia.* Muscat: Society of Petroleum Engineers.

Chang, M.-M., Chung, F.-H., Bryant, R., Gao, H., & Burchfield, T. (1991). Modeling and Laboratory Investigation of Microbial Transport Phenomena in Porous Media. *66th Annual Technical Conference and Exhibition.* Dallas: Society of Petroleum Engineers.

Clement, T., Hooker, B., & Skeen, R. (1996). Macroscopic Models for Predicting Changes in Saturated Porous Media Properties Caused by Microbial Growth. *Ground Water, 34*(5), 934–942.

Corey, A. (1954). The Interrelation Between Gas and Oil Relative Permeabilities. *Producers Monthly*, 38-41.

Dake, L. (1978). *Fundamentals of Reservoir Engineering.* Amsterdam: Elsevier Science B.V.

Delshad, M., Asakawa, K., Pope, G. A., & Sepehrnoori, K. (2002). Simulations of Chemical and Microbial Enhanced Oil Recovery Methods. *75237-MS SPE Conference Paper* . Tulsa Oklahoma: Society of Petroleum Engineers.

Deng, D., Li, C., Ju, Q., Wu, P., Dietrich, F., & Zhou, Z. (1999). Systematic Extensive Laboratory Studies of Microbial EOR Mechanisms and Microbial EOR Application

Results in Changqing Oilfield. *SPE Asia Pacific Oil and Gas Conference and Exhibition.* Jakarta: Society of Petroleum Engineers.

Fredrickson, A., & Stephanopoulos, G. (1981). Microbial Competition. *Science, 213*(4511), 972-979.

Ghazali Abd. Karim, M., Hj Salim, M. A., Md. Zain, Z., & Talib, N. N. (2001). Microbial Enhanced Oil Recovery (MEOR) Technology in Bokor Field, Sarawak. *SPE Asia Pacific Improved Oil Recovery Conference.* Kuala Lumpur: Society of Petroleum Engineers.

Goudarzi, A., Delshad, M., & Sepehrnoori, K. (2013). A Critical Assessment of Several Reservoir Simulators for Modeling Chemical Enhanced Oil Recovery Processes. *SPE 163578-MS.* SPE Reservoir Simulation Symposium,Woodlands, Texas: Society of Petroleum Engineers.

Green, D. W., & Willhite, G. P. (1998). *Enhanced Oil Recovery* (Vol. Volume 6 SPE Textbook Series). Texas: Society of Petroleum Engineers.

Gudiña, E. J., Rodrigues, L. R., Teixeira, J. A., Pereira, J. F., Coutinho, J. A., & Soares, L. P. (2012). Biosurfactant Producing Microorganisms and Its Application to Enhance Oil Recovery at Lab Scale. *SPE EOR Conference at Oil and Gas West Asia.* Muscat: Society of Petroleum Engineers.

Gullapalli, I. L., Bae, J. H., Hejl, K., & Edwards, A. (2000, February). Laboratory Design and Field Implementation of Microbial Profile Modification Process. *SPE Reservoir Evaluation and Engineering, 3*(1), 42-49.

Hou, Z., Dou, X., Jin, R., Wang, R., Wang, Y., Li, W., et al. (2011). The Application of Microbial Enhanced Oil Recovery in Daqing Oilfields. *SPE Enhanced Oil Recovery Conference.* Kuala Lumpur: Society of Petroleum Engineers.

IEA. (2016). *Oil Market Report.* International Energy Agency (OECD/IEA).

Illias, R., Ooi, S., Idris, A., & Rahman, W. (1999). Production of Biosurfactant and Biopolymer from Malaysian Oil Fields Isolated Microorganisms. *SPE Asia Pacific Improved Oil Recovery Conference.* Kuala Lumpur: Society of Petroleum Engineers.

IPIMS. (n.d.). *Permeability*. Retrieved November 29, 2015, from IPIMS Web Site: http://www.ipims.com/data/fe11/G4209.asp?UserID=&Code=23382

Jadhunandan, P. P., & Morrow, N. R. (1995, February). Effect of Wettability on Waterflood Recovery for Crude-Oil/Brine/Rock Systems. *SPE Reservoir Engineering*, 40-46.

Jang, L., & Yen, T. (1990). History of Microbial Enhanced Recovery. In T. F. Yen, *Microbial Enhanced Oil Recovery: Principle and Practice* (pp. 13-27). Boca Raton, Florida: CRC Press.

Jenneman, G. E., Knapp, R. M., McInerney, M. J., Menzie, D., & Revus, D. (1984, February). Experimental Studies of In-Situ Microbial Enhanced Oil Recovery. *Society of Petroleum Engineers Journal*, 33-37.

Khan, H. A., Gbosi, A., Britton, L. N., & Bryant, S. L. (2008). Mechanistic Models of Microbe Growth in Heterogeneous Porous Media. *SPE/DOE Improved Oil Recovery Symposium.* Tulsa, Oklahoma: Society of Petroleum Engineers.

Kianipey, S. A., & Donaldson, E. C. (1986). Mechanisms of Oil Displacement by Microorganisms. *61st Annual Technical Conference and Exhibition.* New Orleans: Society of Petroleum Engineers.

Kowalewski, E., Rueslåtten, I., Boassen, T., Sunde, E., Stensen, J. Å., Lillebø, B.-L. P., et al. (2005). Analyzing Microbial Improved Oil Recovery Processes From Core Floods. *International Petroleum Technology Conference.* Doha: IPTC.

Kowalewski, E., Rueslåtten, I., Steen, K., Bødtker, G., & Torsæter, O. (2006, March). Microbial Improved Oil Recovery - Bacterial Induced Wettability and Interfacial Tension Effects on Oil Production. *Journal of Petroleum Science amd Engineering, 52*(1-4), 275–286.

Kuznetsov, S. I., Ivanov, M. V., & Lyalikova, N. N. (1963). *Introduction to Geological Microbiology* (English ed.). (C. H. Oppenheimer, Ed., & P. T. Broneer, Trans.) New York: McGrawHill.

Lacerda, E., Priimenko, V. I., & Pires, A. P. (2012). Microbial EOR: A Quantitative Prediction of Recovery Factor. *18th SPE Improved Oil Recovery Symposium.* Tulsa, Oklahoma: Society of Petroleum Engineers.

Lake, L. W., Schmidt, R. L., & Venuto, P. B. (1992). A Niche for Enhanced Recovery in the 1990s. *Oilfield Review*, 55-61.

Lie, K.-A. (2015). *An Introduction to Reservoir Simulation Using MATLAB.* Oslo: SINTEF ICT, Departement of Applied Mathematics.

Lomelan, F., Ebeltoft, E., & Thomas, W. H. (2005). A New Versatile Relative Permeability Correlation. *International Symposium of the Society of Core Analysts.* Toronto, Canada, 21-25 August 2005: Society of Core Analysts.

Morrow, N. R. (1990). Wettability and Its Effect on Oil Recovery. *Journal of Petroleum Technology, 42*(12), 1476-1484.

Muggeridge, A., Cockin, A., Webb, K., Frampton, H., Collins, I., Moulds, T., et al. (2014). Recovery rates, enhanced oil recovery and technological limits. *Philosophical Transactions of the Royal Society A, 372*(2006).

Nielsen, S. M. (2010). *Microbial Enhanced Oil Recovery - Advanced Reservoir Simulation.* PhD Thesis, Technical University of Denmark (DTU), Department of Chemical and Biochemical Engineering.

OED and NPD. (2015). *Resource Management in Mature Areas.* Retrieved November 27, 2015, from Norwegian Petroleum: http://www.norskpetroleum.no/en/production/resource-management-in-mature-areas/

Pavlou, S. (2006). Microbial Competition in Bioreactors. *CI&CEQ, 12*(1), 71-81.

Purwasena, I. A., Sugai, Y., & Sasaki, K. (2010). Estimation of the Potential of an Oil-Viscosity-Reducing Bacterium Petrotoga sp. Isolated from an Oil Field for MEOR. *SPE Annual Technical Conference and Exhibition.* Florence: Society of Petroleum Engineers.

Rabiei, A., Sharifinik, M., Niazi, A., Hashemi, A., & Ayatollahi, S. (2013, April). Core Flooding Tests to Investigate the Effects of IFT Reduction and Wettability Alteration on Oil Recovery during MEOR Process in an Iranian Oil Reservoir. *Applied Microbiology and Biotechnology*, *97*(13), 5979–5991.

Range Resources. (n.d.). *Operations - Trinidad*. Retrieved November 29, 2015, from Range Resources: http://www.rangeresources.co.uk/operations-trinidad.asp

Salehi, M., Johnson, S., Liang, J.-T., Fox, S., & Bala, G. (2006). Wettability Alteration of Carbonate Rock Mediated by High-Starch Agricultural Effluents. *9th International Symposium on Evaluation of Wettability and Its Effect on Oil Recovery.* Bergen: Idaho National Laboratory.

Singer, M., & Finnerty, W. (1984). Microbial Metabolism of Straight-Chain and Branched Alkanes. In R. M. Atlas, *Petroleum Microbiology* (pp. 1-60). New York: Macmillan Publishing Company.

Statoil. (2012, August 29). *Aiming High to Improve Recovery*. Retrieved October 29, 2015, from Statoil: http://www.statoil.com/en/NewsAndMedia/News/2012/Pages/29aug_recovery.aspx

Statoil. (2014). *Microbial enhanced oil recovery (MEOR)*. Retrieved March 19, 2016, from Statoil website: http://www.statoil.com/en/TechnologyInnovation/OptimizingReservoirRecovery/RecoveryMethods/WaterAssistedMethodsImprovedOilRecoveryIOR/Pages/MicrobialEnhancedOilRecovery(MEOR).aspx

Sugai, Y., Kishita, A., Hong, C.-X., Enomoto, H., Chida, T., & Zhou, S.-C. (1999). Laboratory Investigation of Polymer Producer TU-15A for MEOR Field Tests. *SPE Asia Pacific Oil and Gas Conference and Exhibition.* Jakarta: Society of Petroleum Engineers.

Tang, B., & Wolkowicz, G. S. (1992). Mathematical Models of Microbial Growth and Competition in the Chemostat Regulated by Cell-Bound Extracellular Enzymes. *Journal of Mathematical Biology, 31*, 1-23.

Thomas, C. E., Mahoney, C. F., & Winter, G. W. (1987). Water-Injection Pressure Maintenance and Waterflood Processes. In *Petroleum Engineering Handbook.* Richardson, Texas: Society of Petroleum Engineers.

Thullner, M. (2010). Comparison of Bioclogging Effects in Saturated Porous Media. *Ecological Engineering, 36*, 176-196.

Tingshan, Z., Xiaohei, C., Guangzhi, L., & Zhaoyong, J. (2005). Microbial Degradation Influences On Heavy Oil Characters And MEOR Test. *18th World Petroleum Congress.* Johannesburg: World Petroleum Council.

Wang, F.-B. (2010). A System of Partial Differential Equations Modeling the Competition for Two Complementary Resources in Flowing Habitats. *Journal of Differential Equations, 249*, 2866-2888.

Wei, X., Liu, K., & Li, D. (2013). Laboratory Investigation of the Effect of Microbial Metabolite on Crude Oil-Water Interfacial Tension Under Reservoir Conditions. *SPE Enhanced Recovery Coneference.* Kuala Lumpur: Society of Petroleum Engineers.

Willey, J. M., Sherwood, L. M., & Woolverton, C. J. (2008). Chapter 6 - Microbial Growth. In *Prescott, Harley, and Klein's Microbiology* (7th ed., pp. 119-148). New York: McGraw-Hill.

Wolicka, D., & Borkowski, A. (2012). Microorganisms and Crude Oil. In L. Romero-Zerón (Ed.), *Introduction to Enhanced Oil Recovery (EOR) Processes and Bioremediation of Oil-Contaminated Sites* (pp. 113-141). InTech.

Yao, C., Lei, G., Ma, J., Wu, C., & Li, W. (2011). Simulation of Indigenous Microbial Enhanced Oil Recovery (IMEOR). *International Petroleum Technology Conference.* Bangkok: IPTC.

Young, T. (1805, January). An Essay on the Cohesion of Fluids. *Philosophical Transactions, 95*, 65-87.

Youssef, N., Elshahed, M. S., & McInerney, M. J. (2009). Microbial Processes in Oil Fields: Culprits, Problems, and Opportunities. In *Advances in Applied Microbiology* (Vol. 66, pp. 141-251). Academic Press.

Zekri, A. Y., Almehaideb, R. A., & Chaalal, O. (1999). Project of Increasing Oil Recovery from UAE Reservoirs Using Bacteria Flooding. *SPE Annual Technical Conference and Exhibition.* Houston, Texas: Society of Petroleum Engineers.

Zekri, A. Y., Ghannam, M. T., & Almehaideb, R. A. (2003). Carbonate Rocks Wettability Changes Induced by Microbial Solution. *SPE Asia Pacific Oil and Gas Conference and Exhibition.* Jakarta: Society of Petroleum Engineers.

Zhang, X., Knapp, R., & Mclnerney, M. (1992). Mathematical Model for Microbially Enhanced Oil Recovery Process. *24202-MS SPE Conference Paper* . Tulsa, Oklahoma: Society of Petroleum Engineers.

Zimmerman, R. (2003). *Fluid Flow in Porous Media.* London: Department of Earth Science and Engineering, Imperial College.

ZoBell, C. E. (1947). Bacterial Release of Oil from Oil-bearing Materials (Part 1). *World Oil, 126*(13), 36-44.

Appendix A

Other Results and Plots

Adsorbed Bacteria vs. Total Bacteria

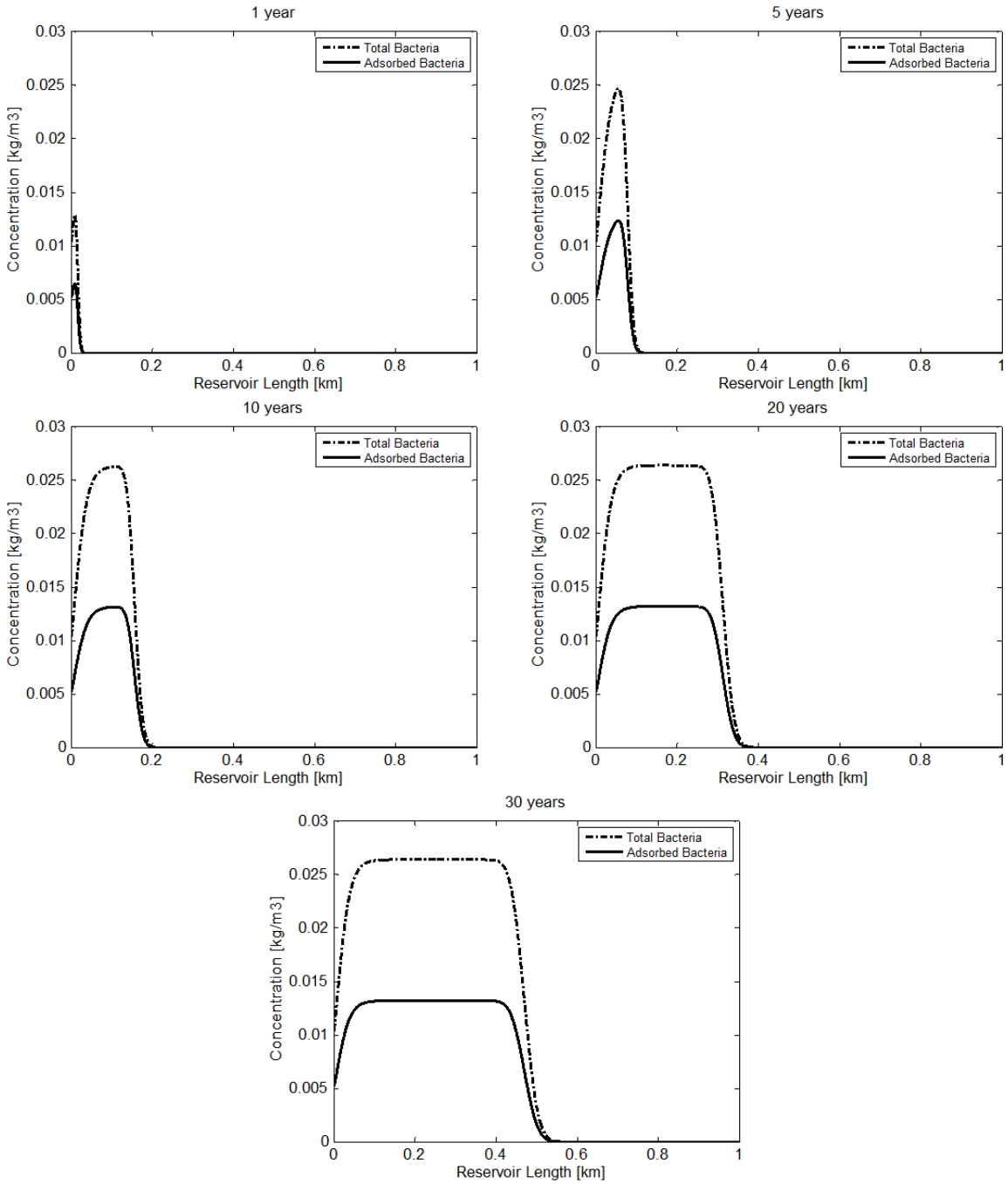

Figure A.1: Bacteria concentration distribution within the biofilm phase and the entire reservoir for the case of MEOR with bacteria adsorption.

Adsorbed Nutrients vs. Total Nutrients

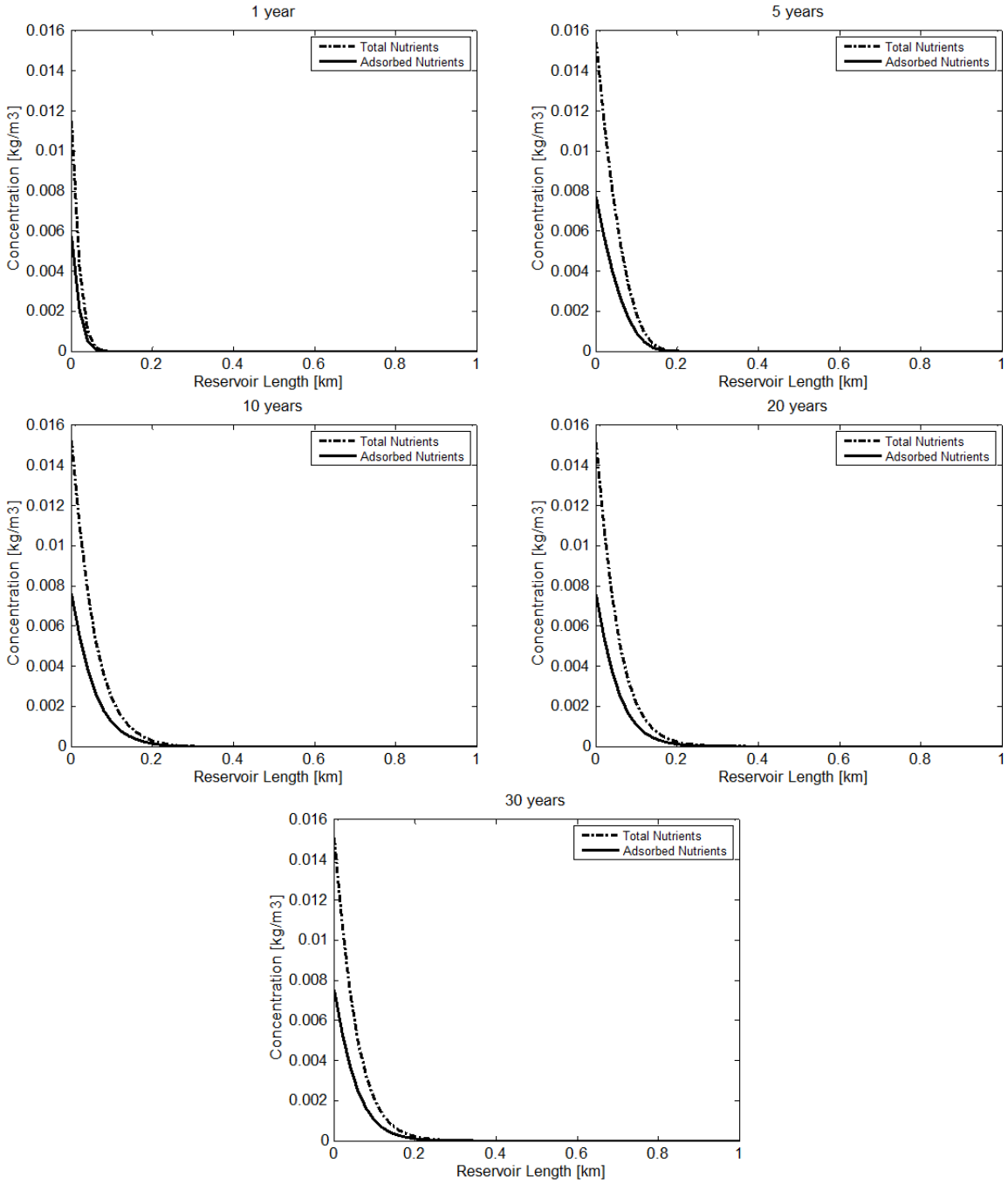

Figure A.2: Nutrient concentration distribution within the biofilm phase and the entire reservoir for the case of MEOR with food adsorption.

Bump in Nutrient Plot during Biofilm Formation

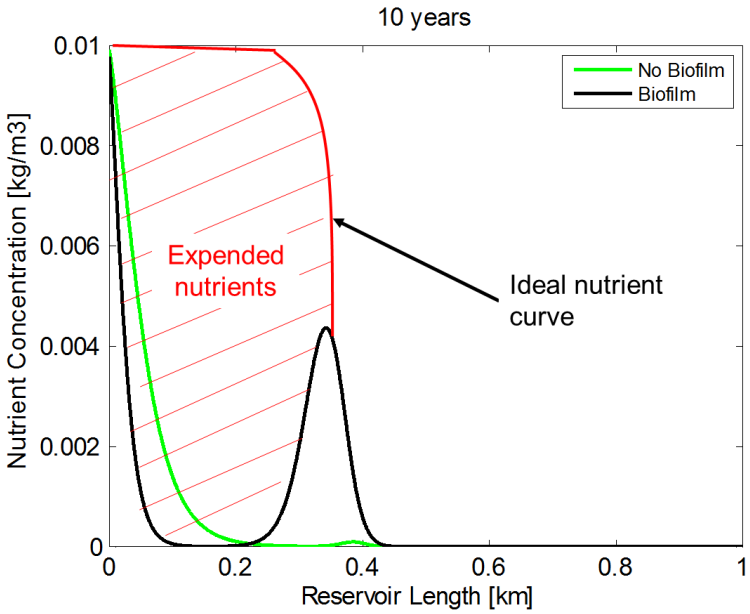

Figure A.3: Comparison of nutrient concentrations for an ideal nutrient front and the nutrient front (bump) of the biofilm case.

This shaded region represents the expended nutrients consumed by the microbes behind the nutrient front. The ideal curve represents a situation where there is no microbial growth and no metabolite production.

Bacteria and Nutrient Concentration Analysis – Single Species Case

Table A.1: Results for the sensitivity analysis on the effect of bacteria and nutrient injection concentration on oil recovery

Nutrient Conc. [kg/m^3]	Bacteria Conc. [kg/m^3]	Oil Recovery [%]
0.00001	0.000005	49.28
	0.00005	49.29
	0.0005	49.31
	0.005	49.35
	0.05	49.36
	0.5	49.36
0.0001	0.000005	49.29
	0.00005	49.31
	0.0005	49.54
	0.005	50.03
	0.05	50.12
	0.5	50.13
0.001	0.000005	49.33
	0.00005	49.81
	0.0005	53.95
	0.005	60.42
	0.05	61.72
	0.5	61.87
0.01	0.000005	65.10
	0.00005	69.22
	0.0005	72.53
	0.005	74.02
	0.05	74.31
	0.5	74.34
0.1	0.000005	73.38
	0.00005	73.81
	0.0005	74.16
	0.005	74.32
	0.05	74.35
	0.5	74.35
1	0.000005	74.22
	0.00005	74.28
	0.0005	74.33
	0.005	74.35
	0.05	74.35
	0.5	74.35

Bacteria and Nutrient Concentration Analysis – Bacteria Adsorption

Table A.2: Results for the sensitivity analysis on the effect of bacteria and nutrient injection concentration on oil recovery for the case of bacteria adsorption

Nutrient Conc. [kg/m^3]	Bacteria Conc. [kg/m^3]	Oil Recovery [%]
0.00001	0.000005	49.28
	0.00005	49.28
	0.0005	49.30
	0.005	49.35
	0.05	49.36
	0.5	49.36
0.0001	0.000005	49.28
	0.00005	49.30
	0.0005	49.46
	0.005	49.98
	0.05	50.12
	0.5	50.13
0.001	0.000005	49.31
	0.00005	49.56
	0.0005	53.23
	0.005	60.42
	0.05	61.77
	0.5	61.87
0.01	0.000005	66.63
	0.00005	70.87
	0.0005	73.24
	0.005	74.13
	0.05	74.32
	0.5	74.34
0.1	0.000005	73.84
	0.00005	74.06
	0.0005	74.24
	0.005	74.33
	0.05	74.35
	0.5	74.35
1	0.000005	74.30
	0.00005	74.33
	0.0005	74.35
	0.005	74.36
	0.05	74.35
	0.5	74.36

Bacteria and Nutrient Concentration Analysis – Nutrient Adsorption

Table A.3: Results for the sensitivity analysis on the effect of bacteria and nutrient injection concentration on oil recovery for the case of food adsorption

Nutrient Conc. [kg/m^3]	Bacteria Conc. [kg/m^3]	Oil Recovery [%]
0.00001	0.000005	49.28
	0.00005	49.28
	0.0005	49.29
	0.005	49.33
	0.05	49.36
	0.5	49.36
0.0001	0.000005	49.30
	0.00005	49.31
	0.0005	49.38
	0.005	49.79
	0.05	50.10
	0.5	50.13
0.001	0.000005	53.79
	0.00005	53.90
	0.0005	54.96
	0.005	59.61
	0.05	61.78
	0.5	61.87
0.01	0.000005	74.12
	0.00005	74.12
	0.0005	74.13
	0.005	74.18
	0.05	74.29
	0.5	74.34
0.1	0.000005	74.35
	0.00005	74.35
	0.0005	74.35
	0.005	74.35
	0.05	74.35
	0.5	74.35
1	0.000005	74.35
	0.00005	74.35
	0.0005	74.35
	0.005	74.35
	0.05	74.35
	0.5	74.35

Bacteria and Nutrient Concentration Analysis – Bacteria Competition Case

Table A.4: Results for the sensitivity analysis on the effect of exogenous bacteria and nutrient injection concentration on oil recovery for MEOR with microbial competition

Nutrient Conc. [kg/m^3]	Bacteria Conc. [kg/m^3]	Oil Recovery [%]
0.00001	0.000005	49.28
	0.00005	49.28
	0.0005	49.29
	0.005	49.63
	0.05	74.30
	0.5	74.35
0.0001	0.000005	49.28
	0.00005	49.28
	0.0005	49.29
	0.005	49.64
	0.05	74.30
	0.5	74.35
0.001	0.000005	49.28
	0.00005	49.28
	0.0005	49.30
	0.005	49.75
	0.05	74.30
	0.5	74.35
0.01	0.000005	49.28
	0.00005	49.29
	0.0005	49.39
	0.005	50.94
	0.05	74.32
	0.5	74.35
0.1	0.000005	49.29
	0.00005	49.39
	0.0005	50.51
	0.005	66.81
	0.05	74.34
	0.5	74.35
1	0.000005	49.39
	0.00005	50.50
	0.0005	66.37
	0.005	74.34
	0.05	74.35
	0.5	74.35

Appendix B

MATLAB Codes

B.1 The Microbial Competition Model

This file is similar to *MeoraModel.m* but with modifications for two bacteria species. The following path **…/ mrst-autodiff / ad-blackoil / models** must be specified in order to access this file. The file must always remain in this directory.

```
classdef MEORIndaModel < TwoPhaseOilWaterModel
    % Oil/water/microbial system
    % This model is a two phase oil/water model, extended with the
    % microbial phase in addition.
    % It accounts for the existence of microbial competition
    % by specifying two bacteria species; microbe_0 and microbe_1
    % microbe_0 are the injected (foreign) microbes and
    % microbe_1 are the indigenous microbes
    % Microbe effects currently available for simulation:

    properties
        % Substances in the reservoir
        microbe_0   % Indigenous microbe
        microbe_1   % Foreign microbe
        nutrient
        metabolite    % Metabolites for both microbes
        biofilm
        biosurf
        biopoly
        biofilmFood
        stateplots
        % Variables
        yield_microbe_0
        yield_microbe_1
        yield_metabolite
        growth_max_microbe_0
        growth_max_microbe_1
        growth_max_metabolite
        halfsat_microbe_0
        halfsat_microbe_1
        halfsat_metabolite
        crit_val
        dist_coeff
        dil_rate
        langmuir
    end

    methods
        function model = MEORIndaModel(G, rock, fluid, varargin)

            model = model@TwoPhaseOilWaterModel(G,rock, fluid);

            model.microbe_0 = true;
```

```
    model.microbe_1 = true;
    model.metabolite = true;
    model.nutrient = true;
                % pre-defining defaults
    model.yield_microbe_0 = .35;
    model.yield_microbe_1 = .50;
    model.yield_metabolite = .15;
    model.growth_max_microbe_0 = .4/day;
    model.growth_max_microbe_1 = .2/day;
    model.growth_max_metabolite = .2/day;
    model.halfsat_microbe_0 = 1;
    model.halfsat_microbe_1 = 1;
    model.halfsat_metabolite = 1;
    model.crit_val = 0;
    model.dil_rate = 50;
    model.dist_coeff = 1;
    model.langmuir = [0, 0];

    % type/types of metabolite to be defined manually
    model.biosurf = false;
    model.biopoly = false;
    model.biofilm = false;
    model.biofilmFood = false;
    model.stateplots = false;
    % not available for more than 3 phases
    % oil/water/microbe/nutrient/metabolite
    model.outputFluxes = true;


    model.wellVarNames = {'qWs', 'qOs', 'qWMEOR', 'bhp'};

    model = merge_options(model, varargin{:});
end


function [problem, state] = getEquations(model, state0, state,...
        dt, drivingForces, varargin)
    [problem, state] = equationsMEORInda(state0, state, model,...
        dt, drivingForces, varargin{:});
end

function [fn, index] = getVariableField(model, name)
    % add metabolites here
    switch(lower(name))
        case 'microbe_0'
            fn = 'm_0';
            index = 1;
        case 'microbe_1'
            fn = 'm_1';
            index = 1;
        case 'nutrient'
            fn = 'n';
            index = 1;
        case 'metabolite'
            fn = 'meta';
            index = 1;
        case 'biofilm'
            fn = 'bio';
            index = 1;
        otherwise
```

```
                    [fn, index] =
getVariableField@TwoPhaseOilWaterModel(model, name);
            end
        end
            function [state, report] = updateState(model, state, problem,
...
                dx, drivingForces)
            [state, report] = updateState@TwoPhaseOilWaterModel(model, ...
               state, problem,  dx, drivingForces);

           if model.stateplots && rem(problem.iterationNo,5)==1
               xvals = linspace(0,1,model.G.cells.num);
       set(0, 'currentfigure', 1);
       plot(xvals, state.pressure);
       title(sprintf('Pressure'));

       set(0, 'currentfigure', 2);
       plot(xvals, state.s);
       title(sprintf('Saturation'));

       set(0, 'currentfigure', 3);
       plot(xvals, state.m_0);
       title(sprintf('Exogenous Microbe concentration'));

       set(0, 'currentfigure', 4);
       plot(xvals, state.m_1);
       title(sprintf('Indigenous Microbe concentration'));

       set(0, 'currentfigure', 5);
       plot(xvals, state.n);
       title(sprintf('Nutrient concentration'));

       set(0, 'currentfigure', 6);
       plot(xvals, state.meta);
       title(sprintf('Metabolite concentration'));

       drawnow;
           end
        end
    end
end
```

B.2 New Equation Files and Helper Function

The new equation files can be accessed by specifying the following path **…/ mrst-autodiff / ad-blackoil / utils**. These files should always remain in this directory.

Food Biofilm Equation (*equationsBiofilmFood.m*)

```
function [problem, state] =
equationsBiofilmFood(state0,state,model,dt,drivingForces,varargin)
% Biofilm effects. Nutrient adsorption only
% Get linearized problem for oil/water/MEOR system with black oil
% properties
```

```
opt = struct('Verbose', mrstVerbose,...
             'reverseMode', false,...
             'resOnly', false,...
             'iteration', -1);

opt = merge_options(opt, varargin{:});

W = drivingForces.Wells;
%assert(isempty(drivingForces.bc) && isempty(drivingForces.src))

% Operators, grid, and fluid model
s = model.operators;
G = model.G;
f = model.fluid;
Y_micro = model.yield_microbe;
Y_meta = model.yield_metabolite;
mu_micro = model.growth_max_microbe;
mu_meta = model.growth_max_metabolite;
K_micro = model.halfsat_microbe;
K_meta = model.halfsat_metabolite;
N = model.crit_val;
D_i = model.dist_coeff;
w = model.langmuir;



% Properties at current timestep
[p, sW, m, meta, n, bioFood, wellSol] = model.getProps(state, 'pressure',
'water',...
    'microbe', 'metabolite', 'nutrient', 'biofilm', 'wellsol');

% Properties at previous timestep
[p0,sW0, m0, meta0, n0,bio0] = model.getProps(state0, 'pressure', 'water',
...
    'microbe', 'metabolite', 'nutrient','biofilm');

pBH = vertcat(wellSol.bhp);
qWs = vertcat(wellSol.qWs);
qOs = vertcat(wellSol.qOs);
qWMEOR = vertcat(wellSol.qWMEOR);

% Initialize independent variables
if ~opt.resOnly,
    % ADI variables needed since we are not only computing residuals.
    if ~opt.reverseMode,
        [p, sW, m, meta, n, bioFood, qWs, qOs, qWMEOR, pBH] = ...
            initVariablesADI( p, sW, m, meta, n, bioFood, qWs, qOs, qWMEOR,
pBH);
    else
        [p0, sW0, m0, meta0, n0,bio0, tmp,tmp,tmp,tmp] = ...
            initVariablesADI(p0, sW0, m0, meta0, n0,bio0,...
            zeros(size(qWs)), zeros(size(qOs)), zeros(size(qWMEOR)),...
            zeros(size(pBH)));
        clear tmp
    end
end

% We will solve for pressure, water saturation (oil saturation follows from
% the definition of saturations) ((may need to change later)), microbe
```

```
% concentration, nutrient concentration, metabolite concentration,
% and well rates and bhp.
primaryVars = {'pressure', 'sW', 'microbe', 'metabolite',
'nutrient','biofilm', 'qWs', 'qOs',...
    'qWMEOR', 'bhp'};

% Evaluate relative permeability
sO = 1 - sW;
sO0 = 1 - sW0;

% Find effective surface area for adsorption
SurfA = 3.*10^5*sW./model.rock.poro;
SurfA0 = 3.*10^5*sW0./model.rock.poro;

[krW, krO] = model.evaluteRelPerm({sW, sO}); % as written

if model.biosurf
    % form is taken from Nielsen
    % constants are as well
    partition = D_i.*(sW.*model.fluid.rhoWS)./(sO.*model.fluid.rhoOS);
    meta_eff = meta.*partition./(partition + 1);
    surfa = [1*10^-4, 0.2, 1.5*10^4];
    ift = @(s) 29.*(-tanh(surfa(3).*s-surfa(2))+1+surfa(1))./...
        (-tanh(-surfa(2))+1+surfa(1));
    sigma = ift(double(meta_eff));
    f = (sigma/29).^(1/6);
    sor = f.*.3;
    %disp(min(sor))
    f = ones(length(f),1);
    wmax = f.*.5+1-f;
    swi = f.*.3;
    omax = f.*.8+1-f;
    a = f.*2+1-f;
    krO_max = omax.*((sO-sor)./(1-swi-sor)).^a;
    krW_max = wmax.*((sW-swi)./(1-swi-sor)).^a;
    inx = meta_eff>1e-16;
    krW = krW + (krW_max - krW).*inx;
    krO = krO + (krO_max - krO).*inx;
end

% Multipliers for properties
[pvMult, transMult, mobMult, pvMult0] = getMultipliers(model.fluid, p,p0);


% Modify relperm by mobility multiplier
krW = mobMult.*krW;
krO = mobMult.*krO;

% Adjustments for pore volume and relperm for biofilm
%m(m<0) = 0; % cheating
%bio(bio<0) = 0; % as well
if model.biofilmFood
    bioeff = bioFood;
    bioeff(bioFood<0) = 0;
    psi = bioeff./1000; % number is biofilm density
    phi_rel = 1 - psi;
   % pvMult = pvMult.*phi_rel;
   % krW = krW.*(phi_rel.^(19/6)); % plenty of other ways found in Thullner
end
```

```
% Compute transmissibility
T = s.T.*transMult;

% Gravity contribution
gdz = model.getGravityGradient();

% Evaluate water and MEOR props
[vW, vMicro, vMeta, vN, bW, mobW, mobM_0, mobPol, mobN, rhoW, pW, upcw] =
...
    getFluxAndPropsMEORbiofilm(model, p, sW, m, meta, n, bioFood, krW, T,
gdz);
bW0 = model.fluid.bW(p0);

% Evaluate Oil properties
[vO,bO,mobO,rhoO,p,upco] = getFluxAndPropsOil_BO(model,p,sO,krO,T,gdz);
bO0 = getbO_BO(model, p0);

if model.outputFluxes
    state = model.storeFluxes(state, vW, vO, vMicro); %add function to
model for more than 1 extra phase
end

if model.extraStateOutput
    state = model.storebfactors(state, bW, bO, []);
    state = model.storeMobilities(state, mobW, mobO, mobM_0, mobN);%add
function if I feel like it same as storeFluxes
    state = model.storeUpstreamIndices(state, upcw, upco, []);
end


% EQUATIONS ------------------------------------------------------------
% Microbe, biofilm, and metabolite calculations
if w(2)~=0
    biocon = (bioFood./SurfA)./(w(1).*w(2)-w(2).*bioFood./SurfA);
else
    biocon = 0;
end
mu_b = mu_micro.*(n)./(K_micro + (n));
mu_m = mu_meta.*((n) - N)./(K_meta + (n) - N);
R_n = -mu_b.*(m.*sW.*bW).*Y_micro - mu_m.*(m.*sW.*bW).*Y_meta;
lang = w(1).*w(2).*(n-bioFood)./(1+w(2).*(n-bioFood));



bWvW = s.faceUpstr(upcw, bW).*vW;
%lang(lang<0) = 0;
bWvMicro = s.faceUpstr(upcw, bW).*vMicro;
bWvMeta = s.faceUpstr(upcw, bW).*vMeta;
bWvN = s.faceUpstr(upcw, bW).*vN;
bOvO = s.faceUpstr(upco, bO).*vO;


% Conservation of oil:
oil = (s.pv/dt).*(pvMult.*bO.*sO - pvMult0.*bO0.*sO0) + s.Div(bOvO);

%Conservation of  water:
```

```
water = (s.pv/dt).*(pvMult.*bW.*sW - pvMult0.*bW0.*sW0) + s.Div(bWvW);

%Conservation of  microbes:
microbe = (s.pv/dt).*((pvMult.*bW.*sW.*m - pvMult0.*bW0.*sW0.*m0)) -
s.pv.*mu_b.*m.*bW.*sW.*pvMult.*Y_micro + s.Div(bWvMicro);


%Conservation of  nutrients:
nutrient = (s.pv/dt).*((pvMult.*bW.*sW.*n - pvMult0.*bW0.*sW0.*n0)) +
s.pv.*pvMult.*SurfA.*lang - s.pv.*R_n.*pvMult+ s.Div(bWvN);
biofilm = (s.pv/dt).*((pvMult.*bioFood - pvMult0.*bio0)) -
s.pv.*pvMult.*SurfA.*lang;

%Conservation of metabolites:
metabolite = (s.pv/dt).*((pvMult.*bW.*sW.*meta - pvMult0.*bW0.*sW0.*meta0))
- s.pv.*mu_m.*(m.*sW.*bW+bioFood).*pvMult.*Y_meta+ s.Div(bWvMeta);

eqs = {water, oil, microbe, nutrient, metabolite, biofilm};
names = {'water', 'oil', 'microbe', 'nutrient', 'metabolite', 'biofilm'};
types = {'cell', 'cell', 'cell', 'cell', 'cell', 'cell'};


% Add in any fluxes/source terms given as boundary conditions
[eqs, qBC, BCTocellMap, qSRC, srcCells] = addFluxesFromSourcesAndBC(...
    model, eqs, {pW, p}, {rhoW, rhoO}, {mobW, mobO}, {bW, bO}, ...
    {sW, sO}, drivingForces);

% Add MEOR boundary conditions
if ~isempty(drivingForces.bc) && isfield(drivingForces.bc,'m')
    injInx = qBC{1} > 0; % Water inflow indicies
    mbc = (BCTocellMap')*m; % m_0 is only type injected
    nbc = (BCTocellMap')*n;
    metabc = (BCTocellMap')*meta;
    mbc(injInx) = drivingForces.bc.m(injInx);
    nbc(injInx) = drivingForces.bc.n(injInx);
    metabc(injInx) = drivingForces.bc.meta(injInx);
    eqs{3} = eqs{3} - BCTocellMap*(mbc.*qBC{1});
    eqs{4} = eqs{4} - BCTocellMap*(nbc.*qBC{1});
    eqs{5} = eqs{5} - BCTocellMap*(metabc.*qBC{1});
end

% Add MEOR source
if ~isempty(drivingForces.src) && isfield(drivingForces.src, 'm')
    injInx = qSRC{1}>0;
    msrc = m(srcCells);
    nsrc = n(srcCells);
    metasrc = meta(srcCells);
    msrc(injInx) = drivingForces.src.m(injInx);
    nsrc(injInx) = drivingForces.src.n(injInx);
    eqs{3}(srcCells) = eqs{3}(srcCells) - msrc.*qSRC{1};
    eqs{4}(srcCells) = eqs{4}(srcCells) - nsrc.*qSRC{1};
 %   eqs{5}(srcCells) = eqs{5}(srcCells) - metasrc.*qSRC{1};
end

% well equations switch to 8 eqns with only 1 meor well
% WELLS NOT READY FOR BIOFILM IMPLEMENTATION (eqs i+1 basically)
if ~isempty(W)
    wm = model.wellmodel;
    if ~opt.reverseMode
```

```
        wc = vertcat(W.cells);
        pw = p(wc);
        rhos = [f.rhoWS, f.rhoOS];
        bw = {bW(wc), bO(wc)};
        tw = {mobW(wc), mobO(wc)};
        s = {sW(wc), sO(wc)};

        [cqs, weqs, ctrleqs, wc, state.wellSol] = ...
            wm.computeWellFlux(model, W, wellSol,...
            pBH, {qWs, qOs}, pw, rhos, bw, tw, s, {},...
            'nonlinearIteration', opt.iteration);

        % Store the well equations (relating well BHP to influx)
        eqs(6:7) = weqs;

        % Store control equations
        eqs{9} = ctrleqs;
        % Add source terms to the equations.
        eqs{1}(wc) = eqs{1}(wc) - cqs{1};
        eqs{2}(wc) = eqs{1}(wc) - cqs{2};

        % MEOR well equations
         [~, wciMEOR, iInxW, MEORc] = getWellMEOR(W);
         mw = m(wc);
         nw = n(wc);
         mw(iInxW) = wciMEOR.*(1-MEORc);
         nw(iInxW) = wciMEOR.*MEORc;
%         [~, wciMICROBE, iInxWM] = getWellMicrobe(W);
%         [~, wciNUTRIENT, iInxWN] = getWellNutrient(W);
%         mw = m(wc);
%         nw = n(wc);
%         mw(iInxWM) = wciMICROBE;
%         nw(iInxWN) = wciNUTRIENT;

        % Totally unsure here
        bWqM = mw.*cqs{1};
        bWqN = nw.*cqs{1};
        eqs{3}(wc) = eqs{3}(wc) - bWqM;
        eqs{4}(wc) = eqs{5}(wc) - bWqN;

        % Well MEOR rate for each well is water rate in each perforation
        % multiplied with microbe and nutrient concentration in that
        % perforated cell
        perf2well = getPerforationToWellMapping(W);
        Rw = sparse(perf2well, (1:numel(perf2well))',
1,numel(W),numel(perf2well));
        eqs{8} = qWMEOR - Rw*(cqs{1}.*(mw+nw)); %UNSURE
%         eqs{7} = qWMICROBE - Rw*(cqs{1}.*mw);
%         eqs{8} = qWNUTRIENT - Rw*(cqs{1}.*nw);

        names(6:9) = {'waterWells', 'oilWells', 'meorWells',
'closureWells'};
        types(6:9) = {'perf', 'perf', 'perf', 'well'};
    else
        [eq, n, typ] = ...
            wm.createReverseModeWellEquations(model, state0.wellSol, p0);
        % add another equation for MEOR well rates. No idea if functional
        [eqs{6:9}] = deal(eq{1});
        [names{6:9}] = deal(n{1});
        [types{6:9}] = deal(typ{1});
```

```
    end
end
problem = LinearizedProblem(eqs,types,names,primaryVars,state,dt);
end

function [wMICROBE, wciMICROBE, iInxWM] = getWellMicrobe(W)
    if isempty(W)
        wMICROBE = [];
        wciMICROBE = [];
        iInxWM = [];
        return
    end
    inj = vertcat(W.sign) == 1;
    mInj = cellfun(@(x)~isempty(x), {W(inj).MICROBE});
    wMICROBE = zeros(nnz(inj),1);
    wMICROBE(mInj) = vertcat(W(inj(mInj)).MICROBE);
    wciMICROBE = rldecode(wMICROBE, cellfun(@numel, {W(inj).cells}));

    % Injection cells
    nPerf = cellfun(@numel, {W.cells})';
    nw = numel(W);
    perf2well = rldecode((1:nw)',nPerf);
    compi = vertcat(W.compi);
    iInx = rldecode(inj, nPerf);
    iInx = find(iInx);
    iInxWM = iInx(compi(perf2well(iInx),1)==1);
end

function [wNUTRIENT, wciNUTRIENT, iInxWN] = getWellNutrient(W)
    if isempty(W)
        wNUTRIENT = [];
        wciNUTRIENT = [];
        iInxWN = [];
        return
    end
    inj = vertcat(W.sign) == 1;
    mInj = cellfun(@(x)~isempty(x), {W(inj).MICROBE});
    wNUTRIENT = zeros(nnz(inj),1);
    wNUTRIENT(mInj) = vertcat(W(inj(mInj)).MICROBE);
    wciNUTRIENT = rldecode(wNUTRIENT, cellfun(@numel, {W(inj).cells}));

    % Injection cells
    nPerf = cellfun(@numel, {W.cells})';
    nw = numel(W);
    perf2well = rldecode((1:nw)',nPerf);
    compi = vertcat(W.compi);
    iInx = rldecode(inj, nPerf);
    iInx = find(iInx);
    iInxWN = iInx(compi(perf2well(iInx),1)==1);
end

function [wMEOR, wciMEOR, iInxW,MEORc] = getWellMEOR(W)
    if isempty(W)
        wMEOR = [];
        wciMEOR = [];
        iInxW = [];
        MEORc = [];
        return
    end
    inj = vertcat(W.sign) == 1;
```

```
    mInj = cellfun(@(x)~isempty(x), {W(inj).meor});
    wMEOR = zeros(nnz(inj),1);
    wMEOR(mInj) = vertcat(W(inj(mInj)).meor);
    wciMEOR = rldecode(wMEOR, cellfun(@numel, {W(inj).cells}));
    MEORcomp = zeros(nnz(inj),1);
    %MEORcomp(mInj) = vertcat(W(inj(mInj)).MEORMIX);
    MEORcomp(mInj) = [.5];
    MEORc = rldecode(MEORcomp, cellfun(@numel, {W(inj).cells}));

    % Injection cells
    nPerf = cellfun(@numel, {W.cells})';
    nw = numel(W);
    perf2well = rldecode((1:nw)',nPerf);
    compi = vertcat(W.compi);
    iInx = rldecode(inj, nPerf);
    iInx = find(iInx);
    iInxW = iInx(compi(perf2well(iInx),1)==1);
end
```

Microbial Competition Equation (*equationsMEORInda.m*)

```
function [problem, state] =
equationsMEORInda(state0,state,model,dt,drivingForces,varargin)
% This function creates MEOR effects for the case of microbial competition
% Get linearized problem for oil/water/MEOR system with black oil
% properties
opt = struct('Verbose', mrstVerbose,...
             'reverseMode', false,...
             'resOnly', false,...
             'iteration', -1);

opt = merge_options(opt, varargin{:});

W = drivingForces.Wells;
%assert(isempty(drivingForces.bc) && isempty(drivingForces.src))

% Operators, grid, and fluid model
s = model.operators;
G = model.G;
f = model.fluid;
Y_micro_0 = model.yield_microbe_0; %% Injected microbes
Y_micro_1 = model.yield_microbe_1; %% Indigenous microbes
Y_meta = model.yield_metabolite;
mu_micro_0 = model.growth_max_microbe_0; %% Injected microbes
mu_micro_1 = model.growth_max_microbe_1; %% Indigenous microbes
mu_meta = model.growth_max_metabolite;
K_micro_0 = model.halfsat_microbe_0;
K_micro_1 = model.halfsat_microbe_1;
K_meta = model.halfsat_metabolite;
N = model.crit_val;
D_i = model.dist_coeff;
dil_rate = model.dil_rate;

% Properties at current timestep
[p, sW, m_0, m_1, meta, n, wellSol] = model.getProps(state, 'pressure',
'water',...
    'microbe_0', 'microbe_1', 'metabolite', 'nutrient', 'wellsol');
```

```
% Properties at previous timestep
[p0,sW0, m_00, m_10, meta0, n0] = model.getProps(state0, 'pressure',
'water', ...
    'microbe_0', 'microbe_1', 'metabolite', 'nutrient');

pBH = vertcat(wellSol.bhp);
qWs = vertcat(wellSol.qWs);
qOs = vertcat(wellSol.qOs);
qWMEOR = vertcat(wellSol.qWMEOR);
%qWMICROBE = vertcat(wellSol.qWMICROBE);
%qWNUTRIENT = vertcat(wellSol.qWNUTRIENT);

% Initialize independent variables
if ~opt.resOnly,
    % ADI variables needed since we are not only computing residuals.
    if ~opt.reverseMode,
        [p, sW, m_0, m_1, meta, n, qWs, qOs, qWMEOR, pBH] = ...
            initVariablesADI( p, sW, m_0, m_1, meta, n, qWs, qOs, qWMEOR,
pBH);
    else
        [p0, sW0, m_00, m_10, meta0, n0, tmp,tmp,tmp,tmp] = ...
            initVariablesADI(p0, sW0, m_00, m_10, meta0, n0,...
            zeros(size(qWs)), zeros(size(qOs)), zeros(size(qWMEOR)),...
            zeros(size(pBH)));
        clear tmp
    end
end

% We will solve for pressure, water saturation (oil saturation follows from
% the definition of saturations) ((may need to change later)), microbe
% concentration, nutrient concentration, metabolite concentration,
% and well rates and bhp.
primaryVars = {'pressure', 'sW', 'microbe_0', 'microbe_1', 'metabolite',
'nutrient', 'qWs', 'qOs',...
    'qWMEOR', 'bhp'};

% Evaluate relative permeability
sO = 1 - sW;
sO0 = 1 - sW0;

[krW, krO] = model.evaluteRelPerm({sW, sO}); % as written


if model.biosurf
    % form is taken from Nielsen
    % constants are as well
    partition = D_i.*(sW.*model.fluid.rhoWS)./(sO.*model.fluid.rhoOS);
    meta_eff = meta.*partition./(partition + 1);
    %meta_eff = meta;
    surfa = [1*10^-4, 0.2, 1.5*10^4];
    ift = @(s) 29.*(-tanh(surfa(3).*s-surfa(2))+1+surfa(1))./...
        (-tanh(-surfa(2))+1+surfa(1));
    sigma = ift(double(meta_eff));
    f = (sigma/29).^(1/6);
    sor = f.*.3;
    %disp(min(sor))
    f = ones(length(f),1);
    wmax = f.*.5+1-f;
    swi = f.*.3;
    omax = f.*.8+1-f;
```

```
    a = f.*2+1-f;
    krO_max = omax.*((sO-sor)./(1-swi-sor)).^a;
    krW_max = wmax.*((sW-swi)./(1-swi-sor)).^a;
    inx = meta_eff>1e-16;

%     krO_max =  .8.*((1 - sW - .08)./(1 - .08 - .3)).^2;
%     krW_max =  .5.*((sW - .3)./(1 - .08 - .3)).^2;
%     meta_eff = meta.*10^3;
%     partition = 1.*(sW.*model.fluid.rhoWS)./(sO.*model.fluid.rhoOS);
%     meta_eff = meta_eff.*partition./(partition + 1);
%     meta_eff(meta_eff<.01) = 0;
%     meta_eff(meta_eff>1) = 1;
     krW = krW + (krW_max - krW).*inx;
     krO = krO + (krO_max - krO).*inx;
    %krW = krW + (sW - krW).*meta_eff;
    %krO = krO + (sO - krO).*meta_eff;
end

% Multipliers for properties
[pvMult, transMult, mobMult, pvMult0] = getMultipliers(model.fluid, p,p0);

% Modify relperm by mobility multiplier
krW = mobMult.*krW;
krO = mobMult.*krO;

% Compute transmissibility
T = s.T.*transMult;

% Gravity contribution
gdz = model.getGravityGradient();

% Evaluate water and MEOR props
[vW, vM_0, vM_1, vMeta, vN, bW, mobW, mobM_0, mobM_1, mobMeta, mobN, rhoW,
pW, upcw] = ...
    getFluxAndPropsMEORX(model, p, sW, m_0, m_1, meta, n, krW, T, gdz);
bW0 = model.fluid.bW(p0);

% Evaluate Oil properties
[vO,bO,mobO,rhoO,p,upco] = getFluxAndPropsOil_BO(model,p,sO,krO,T,gdz);
bO0 = getbO_BO(model, p0);

if model.outputFluxes
    state = model.storeFluxes(state, vW, vO, vM_1); %add function to model
end

if model.extraStateOutput
    state = model.storebfactors(state, bW, bO, []);
    state = model.storeMobilities(state, mobW, mobO, mobM_0, mobM_1,
mobN);%add function
    state = model.storeUpstreamIndices(state, upcw, upco, []);
end


% EQUATIONS ---------------------------------------------------------------

mu_b_0 = mu_micro_0.*n./(K_micro_0 + n);
mu_b_1 = mu_micro_1.*n./(K_micro_1 + n);
mu_m = mu_meta.*(n-N)./(K_meta + n - N);
```

```
R_n = (dil_rate.*m_0 - mu_b_0.*m_0).*Y_micro_0 + (dil_rate.*m_1 -
mu_b_1.*m_1).*Y_micro_1 - mu_m.*(m_0 + m_1).*Y_meta;
% R_n = dil_rate.*n - mu_b_0.*m_0.*Y_micro_0 - mu_b_1.*m_1.*Y_micro_1 -
mu_m.*(m_0 + m_1).*Y_meta;

bWvW = s.faceUpstr(upcw, bW).*vW;
bWvM_0 = s.faceUpstr(upcw, bW).*vM_0;
bWvM_1 = s.faceUpstr(upcw, bW).*vM_1;
bWvMeta = s.faceUpstr(upcw, bW).*vMeta;
bWvN = s.faceUpstr(upcw, bW).*vN;
bOvO = s.faceUpstr(upco, bO).*vO;


% Conservation of oil:
oil = (s.pv/dt).*(pvMult.*bO.*sO - pvMult0.*bO0.*sO0) + s.Div(bOvO);

%Conservation of  water:
water = (s.pv/dt).*(pvMult.*bW.*sW - pvMult0.*bW0.*sW0) + s.Div(bWvW);

%Conservation of  microbes:
% Injected microbes
microbe_0 = (s.pv/dt).*((pvMult.*bW.*sW.*m_0 - pvMult0.*bW0.*sW0.*m_00)) -
s.pv.*(-dil_rate.*m_0 + mu_b_0.*m_0).*bW.*sW.*pvMult.*Y_micro_0 +
s.Div(bWvM_0);

% Indigenous microbes
microbe_1 = (s.pv/dt).*((pvMult.*bW.*sW.*m_1 - pvMult0.*bW0.*sW0.*m_10)) -
s.pv.*(-dil_rate.*m_1 + mu_b_1.*m_1).*bW.*sW.*pvMult.*Y_micro_1 +
s.Div(bWvM_1);

%Conservation of  nutrients:
% nutrient = (s.pv/dt).*((pvMult.*bW.*sW.*n - pvMult0.*bW0.*sW0.*n0) +
Y.*m_0.*n)+ s.Div(bWvN);
nutrient = (s.pv/dt).*((pvMult.*bW.*sW.*n - pvMult0.*bW0.*sW0.*n0)) -
s.pv.*R_n.*bW.*sW.*pvMult+ s.Div(bWvN);

%Conservation of metabolites:
% metabolite = (s.pv/dt).*((pvMult.*bW.*sW.*meta -
pvMult0.*bW0.*sW0.*meta0) - Y.*m_0.*n)+ s.Div(bWvMeta);
metabolite = (s.pv/dt).*((pvMult.*bW.*sW.*meta - pvMult0.*bW0.*sW0.*meta0))
- s.pv.*mu_m.*(m_0+m_1).*bW.*sW.*pvMult.*Y_meta+ s.Div(bWvMeta);

eqs = {water, oil, microbe_0, microbe_1, nutrient, metabolite};
names = {'water', 'oil', 'microbe_0', 'microbe_1', 'nutrient',
'metabolite'};
types = {'cell', 'cell', 'cell', 'cell', 'cell', 'cell'};


% Add microbe processes before boundary conditions? or after?
% before equations? as equations?


% Add in any fluxes/source terms given as boundary conditions
[eqs, qBC, BCTocellMap, qSRC, srcCells] = addFluxesFromSourcesAndBC(...
    model, eqs, {pW, p}, {rhoW, rhoO}, {mobW, mobO}, {bW, bO}, ...
    {sW, sO}, drivingForces);

% Add MEOR boundary conditions
```

```
if ~isempty(drivingForces.bc) && isfield(drivingForces.bc,'m_0')
    injInx = qBC{1} > 0; % Water inflow indicies
    mbc = (BCTocellMap')*m_0; % m_0 is only type injected
    nbc = (BCTocellMap')*n;
    mbc(injInx) = drivingForces.bc.m_0(injInx);
    nbc(injInx) = drivingForces.bc.n(injInx);
    eqs{3} = eqs{3} - BCTocellMap*(mbc.*qBC{1});
    eqs{5} = eqs{5} - BCTocellMap*(nbc.*qBC{1});
end

% Add MEOR source
if ~isempty(drivingForces.src) && isfield(drivingForces.src, 'm_0')
    injInx = qSRC{1}>0;
    msrc = m_0(srcCells);
    nsrc = n(srcCells);
    msrc(injInx) = drivingForces.src.m_0(injInx);
    nsrc(injInx) = drivingForces.src.n(injInx);
    eqs{3}(srcCells) = eqs{3}(srcCells) - msrc.*qSRC{1};
    eqs{5}(srcCells) = eqs{5}(srcCells) - nsrc.*qSRC{1};
end

% well equations switch to 8 eqns with only 1 meor well
if ~isempty(W)
    wm = model.wellmodel;
    if ~opt.reverseMode
        wc = vertcat(W.cells);
        pw = p(wc);
        rhos = [f.rhoWS, f.rhoOS];
        bw = {bW(wc), bO(wc)};
        tw = {mobW(wc), mobO(wc)};
        s = {sW(wc), sO(wc)};

        [cqs, weqs, ctrleqs, wc, state.wellSol] = ...
            wm.computeWellFlux(model, W, wellSol,...
            pBH, {qWs, qOs}, pw, rhos, bw, tw, s, {},...
            'nonlinearIteration', opt.iteration);

        % Store the well equations (relating well BHP to influx)
        eqs(7:8) = weqs;

        % Store control equations
        eqs{10} = ctrleqs;
        % Add source terms to the equations.
        eqs{1}(wc) = eqs{1}(wc) - cqs{1};
        eqs{2}(wc) = eqs{1}(wc) - cqs{2};

        % MEOR well equations
         [~, wciMEOR, iInxW, MEORc] = getWellMEOR(W);
         mw = m_0(wc);
         nw = n(wc);
         mw(iInxW) = wciMEOR.*(1-MEORc);
         nw(iInxW) = wciMEOR.*MEORc;
%        [~, wciMICROBE, iInxWM] = getWellMicrobe(W);
%        [~, wciNUTRIENT, iInxWN] = getWellNutrient(W);
%        mw = m(wc);
%        nw = n(wc);
%        mw(iInxWM) = wciMICROBE;
%        nw(iInxWN) = wciNUTRIENT;

        % Totally unsure here
```

```
        bWqM = mw.*cqs{1};
        bWqN = nw.*cqs{1};
        eqs{3}(wc) = eqs{3}(wc) - bWqM;
        eqs{5}(wc) = eqs{5}(wc) - bWqN;

        % Well MEOR rate for each well is water rate in each perforation
        % multiplied with microbe and nutrient concentration in that
        % perforated cell
        perf2well = getPerforationToWellMapping(W);
        Rw = sparse(perf2well, (1:numel(perf2well))',
1,numel(W),numel(perf2well));
        eqs{9} = qWMEOR - Rw*(cqs{1}.*(mw+nw)); %UNSURE
%         eqs{7} = qWMICROBE - Rw*(cqs{1}.*mw);
%         eqs{8} = qWNUTRIENT - Rw*(cqs{1}.*nw);

        names(7:10) = {'waterWells', 'oilWells', 'meorWells',
'closureWells'};
        types(7:10) = {'perf', 'perf', 'perf', 'well'};
    else
        [eq, n, typ] = ...
            wm.createReverseModeWellEquations(model, state0.wellSol, p0);
        % add another equation for MEOR well rates. No idea if functional
        [eqs{7:10}] = deal(eq{1});
        [names{7:10}] = deal(n{1});
        [types{7:10}] = deal(typ{1});
    end
end
problem = LinearizedProblem(eqs,types,names,primaryVars,state,dt);
end

function [wMICROBE, wciMICROBE, iInxWM] = getWellMicrobe(W)
    if isempty(W)
        wMICROBE = [];
        wciMICROBE = [];
        iInxWM = [];
        return
    end
    inj = vertcat(W.sign) == 1;
    mInj = cellfun(@(x)~isempty(x), {W(inj).MICROBE});
    wMICROBE = zeros(nnz(inj),1);
    wMICROBE(mInj) = vertcat(W(inj(mInj)).MICROBE);
    wciMICROBE = rldecode(wMICROBE, cellfun(@numel, {W(inj).cells}));

    % Injection cells
    nPerf = cellfun(@numel, {W.cells})';
    nw = numel(W);
    perf2well = rldecode((1:nw)',nPerf);
    compi = vertcat(W.compi);
    iInx = rldecode(inj, nPerf);
    iInx = find(iInx);
    iInxWM = iInx(compi(perf2well(iInx),1)==1);
end

function [wNUTRIENT, wciNUTRIENT, iInxWN] = getWellNutrient(W)
    if isempty(W)
        wNUTRIENT = [];
        wciNUTRIENT = [];
        iInxWN = [];
        return
    end
```

```
    inj = vertcat(W.sign) == 1;
    mInj = cellfun(@(x)~isempty(x), {W(inj).MICROBE});
    wNUTRIENT = zeros(nnz(inj),1);
    wNUTRIENT(mInj) = vertcat(W(inj(mInj)).MICROBE);
    wciNUTRIENT = rldecode(wNUTRIENT, cellfun(@numel, {W(inj).cells}));

    % Injection cells
    nPerf = cellfun(@numel, {W.cells})';
    nw = numel(W);
    perf2well = rldecode((1:nw)',nPerf);
    compi = vertcat(W.compi);
    iInx = rldecode(inj, nPerf);
    iInx = find(iInx);
    iInxWN = iInx(compi(perf2well(iInx),1)==1);
end

function [wMEOR, wciMEOR, iInxW,MEORc] = getWellMEOR(W)
    if isempty(W)
        wMEOR = [];
        wciMEOR = [];
        iInxW = [];
        MEORc = [];
        return
    end
    inj = vertcat(W.sign) == 1;
    mInj = cellfun(@(x)~isempty(x), {W(inj).meor});
    wMEOR = zeros(nnz(inj),1);
    wMEOR(mInj) = vertcat(W(inj(mInj)).meor);
    wciMEOR = rldecode(wMEOR, cellfun(@numel, {W(inj).cells}));
    MEORcomp = zeros(nnz(inj),1);
    %MEORcomp(mInj) = vertcat(W(inj(mInj)).MEORMIX);
    MEORcomp(mInj) = [.5];
    MEORc = rldecode(MEORcomp, cellfun(@numel, {W(inj).cells}));

    % Injection cells
    nPerf = cellfun(@numel, {W.cells})';
    nw = numel(W);
    perf2well = rldecode((1:nw)',nPerf);
    compi = vertcat(W.compi);
    iInx = rldecode(inj, nPerf);
    iInx = find(iInx);
    iInxW = iInx(compi(perf2well(iInx),1)==1);
end
```

Helper Function (*getFluxAndPropsMEORX.m*)

This function is required by the equation file *equationsMEORInda.m* for the purpose of fluid and MEOR component property specification. The file can be accessed by specifying the following path **…/ mrst-autodiff / ad-blackoil / utils**. This file should always remain in this directory.

```
function [vW, vM_0, vM_1, vMeta, vN, bW, mobW, mobM_0, mobM_1, mobMeta,
mobN, rhoW, pW, upcw]= ...
```

```
            getFluxAndPropsMEORX(model, pO, sW, m_0, m_1, meta, n, krW, T,
gdz)
fluid = model.fluid;
s = model.operators;

% Check for capillary pressure (p_cOW)
pcOW = 0;
if isfield(fluid, 'pcOW') && ~isempty(sW)
    pcOW = fluid.pcOW(sW);
end
pW = pO - pcOW;

% Fluid props

bW = fluid.bW(pO);
rhoW = bW.*fluid.rhoWS;
% rhoW on face is the average of the neighbouring cells
rhoWf = s.faceAvg(rhoW);
muW = fluid.muW(pO);
muWeff = muW;
mobW = krW./muWeff;
dpW = s.Grad(pO-pcOW) - rhoWf.*gdz;
% water upstream index
upcw = double(dpW)<=0;
vW = -s.faceUpstr(upcw,mobW).*T.*dpW;
if any(bW <0)
    warning('Negative water compressibility present')
end


% MEOR props
mobM_0 = mobW.*m_0;
mobM_1 = mobW.*m_1;
mobMeta = mobW.*meta;
mobN = mobW.*n;
vM_0 = -s.faceUpstr(upcw, mobM_0).*s.T.*dpW;
vM_1 = -s.faceUpstr(upcw, mobM_1).*s.T.*dpW;
vMeta = -s.faceUpstr(upcw, mobMeta).*s.T.*dpW;
vN = -s.faceUpstr(upcw, mobN).*s.T.*dpW;
```